

A REASSESSMENT OF REEF-BUILDING CORALS, AN
ASSESSMENT OF FRAMEWORK BIOEROSION, AND
A REASSESSMENT OF MARINE BENTHIC ALGAE
IN THE REEF AREA AFFECTED BY THERMAL
EFFLUENT AT TANGUSSION POINT, GUAM

By

RICHARD H. RANDALL
ROY T. TSUDA
and
RAYMOND G. BOWMAN

Final Report

Submitted to
Mr. Oscar Duarte
Guam Power Authority
P.O. Box 2977
Agana, Guam 96910-2977

University of Guam
Marine Laboratory
Technical Report No. 98

March, 1990

INTRODUCTION

by

Richard H. Randall

Project Description

TABLE OF CONTENTS

INTRODUCTION by Richard H. Randall.....	1
A REASSESSMENT OF REEF-BUILDING CORALS AND AN ASSESSMENT OF FRAMEWORK BIOEROSION IN THE REEF AREA AFFECTED BY THERMAL EFFLUENT by Richard H. Randall and Raymond Bowman.....	7
REASSESSMENT OF THE MARINE BENTHIC ALGAE by Roy T. Tsuda...	31
APPENDIX	

Scope of Work and Objectives

1. Reassessment of the Coral Community

Determine the areal extent of the coastal fringing reef near Tanguisson Point that is affected by thermal power plant effluent discharge in relation to its effect on the community structure of reef-building corals.

INTRODUCTION

by

Richard H. Randall

Project Description

Pursuant to the certification of NPDES Permit No. GU0000027, the Environmental Protection Agency (EPA) requires the gathering of data by the Guam Power Authority (GPA) to further assess the impact of condenser discharge cooling-water from the Tanguisson Power Plant into adjacent nearshore marine waters (Figs. 1 and 2). In relation to the above EPA permit requirements Stephen G. Nelson and Richard H. Randall of the University of Guam Marine Laboratory jointly submitted a proposal to GPA to further assess impacts from their power plant condenser cooling effluent upon the adjacent marine environment. A proposal, titled "Proposed Chemical and Biological Monitoring of Cooling-Water Effluent from the Tanguisson and Cabras Power Plants and Determination of the Reef Area Impact by the Discharge at Tanguisson Point, Guam", was submitted in November 1988, and a memorandum of understanding and agreement was signed on June 23, 1989. The scope of work objectives of the proposal were divided between the investigators with S.G. Nelson being responsible for those pertaining to temperature monitoring, determination of characteristics of the effluent, and fish and sea urchin bioassays at both the Cabras Island and Tanguisson Point power plants, and R.H. Randall being responsible for a reassessment of the community structure of reef building corals within the reef area affected by effluent discharge, and a first-time assessment of the structural integrity of the reef framework deposits within the area affected by effluent discharge at the Tanguisson Point power plant. This report addresses results of the study that were under the responsibility and supervision of R.H. Randall.

The study was divided into three parts consisting of: 1) a reassessment of the effects of thermal effluent discharge at the Tanguisson Power Plant in relation to the community structure of reef-building corals, 2) an assessment of bioerosion of the reef framework deposits within the area affected by power plant thermal effluent, and 3) an reassessment of marine benthic algae within the area affected by power plant thermal effluent.

Scope of Work and Objectives

Part I. Reassessment of the Coral Community

- 1 . Determine the areal extent of the coastal fringing reef near Tanguisson Point that is affected by thermal power plant effluent discharge in relation to its effect on the community structure of reef-building corals.

2. Compare results of the community structure analysis with the results of a similar study that was conducted in 1974 (Jones et al., 1976). In 1974, the affected reef area consisted of a core zone of 10,300 square meters where >90 percent of the reef-building corals were killed, and a combined core and peripheral zone of 20,000 square meters where to 1 to 90 percent of the corals were killed.

3. From the results of the study determine whether the size of the core and peripheral zones (as defined above) have changed from 1974 to 1989, a period of 15 years of elapsed time.

Part II. Assessment of Bioerosion

1. Determine the amount of bioerosion (borings) within framework reef samples that have been systematically collected in the reef area affected by thermal power plant effluent.
2. Collect reef framework samples for bioerosion analysis along a transect that bisects the entire thermally affected area in the vicinity of the power plant effluent outfall (across the reef flat platform, reef margin, and upper reef front slope to a depth of approximately 6 meters).
3. Compare results of the bioerosion analysis from the thermal effluent affected reef area with a similar bioerosion analysis of samples collected from a nearby control reef area (across the reef flat platform, reef margin, and upper reef front slope to a depth of approximately 6 meters).

Part III. Marine Benthic Algae Reassessment

1. Determine the community structure of marine benthic algae along a transect that bisects the reef flat platform and reef margin zones of the thermally affected reef area, and compare the results with a similar transect in a nearby control reef.

Previous Work and Background Information

During a five-year period between 1969 and 1974, Jones et al., (1976) studied the biological impact brought about by changes on a tropical reef from power plant thermal effluent discharge into the marine environment at Tanguisson Point. In this study R.H. Randall determined the community structure of reef-building corals before, during and after two oil-fired electric generating plants went into

operation at Tanguisson Point. During the same study R.T. Tsuda determined the community structure of marine benthic algae on the reef flat platform and reef margin zones before and after the power plants became operational. In summary this study concluded that effluent from the Tanguisson Power Plant is responsible for the death of corals along the reef margin and upper reef front slope zones that are impinged upon by thermal effluent discharged from the shoreline. Laboratory data indicate that an elevation in the temperature of sea water that is circulated through the power plant condensers and then discharged into marine reef habitats is primarily, but not necessarily the only causal factor responsible.

In a study of the effects of thermal effluent on the coral reef community at Tanguisson, Nuedecker (1976) concluded that: 1) the thermal effluent has a negative effect on the coral community, 2) the amount of coral coverage on the reef front slope at depths of 3 and 6 meters along the seaward margin of the thermally impacted area does not significantly differ from control areas, indicating that the influence of thermal effluent is concentrated along the shallower reef margin and upper reef front slope zones, 3) coral recruitment is less in the thermally impacted area than in control areas, 4) the amount of production in terms of biomass accumulation on plexiglass plates is significantly less in the thermally impacted area than in control areas, and 5) there is no doubt that thermal effluent is responsible for the death of reef-building corals in the thermally impacted area, but the area of coral-kill is not enlarging significantly.

In another study concerned with the development and environmental quality of coral reef communities near the Tanguisson Power Plant, Nuedecker (1977) concluded that: 1) recruitment studies indicate that few corals will settle in the thermally impacted area, and if they do, their chance of survival to reproductive maturity is quite small, and 2) growth-transplant studies demonstrated a negative correlation between and growth rate and increased temperature.

Personnel

- A. Richard A. Randall - University of Guam Marine Laboratory
Faculty (Principal Investigator)
 - 1) Responsibilities - Overall coordination for the study, reassessment of the thermally impacted coral community, and writing of the draft and final reports.
- B. Roy T. Tsuda - University of Guam, Emeritus
 - 1) Responsibilities - Reassessment of the marine benthic algal community within the thermally impacted area.
- C. Raymond G. Bowman - University of Maryland, Dept. of Geology,
Graduate Student

- 1) Responsibilities - An assessment of bioerosion of the reef framework deposits within the thermally-affected area. Partial funding is being provided by this project to R.G. Bowman to conduct a digenetic study of modern and Holocene reef limestones at Tanguisson Point area for his M.S. thesis at the University of Maryland. Preliminary results of this thesis research, in relation to bioerosion of reef framework deposits within the thermally-impacted area, is incorporated into this final report. Since most of the overall proposed thesis research is of fundamental interest to our understanding of the reef ecosystem at Tanguisson Point. Mr. Bowman's completed thesis will be incorporated into the final report as an appendix.

LITERATURE CITED

- Jones, R.S., R.H. Randall, and M.J. Wilder. 1976. Biological impact caused by changes on a tropical reef. U.S. Environmental Protection Agency, Ecological Progress Series, EPA-60013-76-027, Narragansett, Rhode Island, 209 p.
- Nuedecker, S. 1976. Effects of thermal effluent on the coral reef community at Tanguisson. Univ. of Guam Mar. Lab. Tech. Rept. No. 30, 55 p.
- Nuedecker, S. 1977. Development and environment quality of coral reef communities near the Tanguisson Power Plant. Univ. of Guam Mar. Lab. Tech. Rept. No. 41, 68 p.



Figure 1. Map of Guam showing the location of the Tanguisson point study area.

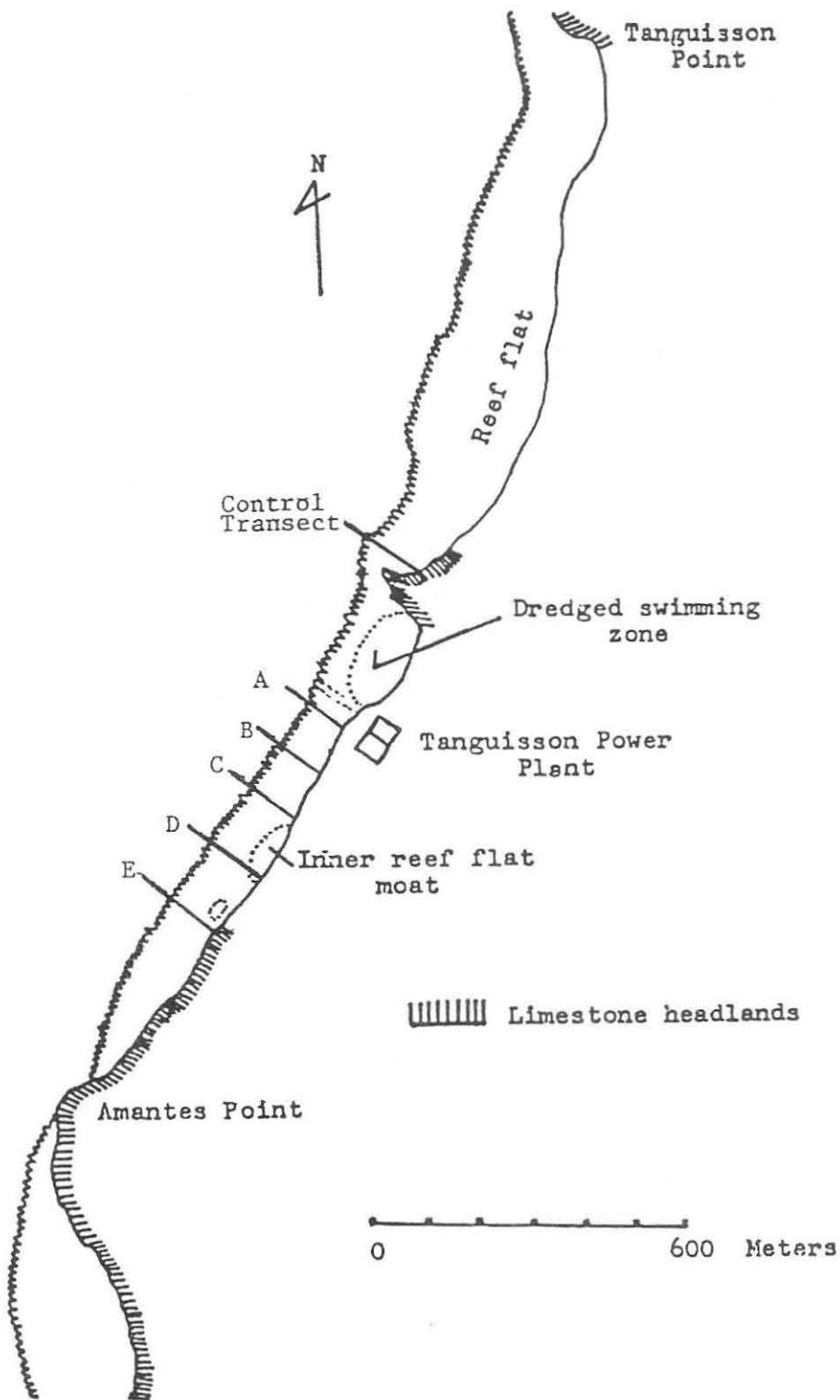


Figure 2. Detailed map of the Tanguisson Point study area showing transect locations

A REASSESSMENT OF REEF-BUILDING CORALS
AND AN ASSESSMENT OF FRAMEWORK
BIOEROSION IN THE REEF AREA AFFECTED
BY THERMAL EFFLUENT

by

Richard H. Randall
and
Raymond G. Bowman

Introduction

The earlier work of Jones et al. (1976) showed that a significant coral-kill occurred in the reef margin and upper reef front slope zones that were affected by thermal effluent discharge from two electric power generating plants at Tanguisson Point. Several questions remaining at the conclusion of this earlier work include: 1) will the original area of significant coral damage enlarge, remain about the same, or contract with passage of more time, and 2) since reef-building corals are major carbonate contributors to reefs, will their death in the effluent-affected area result in a significant net loss of framework deposits by increased rates of bioerosion? In this section the extent of the reef area affected by thermal effluent from power generating plants near Tanguisson Point is reassessed and compared to a similar study conducted between 1971 and 1974 (Jones et al., 1976). In addition a first-time assessment of bioerosion in framework reef deposits within the thermal effluent-affected area is given.

Reassessment of Reef-Building Corals
in Reef Areas by Thermal Effluent

Between 1971 and 1974, the extent of the effluent-affected peripheral coral area increased from 3,776 m², including a core area of 2,080 m² with a >90 percent coral kill, to 20,000 m², with an included core area of 10,300 m² (Jones et al., 1976). Assessment of coral-kill areas during initial plant start-up phases and early years of thermal discharge was a rather straightforward process, in that nearly all stressed corals reacted by expulsion of pigments, or bleaching, and for most eventual death and colonization of corallum surfaces by a succession of algae. Rapid transect assessment was accomplished by laying out a series of plastics surveyor's tapes across the affected area normal to the long plume axis and conducting a line-intercept ratio of bleached and recently killed corals with normally pigmented ones. A core coral-kill region was defined as having more than 90 percent bleached and recently killed corals, and a peripheral coral-kill area as one with 1 to 90 percent of the corals affected by the thermal effluent (Fig. 3).

A reconnaissance trip to the thermal plume area during May 1989, revealed a distinct core area with no living corals, which graded gradually, but almost imperceptibly, into unaffected coral communities in all directions, except toward the adjacent reef flat platform. No pale-colored, bleached, or recently killed corals gave any clue as to where the "normal unaffected" coral community started or ended. Some parameter other than color-stressed corals would have to be used to define the outer limits of the peripherally affected zone. At first it was thought that color-stressed corals might appear later in the wet season when ambient seawater temperatures would rise a slight amount, but throughout the field study period of 1989 none were observed.

To establish community structural parameters of "normal or average" coral density, percentage of substrate coverage, and colony size distribution, a control area must be established for comparison with the thermally-affected experimental area. Such a control area ideally should have, as near as possible, similar habitat characteristics as the experimental area, except for elevated temperatures, and they should also be as near to each other as possible. Although establishing similarity between control and experimental areas is difficult enough when neither has been disturbed, more uncertainty is inherent when one area, as in this case, has been disturbed and its exact previous nature is not known. Even so, such a control area will establish a baseline, or reference, upon which this study, as well as possible future comparisons can be made. With the above uncertainties in consideration, departures of community parameters in the experimental area from those in the control area can be used to estimate the size and nature of the thermally-affected zone.

Methods

A preliminary reconnaissance of fringing reefs within the thermally-impacted area, as well as north and south of it, was made on 12 June, 1989 to determine the best placement locations for transects to sample the community structural parameters of corals within the impacted area, as well as a nearby control area. June 12 was a rather calm day, with relatively little surf activity, which allowed rather thorough observations of both the reef margin and upper reef front slope zones to be made. A thermally elevated layer of surface water about a meter in thickness was present in both the reef margin and upper reef front slope zones adjacent to the power plant outfall (Fig. 4). A nearshore current moving in a southerly direction created an elongate surface plume of warm water that attenuated both in temperature and width toward the south as shown in Figure 3. Normal surface sea water temperatures, as well as what appeared to be nonimpacted coral communities were present at Transect E south of the plume, and again about midway between the power plant intake channel and Transect A as shown in Figure 3. The thermally impacted boundary at the north end of the plume area was quite sharp and conspicuous, because this is where the thermal outfall effluent first impinges upon the reef margin and upper reef front slope coral communities.

Based upon the above qualitative assessment of the thermally impacted reef zones, five transects were established in the thermal effluent area as shown in Figure 3. Transect A bisects the most impacted area at the north end of the thermal plume, Transect E lies just outside or possibly just inside the impacted area at the south end of the thermal plume, and Transects B-D are equally spaced between A and E. A sixth control transect was established about 450 meters north of Transect A in an area that originally was quite similar to the thermally-impacted area in respect to the community structure of corals and reef physiography (Fig. 3). All six transects extend from the shoreline and cross the reef flat platform, reef margin, and upper reef front slope to a depth of about six meters. Since the reef flat platform zone at both the control and thermally-impacted transect areas are mostly intertidal during low spring tides, corals were found to be absent or restricted to a few small holes (data from Jones et al., 1976 for the impacted area). Because corals were never present on these intertidal reef flat platform zones, they were not used in calculating the areas of core and peripheral coral-killed areas in this or the earlier studies.

Coral communities were analyzed along transects by using the plotless pointed-centered or point-quarter technique of Cottam et al. (1953). Six transect areas (A through E) and a control were established within the study area by placing a plastic surveyor's tape along the bottom on the reef flat platform, reef margin, and upper reef front slope locations as shown in Figure 3. Replicate transects were established from the shoreline to the upper reef front slope at each of the six transect areas, one within a five-meter-wide corridor on the right side (when facing seaward) of the transect line and another one within a similar-sized corridor on the left side of transect line. Transect sampling points were established by throwing a geology hammer from the surface at five-meter intervals along the transect line into each of the replicate transect corridors. Actual throws into each replicate corridor were made by tossing the hammer over one's shoulder while facing left for the right-handed corridor and facing right for the left-hand corridor. Such a method provides more randomness of sample point establishment within the corridors. Where the thrown hammer came to a rest, a sample point was established at the intersection of the hammer handle and head. Four quadrants were then formed around the point by establishing one axis along the hammer handle and another at right angles to it along the hammer head. The coral nearest the sample point in each quadrant was located and its specific name, size (diameter or maximum length and width), and the distance from the center of the corallum to the sample point were recorded. From these point-quarter data the following calculations were used to estimate community structure parameters:

1. Total density of all species = $\frac{\text{unit area}}{(\text{mean point-to-colony distance})^2}$
2. Relative density = $\frac{\text{individuals of a species}}{\text{total individuals of all species}}$
3. Density = $\frac{\text{relative density of a species}}{100} \times \text{total density of all species}$

4. Total percentage coverage = $\frac{\text{total density of all species}}{\text{average coverage value for all species}}$

5. Percent coverage = $\text{density of a species} \times \text{average coverage value for the species}$

Colony size distribution data (x = arithmetic mean, s = standard deviation, and w = size range) were also calculated from the point-quarter data. The diameters of irregularly shaped coral colonies were estimated by taking the square root of the product of colony length and width.

To assess the amount of framework bioerosion, sections of reef rock were chisled out from in situ reef deposits along Transect A, where thermal impact is greatest, and along the control transect (Fig. 3). Sampled sections included in situ living and dead coral colonies, crustose algal deposits, and loose cobbles and boulders. Field data accompanying each collected specimen included: 1) the reef zone and distance from shore (collection point within 5-meter interval), 2) water depth corrected to mean low water, 3) the name (taxa) of principal contributors to the sample (generally identifiable to the genus level, or in many sections to a specific level), and 4) the microhabitat of the sample (buttress ridge top, upper channel wall, etc.). To control the amount of variance between transects, that may be introduced because of bioeroding organisms being somewhat selective as to the kinds (taxa) of framework deposits they bore, samples were first collected from Transect A and their principal contributions identified, then samples with the same taxonomic contributors were collected from similar microhabitats and depths from the control transect. Fifty reef deposit samples were collected from Transect A and 43 similar samples were collected from the control transect. Each sample was cut in half with a diamond-bladed rock saw, and then one-half of each was sent to R.G. Bowman at the University of Maryland Geology Department for bioerosion analysis, and the remaining half was retained at the University of Guam Marine Laboratory.

Results and Discussion

Reassessment of the Coral-kill Area

A summary of point-quarter coral density and surface coverage data is presented in Table 1, and a summary of coral colony size distribution data is presented in Table 2. An ANOVA paired comparison test revealed that no significant differences between replicate transects were found at any transect in regard to coral density and surface coverage, but significant differences were found between paired transect stations in regard to the same community structural parameters (Table 3). Since significant differences were not found between replicate transects in regard to coral density and surface coverage the

data were combined (Table 1). The same parameter of coral surface coverage was used to determine the present thermally-affected coral-kill area as was used for estimating the 1974 area. Percentage of coral coverage is plotted at 5-meter station intervals for Transects A through E in Figures 5 through 9, and for the control transect in Figure 10. In Figure 11 all six transects are plotted on the same graph for direct comparison. Since corals were mostly absent on the intertidal reef flat platform, all the graph plots of transect station values of percent surface coverage in Figures 5 through 11 start at the inner part of the reef margin zone.

If an assumption is made that the original surface coral coverage at the thermally-affected transect areas (A-E) was similar to that presently estimated at the control transect, then 10 percent of the control coral coverage values would be equivalent to a 90 percent reduction in the thermally-affected transects. The core coral-kill zone at each thermally-affected transect was then calculated as the interval in meters between the inner reef margin zone (0-meters on Figures 5-9) and the station where the coral surface coverage value first reaches 10 percent of the surface coverage value of the control transect. By using the replicate combined coral coverage values from Table 1, the core coral-kill intervals were interpolated graphically on the coral coverage plots in Figures 5-9 (Transects A-E). The peripheral coral-kill zone at each thermally-affected transect was calculated as the interval in meters between the seaward edge of the core coral-kill zone and where the coral surface coverage value intercepts, or equals, that of the control transect. At this intercept, or equality, point it is assumed that there is no longer any thermal impact sufficient enough to affect coral surface coverage values. By using the replicate combined coral coverage values from Table 1, the peripheral coral-kill intervals were interpolated graphically on the coral coverage plots in Figures 5-9 (Transects A-E). The core and peripheral coral-kill intervals determined from this present study are compared to the 1974 intervals in Table 4.

When core and peripheral coral-kill areas are circumscribed by lines the overall shape of both are somewhat triangular as shown in Figure 3. The thermally-affected areas are widest opposite from the outfall at Transect A, where warm effluent water first impinges upon the coral communities in the reef margin and upper reef front slope zones, and then attenuates southward to about 50 meters past Transect E where no further thermal effects could be detected. The slight contraction of the peripheral coral-kill area at Transect C, during both the present and 1974 studies, is caused by the steepening of the reef front slope along this section of the fringing reef which effectively narrows the zone of the stratified warm water impingement upon the reef surface.

Areas of the core and peripheral coral-kill zones were estimated by using a gridded overlay (1 square per m^2) over a two-dimensional scaled drawing of the thermally-affected reef surface, similar to the method used in the 1974 study. Using the gridded-square method the present area of the overall combined core and peripheral coral-kill zones is $16,400 m^2$, with a central core coral-kill area of $7,300 m^2$ (Table 4). Maximum dimensions of the present overall thermally-affected area is about 45×500 meters with central core of about 40×200 meters. By comparing the present thermally-affected coral-kill areas with those of 1974 (combined core-peripheral coral-kill area of $20,000 m^2$ and a central core coral-kill area of $10,300 m^2$), it appears that there has been reduction in area of the combined core-peripheral coral-kill zone by $3,600 m^2$, and a corresponding reduction in area of the central core area by $3,000 m^2$ (Table 4). This reduction in area of the thermally-affected coral-kill zones is somewhat surprising, because it appeared that during the earlier study period (1971-1974) there was a slow enlargement of the affected region. Nuedecker (1976), though, concluded from a somewhat later study of the effect of thermal effluent on coral reef communities at Tanguisson Point, that the area of the coral-kill zone was not significantly enlarging.

When the power plants first became operational, elevation in ambient sea water temperature was sudden, of considerable magnitude, and permanent where the effluent made contact with shallow-water coral communities living adjacent to the outfall. Such a sudden environmental change provided little opportunity for acclimatization and adjustment for corals, which already live fairly close to their upper thermal tolerance level in normal ambient sea water. Early changes in coral communities within thermally-affected areas at Tanuission are well documented by Jones et al., 1976, and Nuedecker, 1976 and 1977. Long-term changes, such as the 18 percent reduction in area of the thermally-affected coral-kill zone over a period of 15 years reported in this study, have been much less documented. Some factors that might be considered in this particular change in the thermally-affected reef area include: 1) changes in the community structure of corals may occur quite slowly and produce observable differences only through the passage of many years, 2) the coral community may have some kind of resilient rebound effect that only becomes noticeable or operational 3 to 5 years after the initial habitat change, 3) possibly there has been a gradual turnover in coral species composition from a community that was not very tolerant to a community composed of more tolerant species, 4) refugia corals, that include cryptic parts of colonies that survived in holes and crevices, slowly became acclimated to elevated temperatures, and thus grew larger and increased coral coverage without a significant increase in recruitment, and 5) possibly larger established corals are not very tolerant to sudden temperature increases, but a newly

settled planula in such a habitat may develop such a tolerance and recolonize parts of the thermally-affected area.

Assessment of Bioerosion

The following is a summary of a preliminary study of bioerosion at the Tanguisson Point effluent area compared to a control site. Samples of reef rock were first prepared by slabbing with a diamond blade rock saw. Surface area of the slabs was analyzed for percentage of bioerosion using a point count grid. The grid was made of clear plastic and contained 500 points, X Y coordinates generated from a random number tables (Sokal and Rohlf, 1987). The grid was superimposed over a television monitor attached to an image analyzer. The sample was then projected onto the screen. The image analyzer was used to measure surface area (mm²) of the samples. Camera focal length was adjusted to bring surface areas of all samples to within 95% of the surface area of a standard (the largest sample). This allowed approximately the same number of points (175-200) to fall on each sample for point counting.

A statistical analysis was done on 13 Transect A samples (effluent effect) and compared to 13 samples from a control area just north of Tanguisson (Fig. 3). Sample statistics for each group and a t-test were generated using SYSTAT software. These statistics, as well as an analysis of variance (ANOVA) were also calculated by hand. Table 5 lists data used. Table 6 summarizes the statistics performed.

Table 5. Data for preliminary bioerosion study. In the Treatment column a = Transect A and c = control transect.

Sample No.	Erosion	Treatment
RHR 1257-15A	.1429	a
1249B-11A	.0106	c
1249-1A	.0523	c
1247-9A+B	.0734	a
1247-14A	.1251	a
1247-16A	.1271	a
1247-13A	.1381	a
1246-1A	.0230	c
1247-11A	.1667	a
1247-2A	.1518	a
1248-10	.0894	a
1246-2A	.1453	c
1247-5A	.0703	a

1258-1A	.0765	a
1246-12A	.0169	c
1246-9A	.0203	c
1246-9A	.0549	a
1249-5A	.0162	c
1246-11A	.0113	c
1247-4A	.0947	a
1246-5A	.0447	c
1249-3A	.0109	c
1246-6A	.1000	c
1246-8A	.0000	c
1248-1A	.0225	a
1246-3A	.0209	c

Table 6. Statistical summary.

Results for Control (c)
Total observations: 13

Results for Affected (a)
Total observations: 13

	Erosion		Erosion
minimum	0.000	minimum	0.023
maximum	0.145	maximum	0.167
mean	0.036	mean	0.103
standard dev.	0.042	standard dev.	0.043

T-statistic = 3.991

Probability = .001

Bartlett test for homogeneity of group variances:

Chi-square = .007

DF = 1

Probability = .932

ANOVA TABLE

Source of Variation	Degree of Freedom	SS	MS	F
Among groups	1	.0286	.0286	15.930
Within groups	24	.0018		
TOTAL	25	.0716		

Probability of equal variances < .01

The t-test and ANOVA indicate that these groups are significantly different at $\alpha = .01$. Sample statistics indicate that the mean for the control group is $3.6 \pm 4.2\%$ bioerosion, while that for the affected area is $10.3 \pm 4.3\%$. Values of means overlap because of the standard deviations, but I believe that

this is an artifact due to sample size. An increase in the number of samples used for this analysis is planned.

A complete survey of bioeroder types and relative abundances has not been completed, but the affected samples have been extensively bored by polychaetes and sipunculids. Abundances of these groups appear to be higher than those in the control samples. A more thorough study of macro-bioeroders, as well as a study of micro-bioeroders is given in Appendix A.

Literature Cited

- Cottam, G., J.T. Curtis, and B.W. Hale. 1953. Some sampling characteristics of a population of randomly dispersed individuals. *Ecology* 34:731-757.
- Jones, R.S., R.H. Randall, and M.J. Wilder. 1976. Biological impact caused by changes on a tropical reef. U.S. Environmental Protection Agency, Ecological Progress Series. EPA-60013-76-027, 209 p.
- Nuedecker, S. 1976. Effects of thermal effluent on the coral reef community at Tanguisson. Univ. Guam Mar. Lab. Tech. Rept. 30, 55 p.
- Nuedecker, S. 1977. Development and environmental quality of coral reef communities near the Tanguisson Power Plant. Univ. Guam Mar. Lab. Tech. Rept. 41, 68 p.
- Sokal, R.R. and J.F. Rohlf. 1987. Introduction to biostatistics. W.H. Freeman and Company, New York Pub. pp. 93-181.

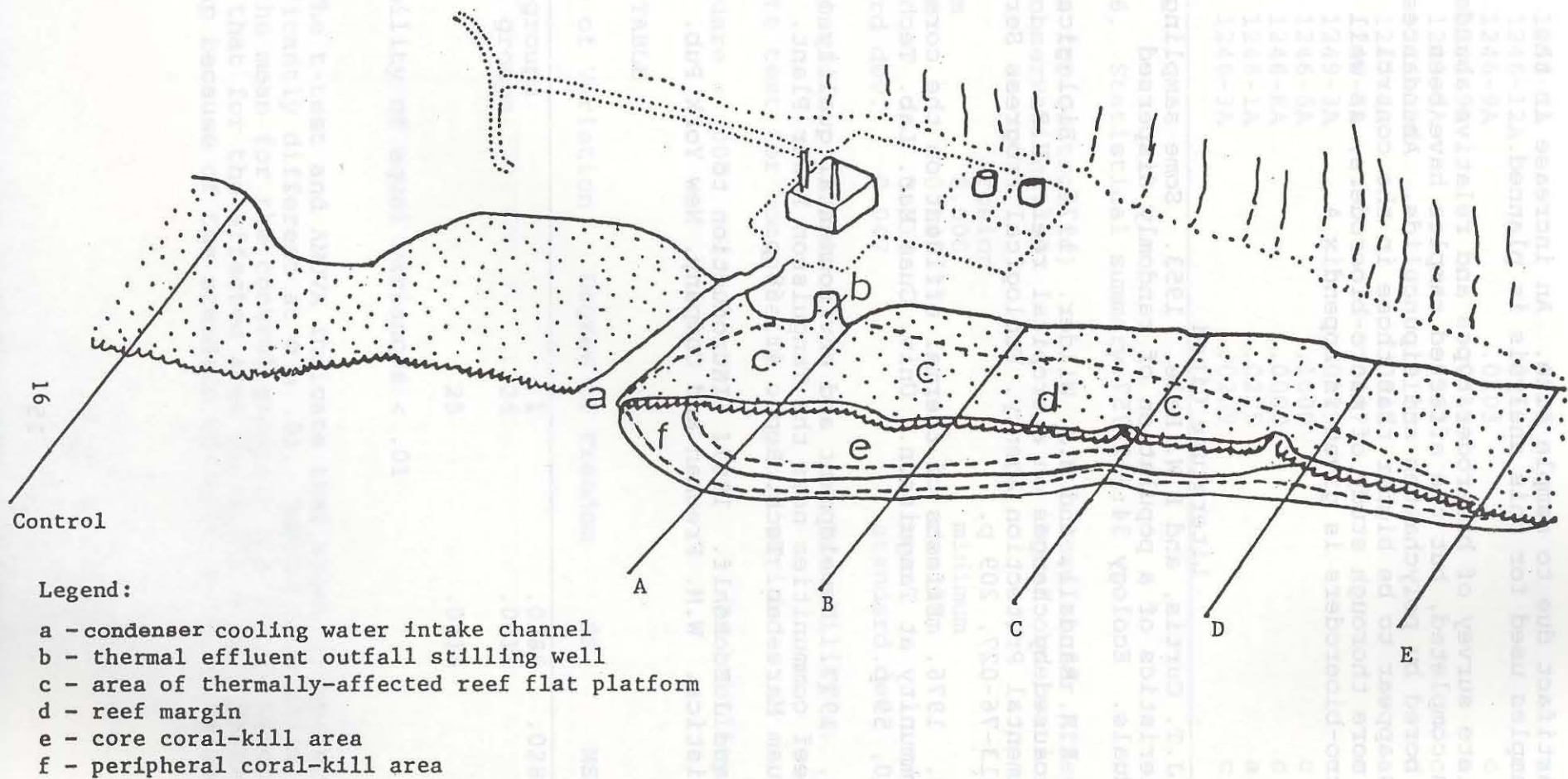


Figure 3. Tanguisson power plant and adjacent fringing reef areas showing transect locations (A-E and a control) and the approximate boundaries (not to scale) of the 1974 (solid lines) and 1990 (dashed lines) thermally-affected core and peripheral coral-kill zones seaward of the reef flat platform. Stippling indicates reef flat platform areas and Transects A-E approximately 100 meters apart.

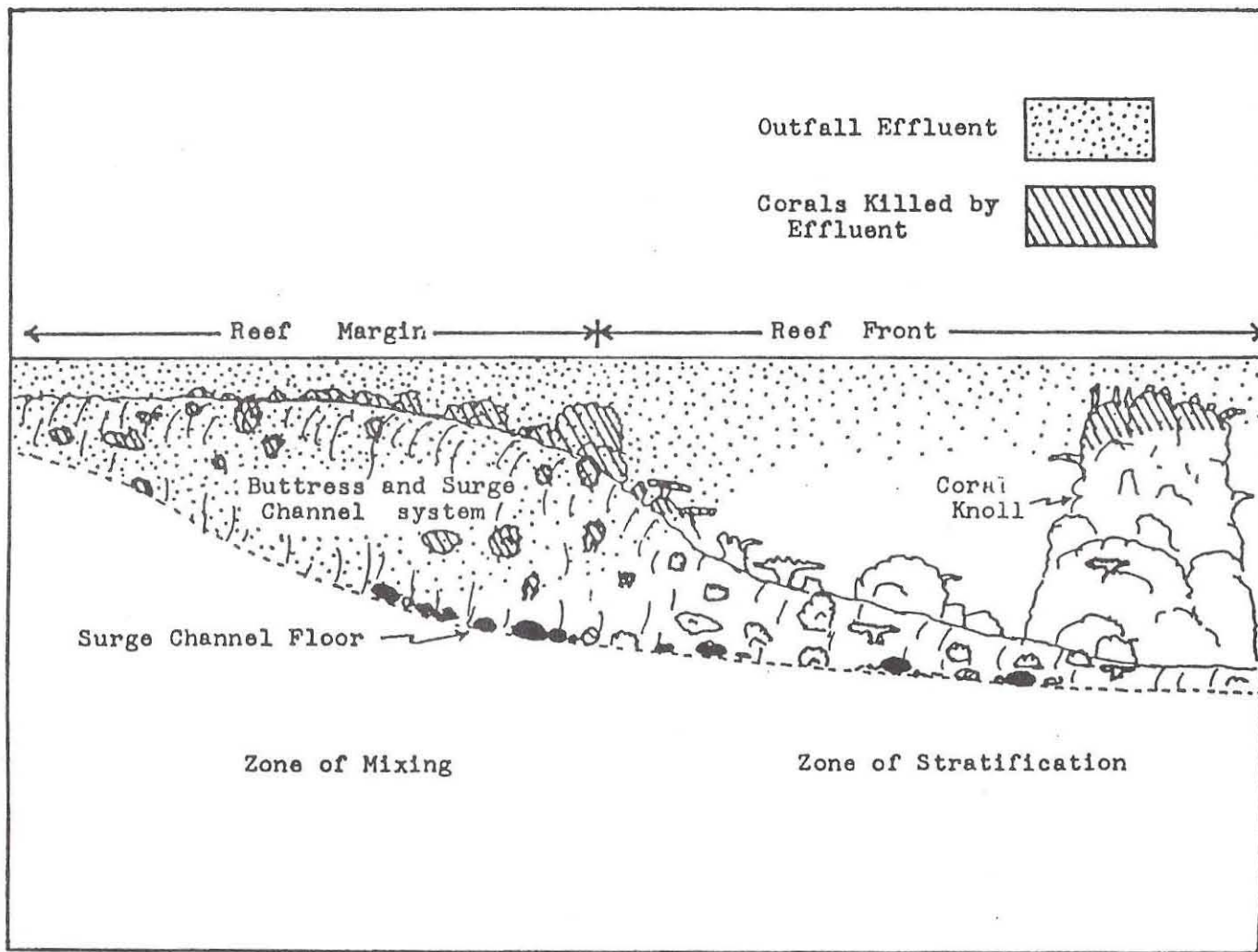
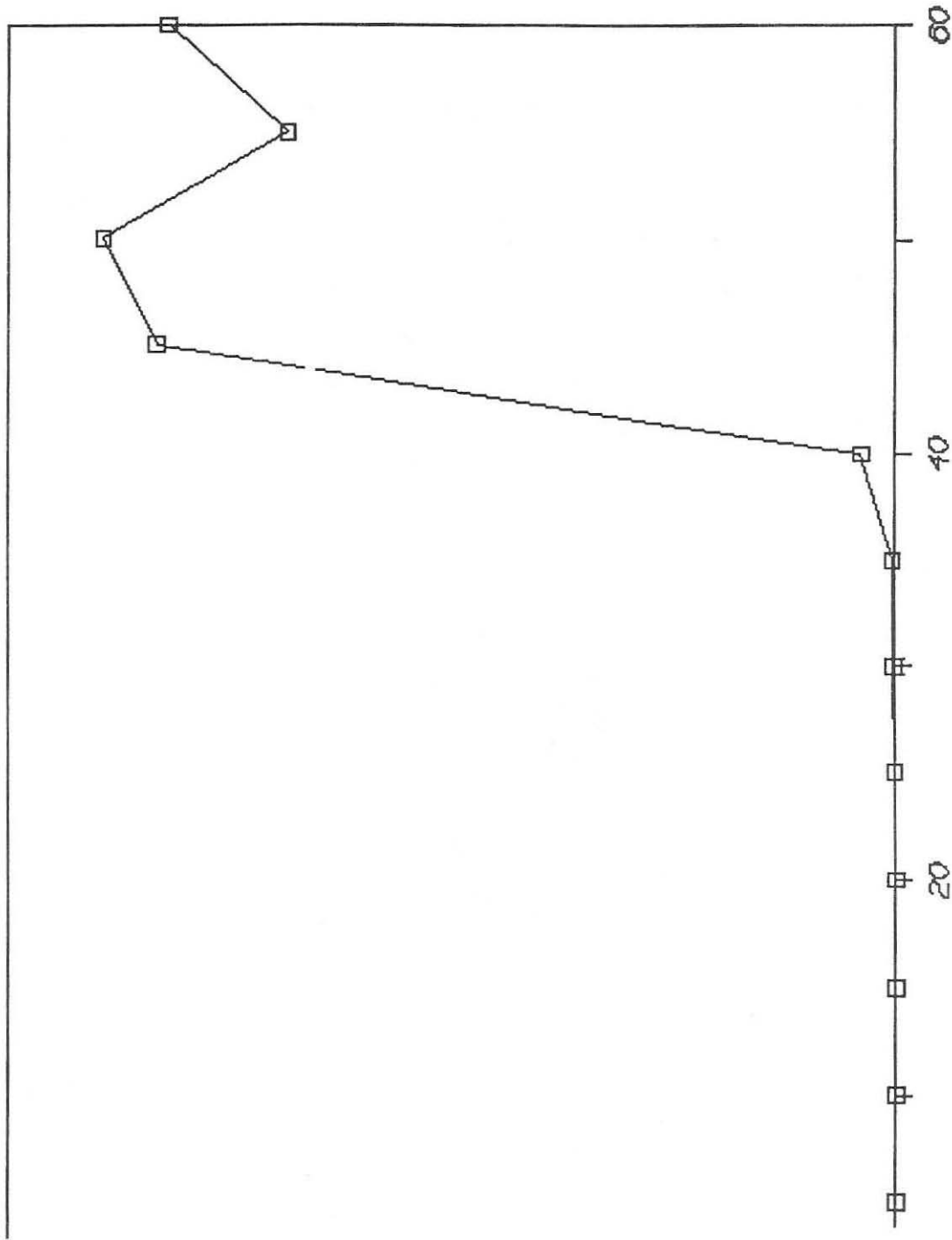


Figure 4. Vertical profile through the reef margin and reef front slope zones in the vicinity of Transect A showing how the thermal plume impinges upon the reef surface. Figure from Jones et al. (1976).

Thermal Effluent Study

Transect A



Thermal Effluent Study

transect B

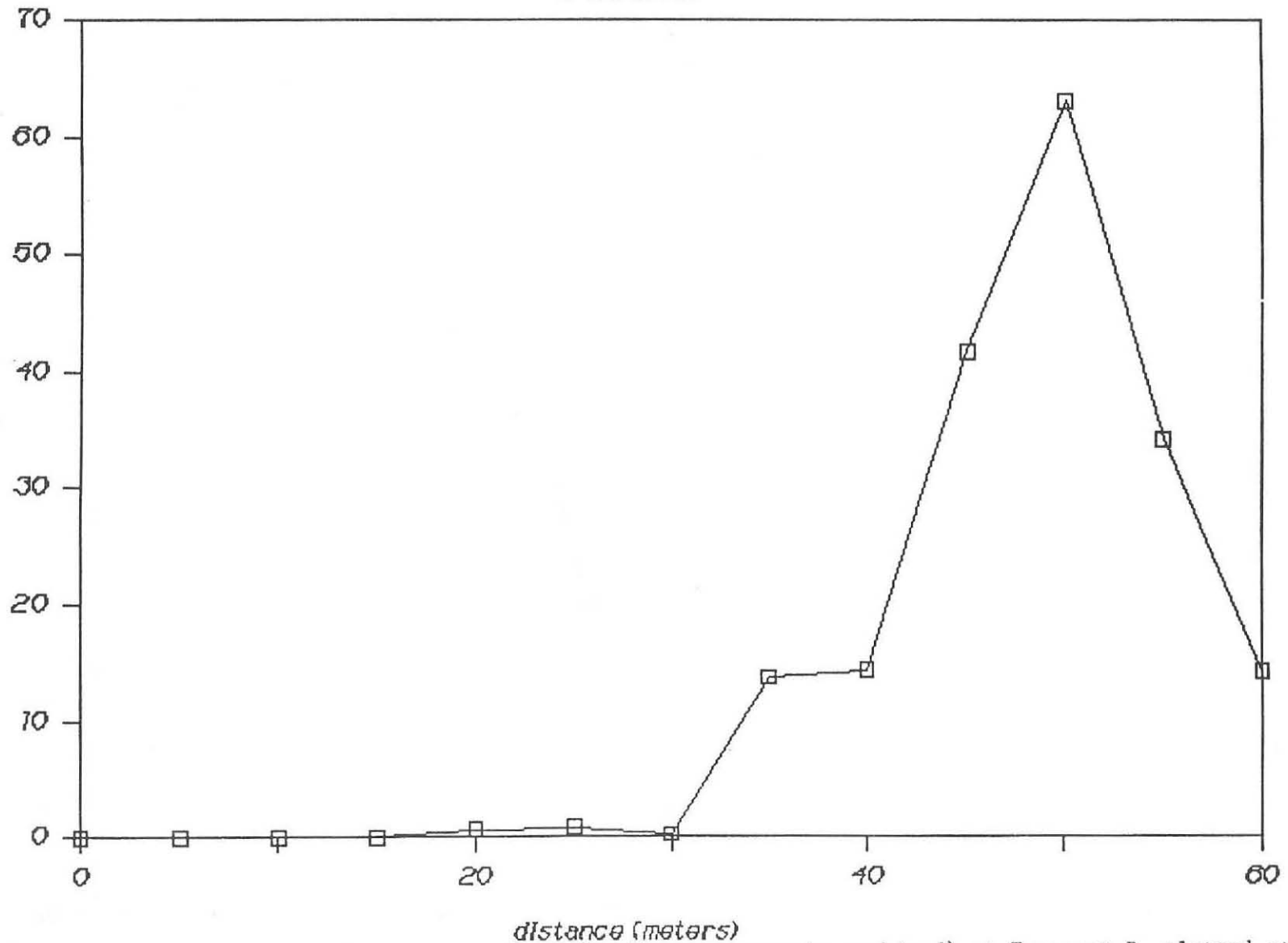
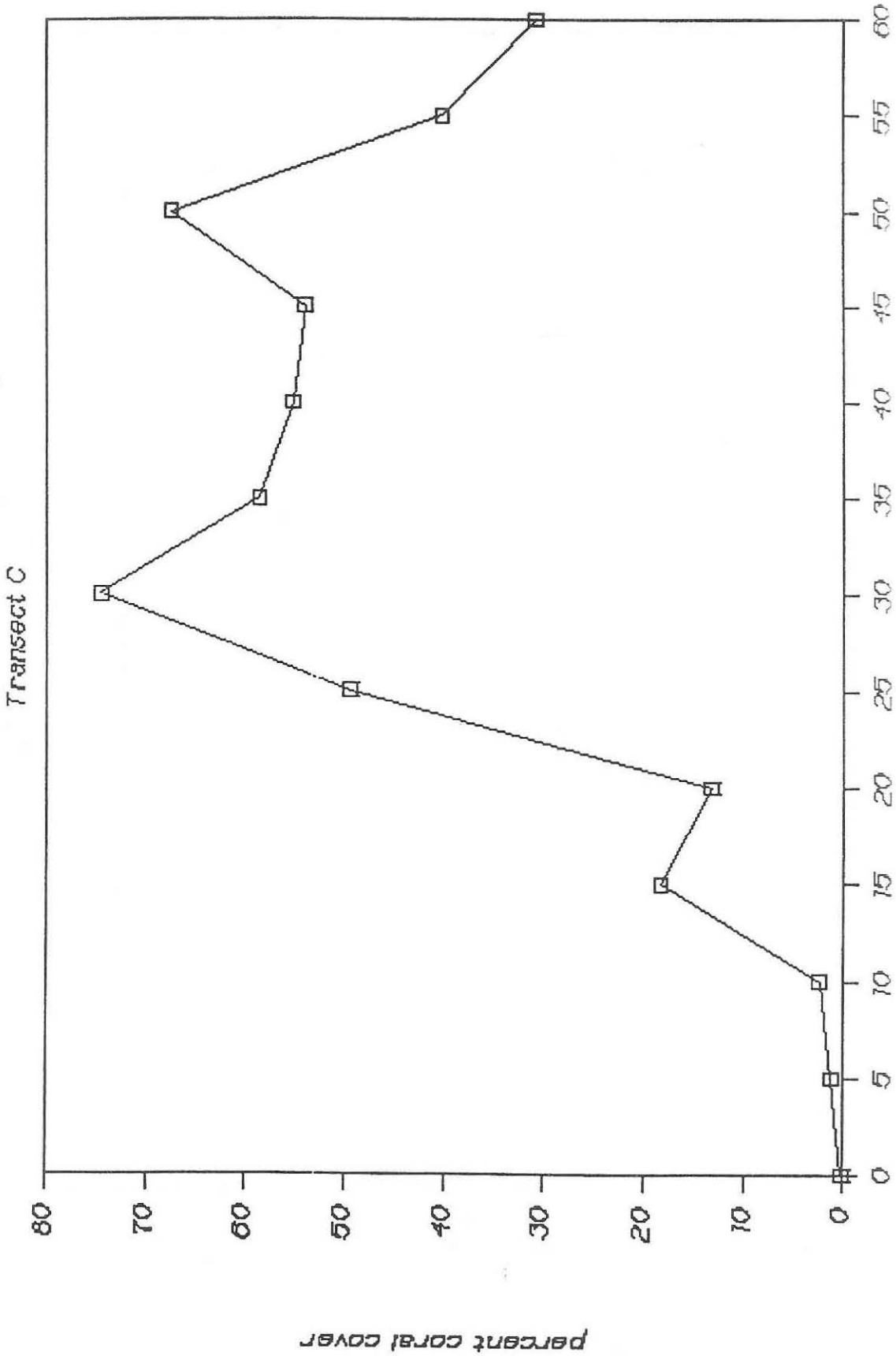


Figure 6. Percent of coral coverage values (replicate transects combined) at Transect B, plotted at 5-meter station intervals in a seaward direction from the innermost part of the reef margin (0 meters) to about 3 to 6 meters depth on the upper reef front slope (60 meters).

Thermal Effluent Study



Thermal Effluent Study

Transect D

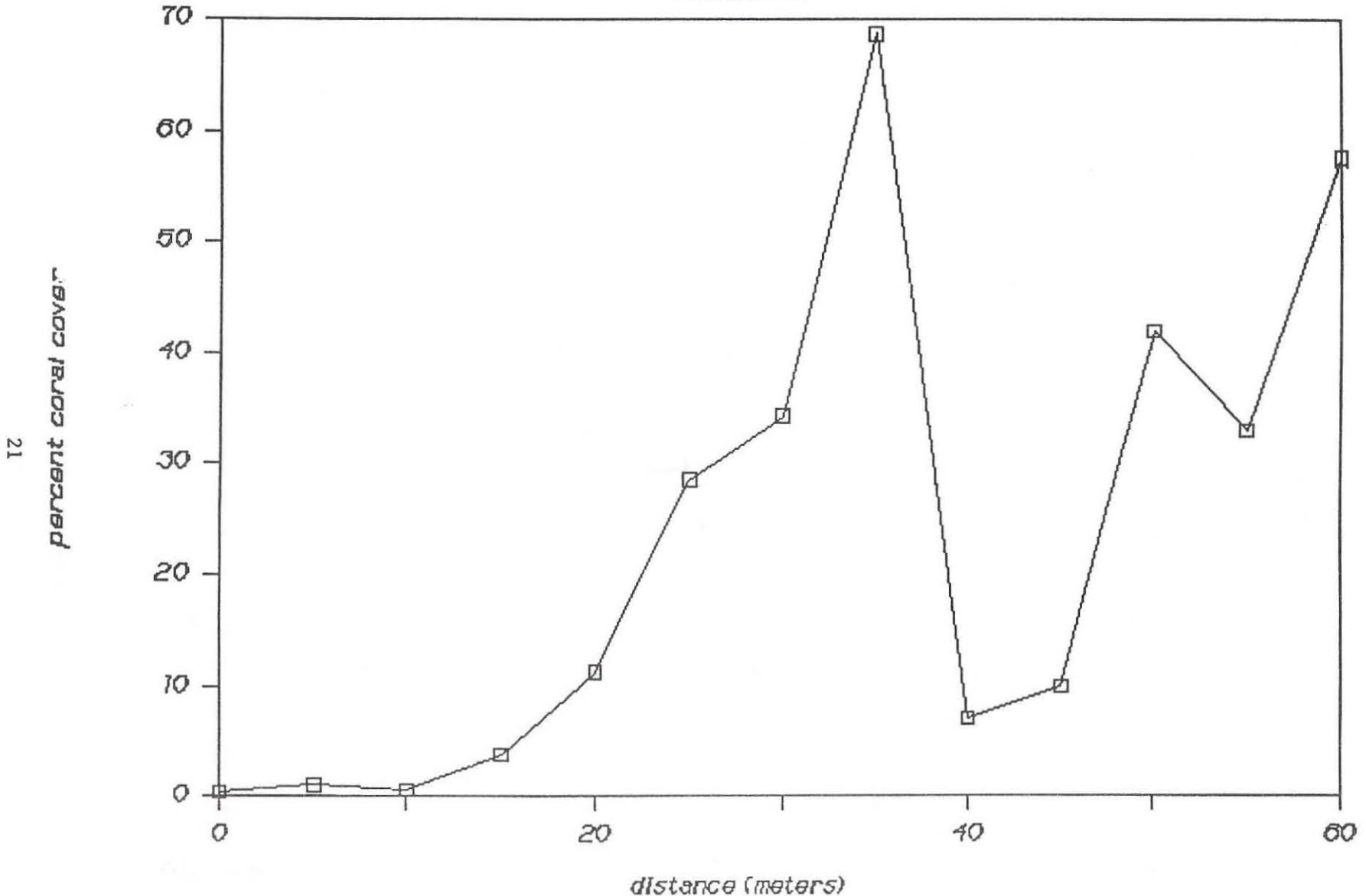
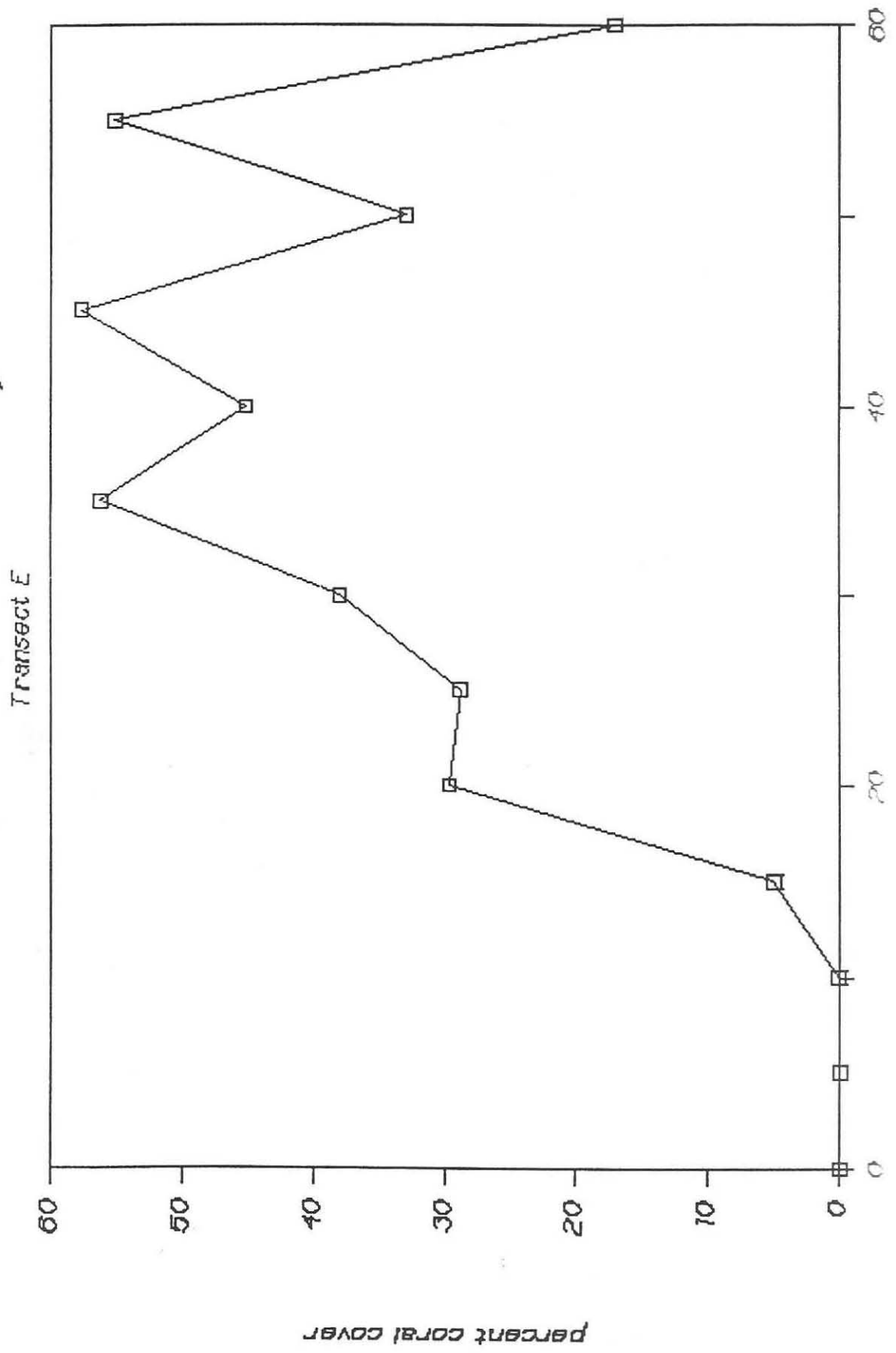


Figure 8. Percent of coral coverage values (replicate transects combined) at Transect D, plotted at 5-meter station intervals in a seaward direction from the innermost part of the reef margin (0 meters) to about 3 to 6 meters depth on the upper reef front slope (60 meters).

Thermal Effluent Study



Thermal Effluent Study

Control transect

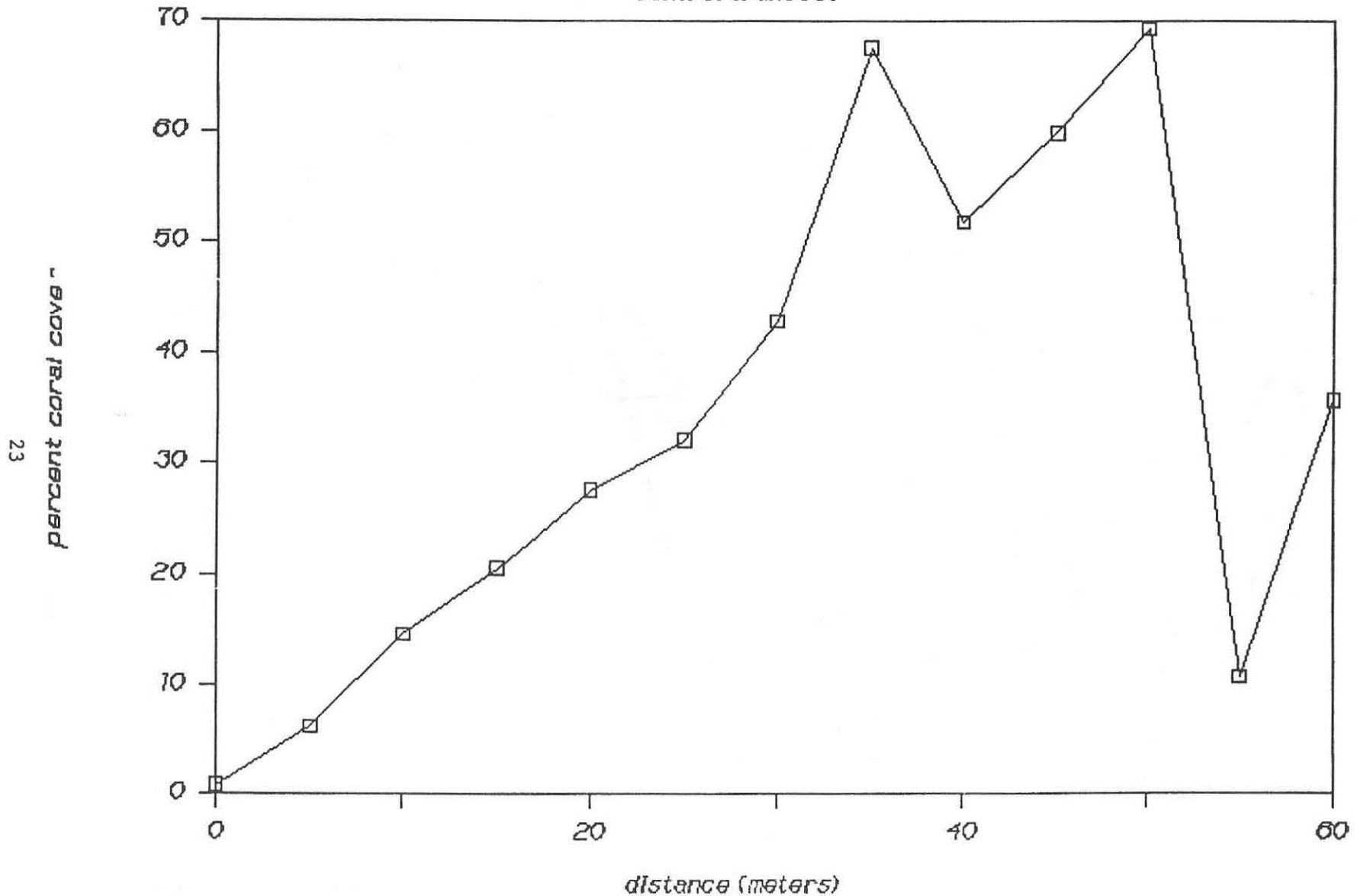


Figure 10. Percent of coral coverage values (replicate transects combined) at Control Transect, plotted at 5-meter station intervals in a seaward direction from the innermost part of the reef margin (0 meters) to about 3 to 6 meters depth on the upper reef front slope (60 meters).

Pooled transect data

all six transects

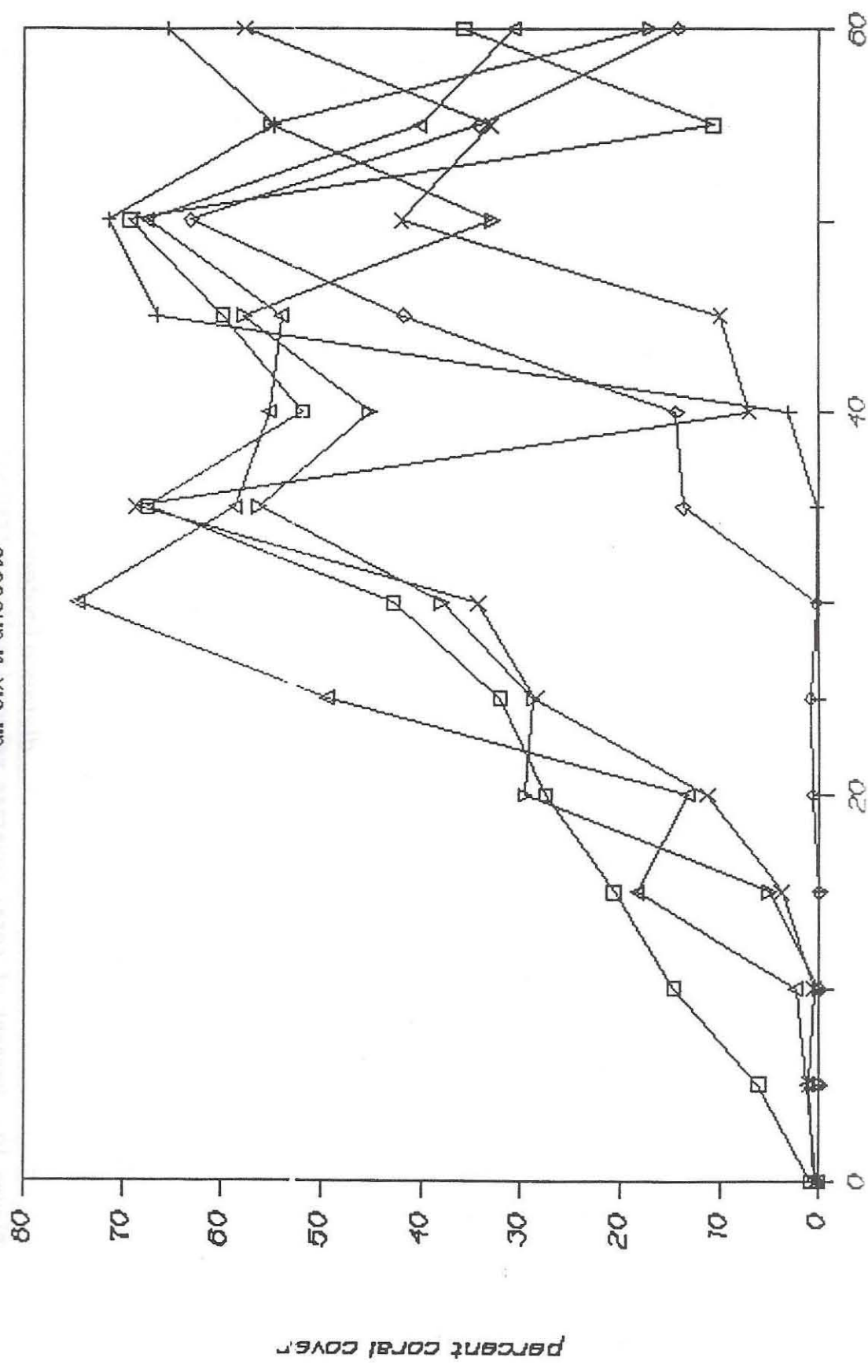


Table 1. Summary of the point-quarter coral density and coral surface coverage data from Transects A through E and a control transect.

Transect Zone on Sta. in meters from shore	Replicate (North)		Replicate (South)		Replicate Combined	
	Coral Density (m ²)	Coral Coverage (%)	Coral Density (m ²)	Coral Coverage (%)	Coral Density (m ²)	Coral Coverage (%)
Transect A						
Reef flat 0-80	no corals		no corals			
Reef margin	no corals		no corals			
85	"	"	"	"		
90	"	"	"	"		
95	"	"	"	"		
100	"	"	"	"		
105	"	"	"	"		
Reef front slope						
110	0.16	0.05	0.41	0.15	0.24	0.11
115	0.21	0.14	1.38	0.91	0.43	0.22
120	3.00	0.91	0.64	0.46	1.20	0.61
125	11.11	3.61	2.61	2.48	4.75	3.11
130	6.66	67.54	3.43	63.35	4.64	66.52
135	12.67	72.29	17.36	69.24	14.79	71.39
140	9.18	60.58	13.42	44.68	11.02	54.71
145	29.17	57.31	19.39	67.47	17.00	65.50
Transect B						
Reef flat 0-75	no corals		no corals			
Reef margin	no corals		no corals			
85	"	"	"	"		
90	"	"	"	"		
95	"	"	"	"		
100	"	"	"	"		
105	"	"	"	"		
Reef front slope						
105	0.51	0.14	0.33	1.29	0.41	0.84
110	0.40	0.55	1.91	0.80	0.76	0.71
115	9.05	14.39	8.40	13.10	8.71	13.72
120	5.11	13.71	8.40	14.88	6.45	14.37
125	7.61	42.62	6.49	40.77	7.01	41.69
130	18.90	62.06	38.87	64.64	25.96	63.07
135	26.30	33.18	10.24	37.34	15.53	34.12
140	8.91	22.87	4.08	9.41	5.81	14.14
Transect C						
Reef flat 0-80	no corals		no corals			
Reef margin						
85	0.48	0.07	0.19	0.83	0.29	0.22
90	0.43	0.44	1.79	4.84	0.77	1.24
95	4.04	1.43	13.47	4.75	6.75	2.38
100	2.78	21.92	8.16	3.27	4.43	18.36
105	5.54	7.97	10.08	22.52	7.30	13.29
110	20.66	23.11	28.44	85.00	24.08	49.48
115	26.30	78.30	7.11	65.80	12.31	74.56
120	33.61	58.82	7.82	59.38	14.24	58.61
125	16.18	27.50	16.66	84.80	16.13	55.18
130	27.70	69.47	40.06	30.44	33.03	53.97
135	5.53	63.28	39.06	68.18	11.65	67.48
140	37.87	48.02	32.65	33.21	35.12	40.14
145	45.96	45.78	25.64	21.44	33.61	30.78
Transect D						
Reef flat 0-20	no corals		no corals			
25	0.33	0.14	0.23	0.11	0.28	0.12
30	0.22	0.12	0.20	0.12	0.21	0.12
35	0.28	0.63	2.39	1.61	0.62	0.75
40	0.00	0.00	1.18	0.37	0.34	0.11
45	0.00	0.00	0.57	0.40	0.27	0.19
50	0.00	0.00	0.27	0.15	0.21	0.11

Table 1. Continued.

Transect Zone on Sta. in meters from shore	Replicate (North)		Replicate (South)		Replicate 13
	Coral Density (m ²)	Coral Coverage (%)	Coral Density (m ²)	Coral Coverage (%)	Coral Density (m ²)
55-65	no corals		no corals		
70	0.00	0.00	0.19	0.15	0.17
75	0.18	0.27	0.53	0.23	0.28
Reef margin					
80	0.47	0.41	0.37	0.35	0.24
85	0.25	0.12	1.53	3.08	0.77
90	0.87	0.56	0.92	0.62	0.90
95	1.01	4.67	2.12	1.59	1.41
100	7.32	15.03	0.85	7.60	2.33
Reef front slope					
105	5.47	24.37	3.13	30.09	4.06
110	11.00	35.59	4.25	39.74	7.56
115	11.89	69.71	29.22	67.94	17.73
120	16.00	7.82	15.68	6.29	15.84
125	9.32	12.94	15.08	7.89	11.69
130	28.44	42.43	20.20	41.21	23.79
135	27.71	34.10	18.90	31.70	22.68
140	17.00	56.44	28.44	58.20	21.63
Transect E					
Reef flat 0-90	no corals		no corals		
Reef margin					
95	0.32	0.15	0.24	0.10	0.27
100	0.00	0.00	0.00	0.00	0.00
105	0.00	0.00	0.18	0.10	0.17
110	2.95	3.49	2.46	6.72	2.69
115	3.88	77.48	10.58	9.75	6.02
Reef front slope					
120	6.17	29.41	16.66	33.41	9.54
125	13.72	39.62	17.73	34.78	15.53
130	13.14	51.26	13.46	57.30	13.02
135	11.89	46.72	15.68	44.10	13.59
140	24.60	53.89	13.47	59.96	20.43
145	24.39	40.76	17.36	23.56	20.43
150	30.86	30.74	15.08	64.59	20.90
155	12.53	10.78	14.51	24.32	13.47
Control Transect					
Reef flat 0-60	no corals		no corals		
65	0.00	0.00	0.16	0.09	0.16
70	0.00	0.00	0.17	0.02	0.17
75	0.20	0.21	0.23	0.62	0.22
80	0.57	0.14	5.22	0.90	1.29
85	0.60	0.42	0.67	1.18	0.63
90	0.66	0.17	0.28	0.35	0.44
Reef margin					
95	2.24	1.17	0.70	0.67	1.15
100	3.53	6.30	5.05	6.09	4.25
105	15.38	13.26	12.10	15.99	13.59
110	18.63	19.16	23.80	23.64	20.20
115	17.36	28.55	22.11	23.64	20.20
Reef front slope					
120	6.75	35.31	8.52	27.85	7.56
125	23.80	51.02	22.68	34.99	23.21
130	6.10	66.20	14.86	67.94	11.69
135	25.00	63.71	10.93	47.88	15.84
140	27.73	73.24	18.53	44.79	25.65
145	21.13	53.29	22.68	86.33	21.89
150	15.08	7.73	7.02	15.85	9.92
155	11.49	28.18	22.15	47.75	15.53

Table 2. Summary of coral colony size (diameter in cm) distribution for the core and periphery coral-kill areas of the thermally affected parts of the reef margin and upper reef front slope zones, and for the region that lies seaward (outside) of the thermally affected reef areas.

	Core Zone	Peripheral Zone	Unaffected Zone
Transect A			
n	18	8	32
x	6.8	8.3	24.3
s	4.8	4.0	17.6
w	1-16.9	2.4-14.7	4.5-81.7
Transect B			
n	17	16	72
x	15.9	13.4	16.5
s	12.1	8.1	12.0
w	3.0-53.9	3.0-32.0	3.0-54.1
Transect C			
n	11	16	72
x	10.7	10.7	14.8
s	10.9	13.6	12.8
w	1.0-36.5	2.8-50.9	3.0-69.0
Transect D			
n	27	24	48
x	12.6	21.7	12.6
s	7.3	15.3	8.1
w	5.5-25.5	3.0-53.2	4.5-50.0
Transect E			
n	no corals	no corals	81
x			15.0
s			11.1
w			3.5-78.9
Control Transect (no coral-kill zone, reef margin and upper reef front slope zones combined)			
n	104		
x	15.6		
s	10.1		
w	3.5-59.5		

Table 4. A comparison of core and peripheral coral-kill distance intervals at Transects A-E determined during the present and 1974 studies. Distances are in meters.

Transect	Present study		1974 study	
	Core	Core and Peripheral Combined	Core	Core and Peripheral Combined
A	40	44	40	63
B	33	45	40	57
C	0	22	20	24
D	0	35	3	36
E	0	18	0	20
Affected Area	7,300 m ²	16,400 m ²	10,300 m ²	20,000 m ²

REASSESSMENT OF THE MARINE BENTHIC ALGAE

by
Roy T. Tsuda

Methods

Field Collection

Pieces of limestone substrata, ranging in diameter from 10 to 35 cm, were collected intact or chiseled along the thermal effluent transect (Transect A) on 21 November 1989 by R.H. Randall and R.T. Tsuda, and along in the control transect (Transect B), just north of NCS Beach, on 6 November 1989 by R.H. Randall. The pieces of substrata were labeled and brought to the Laboratory where the substrata were preserved with 10% formaldehyde in separate plastic bags.

Laboratory Examination and Quantification

Prior to examination with a dissecting microscope, the larger pieces of substrata were broken into smaller pieces with a hammer and chisel. Since the majority of algae represented the smaller filamentous-like species or immature thalli of larger macroalgae, verification of species identification were done with the use of a compound microscope either at 100x or 450x.

A rather rough estimate of percent cover of the various species was mainly done with the naked eye after all species present at a station were compiled. The percent cover is basically an estimate and does provide a general idea of which algae were dominant in terms of percent cover.

Results

The following pages provide a species listing and a rough quantitative estimate of the percent cover of the dominant algae found at the respective stations along the Thermal Effluent Transect A (13 stations) and along the Control Transect (7 stations). Table 1 provides a comparison of the different algae species along the two transects. The Control Transect B had exactly double the number of species than at the Thermal Effluent Transect A - 40 algal species compared to 20 algal species, respectively.

	Thermal Outfall Transect A	Control Transect
Cyanophyta	7 spp.	3 spp.
Chlorophyta	7	13
Phaeophyta	3	5
Rhodophyta	3	19
TOTAL	20 spp.	40 spp.

Tables 2 and 3 provide a summarized account of the presence of algal species along the two transects.

Brief Discussion

Based on the assumption that both transects were inhabited by similar algae prior to the construction of the thermal outfall, it is obvious that the thermal outfall did affect the diversity of algae (especially, the greens, browns and reds). There was, however, a much more diverse blue-green algal flora along the Thermal Effluent Transect A. In fact, the three blue-greens - Microcoleus lyngbyaceus, Schizothrix tenerrima and Calothrix crustacea - were the dominant species within 40 m of the thermal outfall source. In comparison, species of red algae - Gracilaria salicornia, Gelidiella acerosa, Hypnea pannosa and Rhodomenia divaricata - were dominant, with Cladophoropsis sundanensis and Ralfsia pangoensis, within 50 m from shore along the Control Transect.

Schizothrix tenerrima is of particular interest because of its abundance in the thermal channel. This species is rare around Guam and could easily be mistaken for Schizothrix mexicana. The conspicuous characteristic of S. tenerrima is that the terminal cell is attenuated (pointed), after growth or cell division ceases. Trichomes of S. tenerrima possess rounded terminal cells while it is still growing. The only other species of Schizothrix which possess terminal cells which are attenuated, but shorter attenuation, is S. monticulosa (Bory) Drouet reported from freshwater hot springs only.

Whether the thermal effluent affects the algal community at the reef margin is not known. During low spring tides during period of calm seas, one would expect the subtidal algae, i.e., those inhabiting crevices to be most affected. The dominant algal community is different at each transect. Gelidiella tenuissima, Microcoleus lyngbyaceus and Cladophoropsis sundanensis were the dominant component on the subtidal reef margin along the Thermal Effluent Transect A. Rhodomenia divaricata, Jania capillacea, Amphiroa fragilissima and Dictyota bartayresii were the dominant algal flora on the subtidal reef margin along the Control Transect.

The dominant algal flora also differed on the intertidal reef margin, where one would not expect any effect of thermal waters during low spring tides. Gelidiella tenuissima, Cladophora albida and Boodlea composita were the dominant algae the Thermal Effluent Transect A, while Porolithon spp. Hypnea pannosa, Rhodomenia divericata and Polysiphonia tenuis were dominant along the Control Transect.

Cyanophyta	7 spp.	3 spp.
Chlorophyta	7 spp.	13
Phaeophyta	3	5
Rhodophyta	3	19
TOTAL	20 spp.	40 spp.

THERMAL EFFLUENT TRANSECT A

November 21, 1989

Station 1 - Intertidal knob, reef margin (80-90 m from concrete outfall source).

Gelidiella tenuissima (ca. 40% cover)

Cladophora albida (ca. 40% cover)

Fine filaments about 10 mm long and less than 32 μ in diameter.

Boodlea composita (ca. 20% cover)

Remaining algae comprise less than 1% cover.

Microcoleus lyngbyaceus

Schizothrix calcicola

Acetabularia moebii

Padina sp. (only vaughaniella form)

Sphacelaria sp. (no attached propagulum)

Rhodymenia divaricata

Station 2 - Subtidal beachrock, reef margin (80-90 m from concrete outfall source).

Gelidiella tenuissima (ca. 55% cover)

Microcoleus lyngbyaceus (ca. 30% cover) epiphytic on Gelidiella tenuissima.

Cladophoropsis sundanensis (ca. 10% cover)

Porolithon spp. (ca. 5% cover) deep red in color

Remaining algae comprise less than 1% cover.

Schizothrix mexicana (dark green filaments interspersed among other algae)

Schizothrix calcicola

Calothrix crustacea

Acetabularia moebii

Boodlea composita

Cladophora albida

Enteromorpha clathrata

Feldmannia cf. indica

Sphacelaria sp. (no attached propagulum)

Station 3.- Subtidal shelf where reef margin grades into reef flat (75-80 m concrete outfall source).

A. Upper side of shelf

Gelidiella tenuissima (ca. 60% cover)

Microcoleus lyngbyaceus (ca. 30% cover)

Boodlea composita (ca. 10% cover)

Remaining algae comprise less than 1% cover.

Cladophora albida

Cladophoropsis sundanensis

Enteromorpha clathrata

Padina sp. (vaughaniella form)

Porolithon spp. (purple in color)

Station 3. Continued.

B. Lower side of shelf

Porolithon spp. (ca. 50% cover) reddish-purple in color
Boodlea composita (ca. 50% cover)

Remaining algae comprise less than 1% cover.

Microcoleus lyngbyaceus
Schizothrix mexicana (dark green filaments)
Acetabularia moebii (1 specimen)
Boergesenia forbesii
Enteromorpha clathrata
Gelidiella tenuissima

Station 4 - Chiseled reef ledge, intertidal reef flat, between Mariana limestone shelf and inner part of the reef margin (55-65 m from concrete outfall source). SAME AS Station 5.

A. Upper side of ledge

Combination of the following species causes the substratum to be green in color. (ca. 90% cover).

Ostreobium reineckeii
Calothrix crustacea
Schizothrix calcicola

Gelidiella tenuissima (ca. 10% cover) in grooves/holes

Remaining algae comprise less than 1% cover.

Anacystis dimidiata
Cladophora albida (6 u wide, cells 2x long as wide)
Cladophoropsis sundanensis
Enteromorpha clathrata

B. Lower side of ledge.

Porolithon spp. (ca. 50% cover) deep purple in color
Mussels (ca. 50% cover)

Station 5 - Chiseled reef rock, intertidal reef flat, between Mariana limestone shelf and inner part of the reef margin (60-70 m from concrete outfall source). SAME AS Station 4.

A. Upper side of reef rock.

Bare limestone (ca. 50% cover)
Gelidiella tenuissima (ca. 20% cover)
Microcoleus lyngbyaceus (ca. 20% cover) 25 u wide
Calothrix crustacea (ca. 10% cover)

Remaining algae comprise less than 1% cover.

Anacystis dimidiata (14 u diameter)
Schizothrix tenerrima
Boodlea composita (immature)
Enteromorpha clathrata (1 mm long)

Station 5. Continued.

B. Lower side of reef rock

Porolithon spp. (deep purple crust covering about 40% of lower ledge).

Station 6.- Chiseled intertidal Mariana limestone shelf, 3 m from seaward margin of reef flat platform (35-40 m from concrete outfall source).

Limestone with no algae (ca. 80% cover; however, 40% of limestone appeared green in color but no algae could be recognized during observations through microscope)

Calothrix crustacea (ca. 10% cover) 9.2 u in diameter

Forming hard black crust, Ralfsia-like, in patches.

Schizothrix tenerrima (ca. 10% cover).

Forming dark greenish black spongy clumps. Filaments, with few tapered terminal cell; majority with rounded terminal cell. Except for the tapered terminal cell of a few filaments, the alga appeared much like Schizothrix mexicana.

Remaining algae comprise less than 1% cover.

Schizothrix calcicola

Cladophora albida (1 cm high, 41 u diameter, .8 to .9x as long as wide)

Gelidiella tenuissima (2 mm high, 81 u diameter)

Station 7 - Intact loose boulders, mid part of outfall discharge channel (15-25 m from concrete outfall source).

Microcoleus lyngbyaceus (ca. 50% cover)

Reddish-brown turfs, up to 4 mm high, 10.6 u diameter, with conspicuous hormogone packets. Filaments on side of channel up to 16 mm long where force of water is less.

Schizothrix tenerrima (ca. 50% cover)

Greenish brown to black loose or compact slimy mats, 4.6 u diameter filaments, length of cells 1-1.5 times diameter; cross walls usually not visible under high power (450X); few filaments with tapered terminal cell.

Remaining algae comprise less than 1% cover.

Calothrix crustacea (9.2 u wide, with basal heterocyst only)

Schizothrix calcicola (1 u diameter)

Spirulina subsalsa (only one trichome seen)

CONTROL TRANSECT
November 6, 1989

Station 1 - Piece of chiseled intertidal knob, inner reef margin (95-100 m from shore).

Porolithon spp. (ca. 40% cover)
Hypnea pannosa (ca. 35% cover)
Rhodymenia divaricata Dawson (ca. 25% cover)
Remaining algae comprise less than 1% cover.
Microcoleus lyngbyaceus
Bryopsis pennata
Feldmannia indica (with plurilocular reproductive organs)
Dictyota bartayresii (prostrate thalli)
Lobophora variegata
Jania capillacea
Polysiphonia tenuis

Station 2 - Intact beachrock, intertidal knob, but 25 cm lower than Station 1, reef margin (110-115 m from shore).

A. Upper side of beachrock

Polysiphonia tenuis (ca. 60% cover)
Thallus appearing as fine red turf, 3 mm high and ca. 40 μ in diameter; tetrasporic.
Rhodymenia divaricata (ca. 40% cover)
Thalli immature, mostly comprised of unbranched blades ca. 4 mm high.

Remaining algae comprise less than 1% cover.

Microcoleus lyngbyaceus
Schizothrix calcicola
Feldmannia indica
Jania capillacea
Gelidiella acerosa

B. Lower Edge and bottom of beachrock

Porolithon spp. (ca. 50% cover) primarily in center
Hypnea pannosa (ca. 45% cover) primarily on edge
Rhodymenia divaricata (ca. 5% cover)
Boodlea composita (less than 1% cover)

Microcoleus lyngbyaceus (ca. 25% cover)
Calothrix crustacea (ca. 10% cover)

Remaining algae comprise less than 1% cover.

Anacystria dimidiata
Schizothrix calcicola
Boodlea composita
Enteromorpha linza

Station 3 - Intact beachrock, subtidal, inner reef margin (95-100 m from shore).

A. Upper side of beachrock

Rhodymenia divaricata (ca. 45% cover)

Jania capillacea (ca. 35% cover)

Dictyota bartayresii (ca. 10% cover)

Remaining algal assemblage (ca. 10% cover)

Microcoleus lyngbyaceus

Boodlea composita

Single immature filament.

Bryopsis pennata

Caulerpa racemosa (one thallus)

Chlorodesmis fastigiata

Halimeda opuntia (one thallus)

Sargassum cristaefolium

Amphiroa fragilissima

Centroceras clavulatum

Ceramium mazatlanense (ca. 40 u diameter)

Gelidium pusillum

Hypnea pannosa

B. Lower Edge and bottom of beachrock

Dictyota bartayresii (primarily on edge)

Porolithon spp. (primarily in center)

Station 4 - Chiseled beachrock, subtidal, inner reef margin (100-105 m from shore).

Amphiroa fragilissima (ca. 60% cover) fertile

Rhodymenia divaricata (ca. 30% cover)

Four species comprising ca. 10% cover.

Microcoleus lyngbyaceus

Chlorodesmis fastigiata

Halimeda opuntia

Dictyota bartayresii

Remaining species comprising less than 1% cover

Avrainvillea lacerata

Boodlea composita

Caulerpa antoensis

Caulerpa racemosa (peltata form)

Champia parvula

Cheilosporum multifidum (4 mm high)

Ceramium mazatlanense (ca. 120 u
in diameter)

Galaxaura marginata

Gelidiella tenuissima

Hypnea pannosa

Jania capillacea

Peyssonelia rubra

Polysiphonia tenuis (on rock, dark
red carpet, 2 mm high, 46 u
in diameter)

Station 5 - Chiseled beachrock, intertidal reef flat platform (55-60 m from shore).

Gelidiella acerosa (ca. 95% cover) up to 3.7 cm high

Two species comprising ca. 5% cover.

Hypnea pannosa

Centroceras clavulatum (as turfs or epiphytic on Gelidiella acerosa)

Remaining two species comprising less than 1% cover.

Rhodomenia divaricata

Porolithon spp. (on bivalve)

Station 6 - Chiseled beach rock, subtidal depression, reef flat platform (55-60 m from shore).

Gelidium pusillum (ca. 40% cover)

Gelidiella acerosa (ca. 30% cover)

Jania capillacea (ca. 30% cover)

Remaining algae comprising less than 1% cover.

Boodlea composita (immature)

Dictyosphaeria versluysii

Dictyota cf. bartayresii (3 mm high, prostrate)

Sargassum cristaefolium (immature)

Ceramium mazatlanense

Porolithon spp.

Station 7.- Chiseled beach rock, intertidal, on side of block, reef flat platform (75-80 m from shore)

Jania capillacea (ca. 50% cover)

Centroceras clavulatum (ca. 45% cover) tetrasporic

Hypnea pannosa (ca. 5% cover)

Remaining algae comprising less than 1% cover.

Microcoleus lyngbyaceus

Boodlea composita (immature, 6 mm high)

Enteromorpha clathrata (ca. 4 mm high)

Gelidiella acerosa

Polysiphonia tenuis (unbranched thallus 2 mm high)

Rhodomenia divaricata (immature single blade, 8 mm high)

Station 8 - Chiseled beachrock, intertidal on platform pinnacle, outer intertidal/supratidal zone (40-45 m from shore).

Calcified worm tube (ca. 80% cover)

Bare beachrock (ca. 15% cover)

Porolithon spp. (ca. 5% cover)

Fleshy algae present on side of beachrock.

Boodlea composita (ca. 3 mm high)

Dictyosphaeria versluysii (in minute crevise)

Centroceras clavulatum (tetrasporic)

Gelidiella acerosa (immature)

NOTE: No Jania capillacea.

Station 9 - Low tide reef flat pool between supratidal and beach (15-20 m from shore).

A. Loose macroalgae

Gracilaria salicornia (ca. 75% cover) 18 by 9 cm in diameter clump

Cladophoropsis sundanensis (ca. 25% cover) epiphytic on Gracilaria salicornia.

B. Intact beachrock (ca. 13 x 11 cm) Bottom with no algae

Cladophoropsis sundanensis (ca. 45% cover)

Gelidiella tenuissima (ca. 40% cover) prostrate, 3 mm high, 120 u diameter.

Gelidiella acerosa (ca. 10% cover) 10 mm high

Rhodymenia divaricata (ca. 5% cover) immature single blades, 4 mm high

C. Intact beachrock (ca. 18 x 15 cm) Bottom with no algae

Gelidiella acerosa (ca. 95% cover)

Remaining algae comprising 5% cover.

Chlorodesmis fastigiata (2 mm high)

Dictyosphaeria versluysii (8 mm across)

Lobophora variegata

Amphiroa fragilissima

Gelidiella tenuissima

Jania capillacea

Peyssonelia cf. rubra

Polysiphonia tenuis

Rhodymenia divaricata

Tolypocladia glomerulata

Station 10 - Chiseled beachrock, intertidal just seaward of supratidal limestone remnants, 45-50 m from shore.

Hypnea pannosa (ca. 45% cover) prostrate, adhering to beachrock
Rhodomenia divaricata (ca. 30% cover)
Cladophoropsis sundanensis (ca. 15% cover) fine light green mat, filaments 100-120 u in diameter, growing on beachrock or epiphytic on Rhodomenia divaricata
Gelidiella acerosa (ca. 5% cover) with stichidia, ca. 1.5 cm high
Boodlea vanbosseae (ca. 5% cover)
Clump, dark green, filaments (330-400 u in diameter) with thick walls and with distinct rhizoids adhering to coral or to other branches. Resembles a coarse Cladophoropsis or Rhizoclonium.

Remaining species comprising less than 1% cover.

Microcoleus lyngbyaceus (mixed with Centroceras clavulatum)
Dictyosphaeria versluysii (immature patches, ca. 2 mm in diameter, with Hypnea pannosa)
Amphiroa fragilissima (on beachrock with Rhodomenia divaricata and Hypnea pannosa)
Centroceras clavulatum (epiphytic on Rhodomenia divaricata or occurring in 5 mm diameter patches with Hypnea pannosa)
Champia parvula (epiphytic on Rhodomenia divaricata and on beachrock with Hypnea pannosa)
Jania capillacea (epiphytic on Rhodomenia divaricata and among Hypnea pannosa)
Porolithon spp. (pink crustose)

Station 11 - Intact beachrocks, subtidal on loose cobbles, reef flat platform (65-70 m from shore).

A. Beachrock (ca. 19 x 11 cm)

Gelidium pusillum (ca. 45% cover) 2 mm high, green in color, thallus with fine rhizoids in medullary area
Porolithon spp. (ca. 25% cover)
Gelidiella tenuissima (ca. 20% cover)
Schizothrix calcicola (ca. 5% cover)
Entophysalis deusta (ca. 5% cover)

Remaining algae comprise less than 1% cover.

Champia parvula
Hypnea pannosa (pink in color)

Bottom of beachrock consists of 30% cover of

Schizothrix calcicola

Station 11 (Continued)

B. Beachrock (ca. 16 x 12 cm)

Gelidium pusillum (ca. 45% cover)
(ca. 45% cover)

Porolithon spp. (ca. 5% cover) deep red in color

Remaining four species comprise less than 5% cover.

Entophysalis deusta

Schizothrix calcicola

Centroceras apiculatum (few thalli, 110 u in diameter, intermixed
with Gelidium pusillum and Gelidiella tenuissima)

Bottom of beachrock consists of 30% cover of

Schizothrix calcicola

Station 12 - On intact boulder, just seaward of intertidal boulder field
(40-45 m from shore).

A. Top

Ralfsia pangoensis (ca. 100% cover)

B. Bottom

Entophysalis deusta (ca. 65% cover) green in color

Porolithon spp. (ca. 35% cover) red in color

Station 13 - Selected algal samples from the reef margin (inner part).

Schizothrix calcicola

Boergesenia forbesii

Boodlea composita

Bryopsis pennata

Caulerpa racemosa

Caulerpa sertularioides

Dictyosphaeria versluysii

Halimeda opuntia

Amphiroa fragilissima

Centroceras clavulatum (epiphytic on

Bryopsis pennata, Dictyosphaeria
versluysii, Halimeda opuntia)

Galaxaura marginata

Gracilaria salicornia

Gelidiella acerosa

Hypnea pannosa

Jania capillacea

Mastophora rosea

Rhodomenia divaricata

Table 1. Checklist of marine benthic algae present along Thermal Effluent Transect A (collection made on 21 November 1989) and along Control Transect B (collection made on 6 November 1989), Tanguisson Power Plant, NCS Beach.

Species	Thermal Effluent Transect	Control Transect
Division CYANOPHYTA (blue-greens)		
<u>Anacystis dimidiata</u> (Kuetz.) Drouet & Daily	X	
<u>Calothrix crustacea</u> Schousbee & Thuret	X	
<u>Entophysalis deusta</u> (Meneg.) Drouet & Daily		X
<u>Microcoleus lyngbyaceus</u> (Kuetz.) Crouan	X	X
<u>Schizothrix calcicola</u> (Ag.) Gomont	X	X
<u>Schizothrix mexicana</u> Gomont	X	
<u>Schizothrix tenerrima</u> (Gomont) Drouet	X	
<u>Spirulina subsalsa</u> Oersted	X	
Division CHLOROPHYTA (greens)		
<u>Acetabularia moebii</u> Solms-Laubach	X	
<u>Avrainvillea lacerata</u> Harv.		X
<u>Boergesenia forbesii</u> (Harv.) Feldmann	X	X
<u>Boodlea composita</u> (Harv.) Brand	X	X
<u>Boodlea vanbosseae</u> Reinbold		X
<u>Bryopsis pennata</u> Lamx.		X
<u>Caulerpa antoensis</u> Yamada		X
<u>Caulerpa racemosa</u> (Forsk.) J. Ag.		X
<u>Caulerpa sertularioides</u> (Gmel.) Howe		X
<u>Chlorodesmis fastigiata</u> (C. Ag.) Ducker		X
<u>Cladophora albida</u> (Huds.) Kuetz.	X	
<u>Cladophoropsis sundanensis</u> Reinbold	X	X
<u>Dictyosphaeria versluysii</u> W. v. Bosse		X
<u>Enteromorpha clathrata</u> (Roth) J. Ag.	X	X
<u>Halimeda opuntia</u> (L.) Lamx.		X
<u>Ostreobium reineckeii</u> Bornet	X	

Table 1. Continued.

Species	Thermal Effluent Transect	Control Transect
Division PHAEOPHYTA (browns)		
<u>Dictyota bartayresii</u> Lamx.		X
<u>Feldmannia indica</u> (Sonder) Womersley & Bailey	X	X
<u>Lobophora variegata</u> (Lamx.) Womersley		X
<u>Padina</u> sp. (vaughaniella form only)	X	
<u>Ralfsia pangoensis</u> Setch.		X
<u>Sargassum cristaefolium</u> C. Ag.		X
<u>Sphacelaria</u> sp. (no propagulum)	X	
Division RHODOPHYTA (reds)		
<u>Amphiroa fragilissima</u> Lamx.		X
<u>Centroceras apiculatum</u> Yamada		X
<u>Centroceras clavulatum</u> (C. Ag.) Montagne		X
<u>Ceramium mazatlanense</u> Dawson		X
<u>Champia parvula</u> (Ag.) J. Ag.		X
<u>Cheilosporum multifidum</u> (Kuetz.) Manza		X
<u>Galaxaura marginata</u> Lamx.		X
<u>Gelidiella acerosa</u> (Forsk.) Feldmann & Hamel		X
<u>Gelidiella tenuissima</u> Feldmann & Hamel	X	X
<u>Gelidium pusillum</u> (Stackh.) Le Jolis		X
<u>Gracilaria salicornia</u> (C. Ag.) Dawson		X
<u>Hypnea pannosa</u> J. Ag.		X
<u>Jania capillacea</u> Harv.		X
<u>Mastophora rosea</u> (C. Ag.) Setch.		X
<u>Peyssonelia rubra</u> (Grev.) J. Ag.		X
<u>Porolithon</u> spp.	X	X
<u>Rhodymenia divaricata</u> Dawson	X	X
<u>Tolypiocladia glomerulata</u> (Ag.) Schmitz		X
<u>Polysiphonia tenuis</u> Hollenberg		X

Table 2. Species diversity at each of the 7 stations. Thermal Effluent Transect A.

Species	Stations						
	1	2	3	4	5	6	7
Cyanophyta (7 spp.)							
<u>Anacystis dimidiata</u>				X	X		
<u>Calothrix crustacea</u>		X		X	X	X	X
<u>Microcoleus lyngbyaceus</u>	X	X	X		X		X
<u>Schizothrix calcicola</u>	X	X		X		X	X
<u>Schizothrix mexicana</u>		X	X				
<u>Schizothrix tenerrima</u>					X	X	X
<u>Spirulina subsalsa</u>							X
Chlorophyta (7 spp.)							
<u>Acetabularia moebii</u>	X	X	X				
<u>Boergesenia forbesii</u>			X				
<u>Boodlea composita</u>	X	X	X		X		
<u>Cladophora albida</u>	X	X	X	X		X	
<u>Cladophoropsis sundanensis</u>		X	X	X			
<u>Enteromorpha clathrata</u>		X	X	X	X		
<u>Ostreobium reineckei</u>				X			
Phaeophyta (3 spp.)							
<u>Feldmannia indica</u>		X					
<u>Padina sp. (vaughaniella form)</u>	X		X				
<u>Sphacelaria sp.</u>	X	X					
Rhodophyta (3 spp.)							
<u>Gelidiella tenuissima</u>	X	X	X	X	X	X	
<u>Porolithon spp.</u>		X	X	X	X		
<u>Rhodymenia divaricata</u>	X						
NO. OF SPECIES	9	13	11	9	8	5	5

Table 3. Species diversity at each of the 12 stations. Station 13, which comprises of collection of selected algae, is not considered in this table. Control Transect.

Species	Stations											
	1	2	3	4	5	6	7	8	9	10	11	12
Cyanophyta (3 spp.)												
<u>Entophysalis deusta</u>											X	X
<u>Microcoleus lyngbyaceus</u>	X	X	X	X			X			X		
<u>Schizothrix calcicola</u>		X									X	
Chlorophyta (13 spp.)												
<u>Avrainvillea lacerata</u>				X								
* <u>Boergensia forbesii</u>												
<u>Boodlea composita</u>		X	X	X		X	X	X				
<u>Boodlea vanbosseae</u>										X		
<u>Bryopsis pennata</u>	X		X									
<u>Caulerpa antoensis</u>				X								
<u>Caulerpa racemosa</u>			X	X								
<u>Caulerpa sertularioides</u>												
<u>Chlorodesmis fastigiata</u>			X	X					X			
<u>Cladophoropsis sundanensis</u>									X	X		
<u>Dictyosphaeria versluysii</u>						X		X	X	X		
<u>Enteromorpha clathrata</u>							X					
<u>Halimeda opuntia</u>			X	X								
Phaeophyta (5 spp.)												
<u>Dictyota bartayresii</u>	X		X	X		X						
<u>Feldmannia indica</u>	X	X										
<u>Lobophora variegata</u>	X								X			
<u>Ralfsia pangoensis</u>												X
<u>Sargassum cristaefolium</u>			X			X						
Rhodophyta (19 spp.)												
<u>Amphiroa fragilissima</u>			X	X					X	X		
<u>Centroceras apiculatum</u>											X	
<u>Centroceras clavulatum</u>			X		X		X	X		X		
<u>Ceramium mazatlanense</u>			X	X		X						
<u>Champia parvula</u>				X						X	X	
<u>Cheilosporum multifidum</u>				X								
<u>Galaxaura marginata</u>				X								
<u>Gelidiella acerosa</u>		X			X	X	X	X	X	X		
<u>Gelidiella tenuissima</u>				X					X		X	
<u>Gelidium pusillum</u>			X			X						X
<u>Gracilaria salicornia</u>									X			
<u>Hypnea pannosa</u>	X	X	X	X	X		X			X	X	
<u>Jania capillacea</u>	X	X	X	X		X	X		X	X		
* <u>Mastophora rosea</u>												
<u>Peyssonelia rubra</u>				X					X			
<u>Polysiphonia tenuis</u>	X	X		X			X		X			
<u>Porolithon app.</u>	X	X	X		X	X		X	X	X	X	X
<u>Rhodymenia divaricata</u>	X	X	X	X	X		X		X	X		
<u>Tolypocladia glomerulata</u>									X			
NO. OF SPECIES	10	10	16	19	5	9	9	5	14	12	8	3

* Present in collections from Station 13 only.

APPENDIX

DIAGENETIC EFFECTS RELATED TO HOT WATER EFFLUENT
IN MODERN AND HOLOCENE REEF LIMESTONES ON GUAM

by
Raymond G. Bowman

Thesis submitted to the faculty of the Graduate School
of the University of Maryland in partial fulfillment
of the requirements for the degree of
Master of Science
1990

INTRODUCTION

The fringing reef just south of Tanguisson Point on Guam, Mariana Islands, is the site of an oil-fired thermoelectric plant. Tanguisson No. 1, completed in 1971, went into operation at that time. Tanguisson No. 2 was constructed adjacent to No. 1 and went into operation in 1973. Cooling water is taken in from the Philippine Sea by means of a 14-meter-wide intake channel; plant effluent is then discharged directly onto the reef flat (Figure 1). In 1972, mean temperature of intake water was 27.3°C , in contrast to a mean of 33.8°C for effluent water (Jones and Randall, 1973).

Jones and Randall (1973) noted from coral kill data that the elevated temperatures of effluent affected an approximate $10,000\text{m}^2$ area of the modern fringing reef (Figure 1). This study is part of a re-evaluation of the affected area.

Hypothesized temperature-dependent scenarios to be tested include:

1. increased bioerosion in the affected area caused by increased temperature, absence of coral cover, or a combination thereof;
2. increased rate of deposition and possible increase in magnesium content of carbonate cements; and/or
3. alteration of original biologically fractionated strontium concentration in coral skeletons.

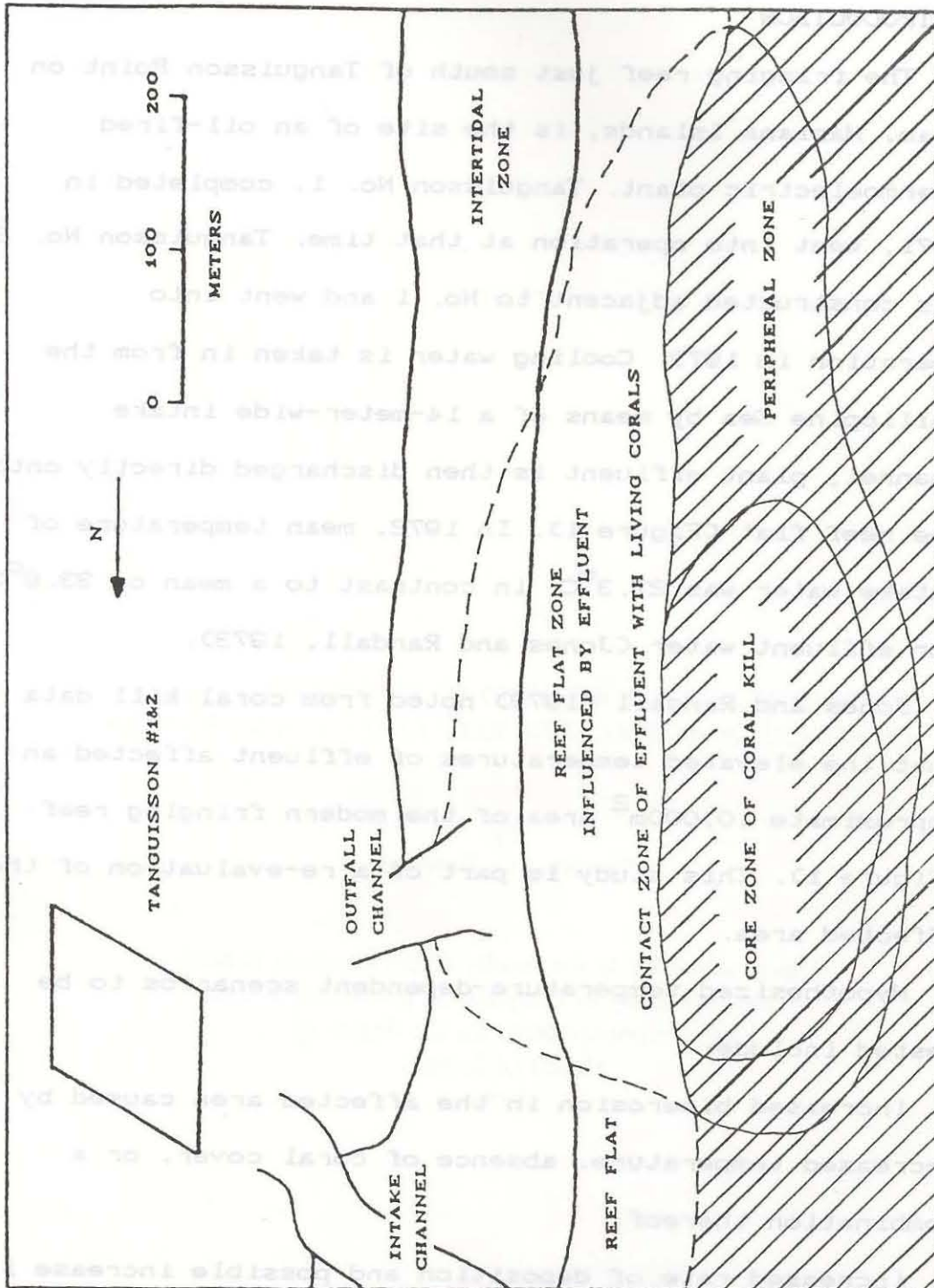


Figure 1. Area of reef flat affected by hot water effluent as of January, 1973. Shading indicates area of abundant coral prior to plant operation (after Jones and Randall, 1973).

The principal objective of this study is to document, describe and interpret diagenetic changes in the modern corallgal reef environment linked to thermal and/or geochemical stress from power plant effluent.

Secondarily, this study is an assessment of a possible power plant-related alteration of intertidal Holocene limestone outcrops located within the discharge plume.

The specific research tasks are to contrast major taxonomic groups within bioeroder populations, cementation types and styles, and trace element geochemistry of cements and coral skeletal material between the area affected by the thermal plume and control areas for both Modern and Holocene reef material.

The obvious implication of this study is related to the question of increased bioerosion in the affected area. If there is indeed an increase in bioerosion (i.e. breakup and removal of reef framework) in the absence of generation of new reef framework by living corals and/or coralline algae, then destruction of the fringing reef at Tanguisson could translate to eventual loss of a natural protective barrier. Increased wave energy during major storms would impact directly on the shoreline, severely jeopardizing the shoreline and the power plant itself. On the other hand, increased cementation in this area could increase the integrity of this natural barrier, in effect strengthening its protective

capabilities.

The model generated by this study also may have implications on a larger scale. Glynn (1988) has studied the effects of El Niño-Southern Oscillation (ENSO) in the eastern Pacific and the Caribbean. His model includes the incidence of coral bleaching and death, similar to that found at Tanguisson, due to elevated surface sea water temperatures. It is possible that trends in reef degradation seen at Tanguisson may be anticipated on coral reefs worldwide as a result of ENSO events.

Of strictly geological importance, the effects documented by this study may help to explain certain diagenetic fabrics observed in ancient limestones. Abrupt stratigraphic or facies-controlled changes in carbonate cement geochemistry, as well as type and extent of bioerosion observed in ancient limestones, may be related to relatively rapid rises in surface seawater temperatures.

General Geology:

The study area is located on the west coast of Guam, Mariana Islands ($13^{\circ}28'$ N. Lat., $144^{\circ}45'$ E. Long.), near Tanguisson Point (Figure 2). This area is approximately 10 km northeast of Agana, and is located on the Limestone Plateau of northern Guam. This location has a well-developed calcium carbonate sand beach and

lowland area surrounded by steep cliffs (approximately 100m relief) of Pleistocene Mariana Limestone. A pronounced gap in the Mariana scarp is the location of Tanguisson Nos. 1 and 2 thermoelectric plant.

At Tanguisson, outcrops of Holocene Merizo Limestone are found in the intertidal zone. It is thought that these are exposed due to both eustatic sea level adjustment and tectonic effects (Randall and Siegrist, 1988). Coral, red algal, and associated detrital limestone facies are present. Intertidal Holocene outcrops are concentrated near the outfall channel and within approximately 200 meters south of the power plant in the effluent-affected area. Presumably unaffected Merizo crops out 1000 meters north of the power plant at Shark Hole, where it intersperses with intertidal to low supratidal outcrops of Mariana Limestone. In the field, Merizo Limestone is identified by its unrecrystallized texture and by its perceptively low bulk density. The Mariana Limestone is less porous and has been thoroughly recrystallized to calcite, giving it a sucrosic texture and sparkling appearance.

At Tanguisson a 60 to 100 meter-wide reef flat (Figure 3) is exposed during extreme low tides (Jones and Randall, 1973). The reef margin represents the seaward edge of the reef flat, and is elevated approximately 20cm above it. Located seaward of the reef margin, the reef front represents an abrupt increase in

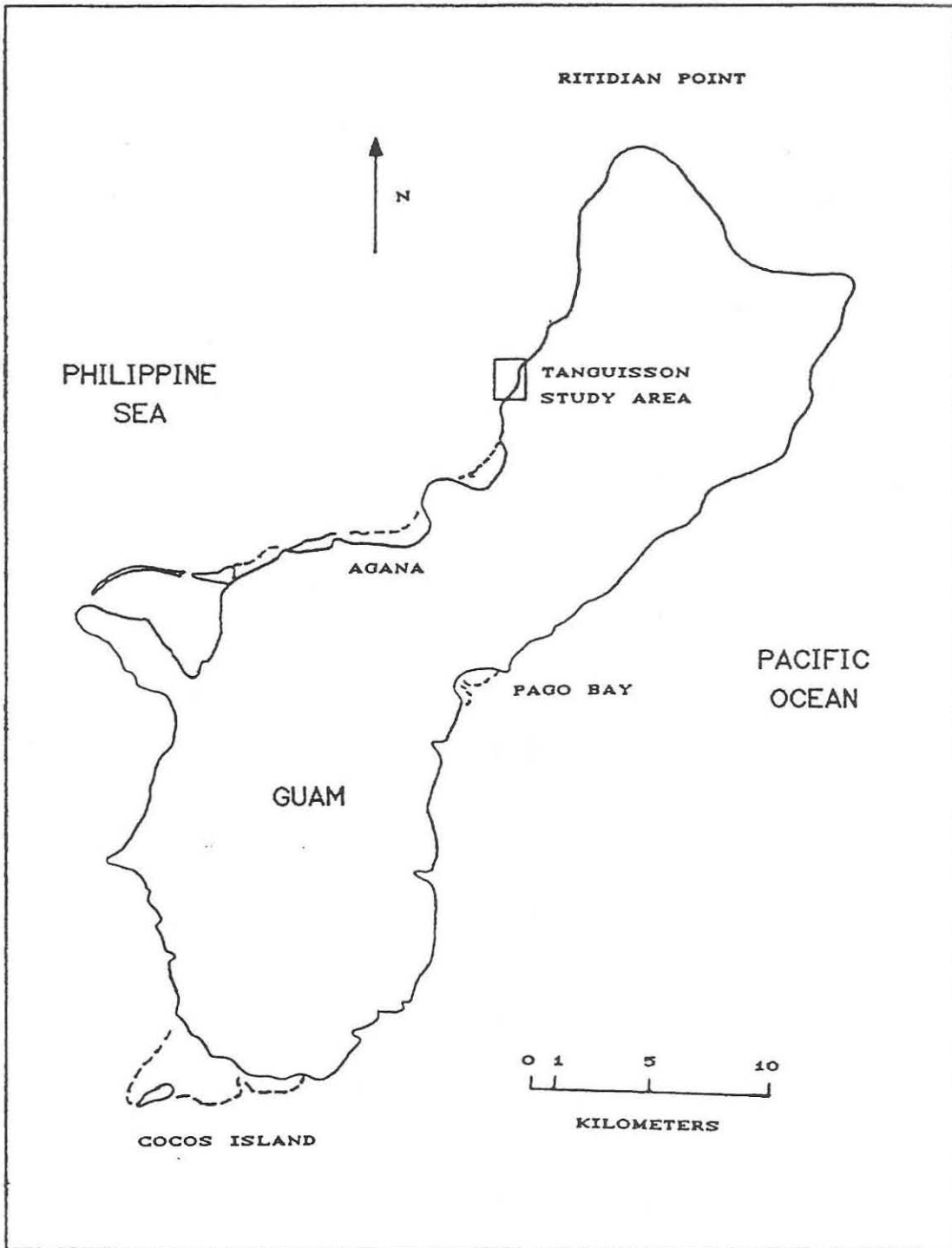


Figure 2. Map of Guam showing the location of the Tanguisson Point study area (after Randall et al., 1990).

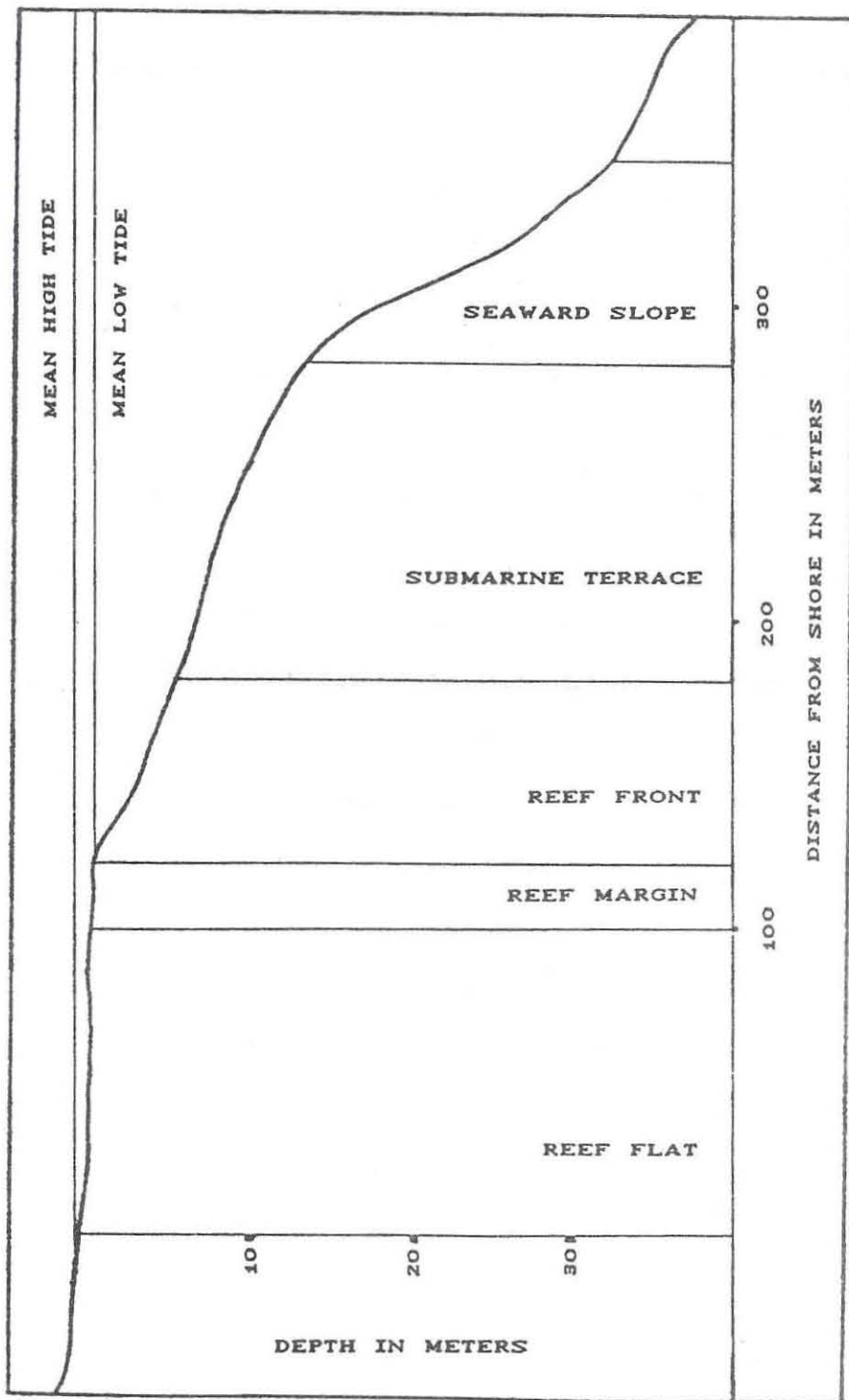


Figure 3. Vertical profile of the fringing reef system at Tanguisson Point (after Jones and Randall, 1973).

depth and slope. It extends to approximately 7 meters below mean low tide level (Jones and Randall, 1973). Both the reef front and reef slope are dissected by surge channels, giving the reef limestone a buttress-like morphology. An approximately 70 meter-wide submarine terrace at 7 to 15 meters depth is located adjacent to the reef front. This is followed by a series of deeper terraces seaward (Jones and Randall, 1973; Tracey, et al., 1964).

Most reefs have been shown through carbonate budget studies to be net exporters of material (Warne, 1977), but loss of material is usually partly offset by new skeletal growth. Tanguisson may represent an area of relatively great loss of solid CaCO_3 due to the lack of new CaCO_3 bioskeletal formation. Because the fringing reef acts as a natural protective barrier against storm wave activity, damage to the shoreline and power plant at Tanguisson is probable if removal of material by physical- and bioerosion is greater than deposition of CaCO_3 as cements and skeletal material. A model for dead reef framework preservation/destruction for a mature reef environment, such as at Tanguisson, includes bioerosion of internal framework by borers (destruction). These borings provide areas for the precipitation of carbonate cements. This, along with encrustation by coralline algae, vermetid gastropods, etc. (construction), may result in increased

preservation of the mature dead reef (Kiene, 1988). An overview of these processes and their relation to this study is presented here.

Bioerosion:

Bioerosion of coral reefs is facilitated by grazers such as parrotfish and echinoids through scraping and chewing of the coral exterior in a search for food (Hutchings, 1986). Bacteria, algae, and fungi bioerode carbonate surfaces, probably as a result of biochemical dissolution of CaCO_3 (Bathurst, 1976). A discussion of microbioeroders is located in Appendix C. More of a factor in this study is bioerosion caused by endolithic macroboring organisms.

The major macroborers identified on Guam are sipunculans, polychaetes, and clionid sponges (Randall, 1983). Rice (1969) indicates that a possible boring mechanism for sipunculans includes secretion of products causing some chemical dissolution of CaCO_3 , along with mechanical removal of material by rigid papillae located along the body and at the posterior end which is located at the base of the boring. Actual borings can be simple or highly sinuous, straight or curved, are usually blind, and contain a single specimen (Rice, 1969).

Polychaetes have been found to bore predominantly by secretion of acids which dissolve the CaCO_3 substrate (Hutchings, 1986). This was found to be true for

Polydora websteri, an oyster-boring polychaete, experimentally in various calcareous substrates and Iceland spar by Haigler (1969). Individual borings are either blind straight or U-shaped circular tubes from 1-5mm in diameter (Warme, 1975).

Clionid sponges bore primarily by chemical dissolution. Hutchings (1986) indicates that etching (dissolution) of CaCO_3 substrate is carried out by specialized cells located on filopodia. As etching proceeds, these filopods wrap around a substrate chip. When opposing filopodia meet behind the chip, the chip is dislodged and transferred to an excurrent opening where it is expelled. Chips have a characteristic multi-sided angular shape possessing concave and/or convex facets (Cobb, 1969). Chips are 15 to 100 μm in size (Fütterer, 1974).

The major superficial characteristic of the affected area at Tanguisson is the absence of live coral cover due to the death of living coral substrate. It is suspected that the activity of bioeroders has increased in the affected area as a result of the absence of live coral cover. Warme (1977) has observed that "dead substrates are colonized and more heavily attacked than those covered with coral polyps or lush growth." Unfortunately, no work has been done which relates bioerosion or bioeroders to changes in surface seawater temperatures similar to what has been observed at

Tanguisson. This subject will be discussed in greater detail later.

Hutchings (1986) indicates that bioerosion may facilitate cementation of the reef by production of fine-grained sediment which could become cemented in situ. She also indicates that some infaunal organisms actually carry sediment into their borings for feeding purposes. This "allochthonous" sediment could also become cemented within the reef framework.

Removal of CaCO_3 is accompanied by the weakening and eventual breakup of reef material into boulder- to sand-sized particles which can be transported away from the reef by currents, or can be deposited on the reef or seaward of the reef margin (Warne, 1977). Much of this material will become cemented in natural reef cavities and crevices to form reef detrital limestone (Scoffin, 1987).

Cementation:

The standard form for the solubility product (K_{sp}) of CaCO_3 is: $K_{sp} = a_{\text{Ca}^{+2}} \cdot a_{\text{CO}_3^{2-}}$ (Milliman, 1974).

Unfortunately it cannot be used easily for calculating the solubility of CaCO_3 in sea water, as salinity is not taken into account. Milliman (1974) uses the apparent solubility product (K'_{sp}), which is a function of pressure, temperature, and salinity. Computed activity products using K'_{sp} indicate that tropical surface sea

water is supersaturated with respect to both aragonite and calcite, the two most common marine cements (Milliman, 1974). Factors favoring either precipitation of aragonite or calcite in sea water are shown in Table 1.

The first factor from Table 1, presence of Mg^{2+} in solution, is of interest. Berner (1975) experimentally precipitated $CaCO_3$ under constant temperature, pressure, and $CaCO_3$ supersaturation, but with varying Mg^{2+} concentrations. He found that in general "(1) changing P_{CO_2} has no measurably consistent effect upon the rate of precipitation of either calcite or aragonite. (2) Dissolved Mg^{2+} in sea water has virtually no effect

Table 1. Factors favoring aragonite and calcite precipitation (after Milliman, 1974).

<u>Factors favoring aragonite precipitation</u>	<u>Factors favoring calcite precipitation</u>
1. Mg in solution	1. absence of Mg
2. high temperature	2. low temperature
3. high pH	3. low pH
4. sodium succinate, chondroitin sulfate	4. SO_4
5. Sr, Ba, Pb	5. $NaCO_3$, $(NH_4)_2CO_3$
	6. presence of many organic compounds, such as sodium citrate and sodium malate

upon the rate of seeded precipitation of aragonite. (3) Dissolved Mg^{2+} in sea water severely retards the rate of seeded precipitation of calcite. (4) Calcite precipitated from sea water on pure calcite seeds is magnesian, containing 7-10 mole per cent $MgCO_3$ in solid solution. It occurs as a true overgrowth on the calcite seed particles. (5) In Mg-deficient 'sea water' containing less than (approximately) 5 per cent of the normal Mg content, Mg does not appreciably retard the seeded precipitation of calcite." From these results he hypothesized that either "(1) magnesium acts as a surface poison by being adsorbed as hydrated ions on active growth sites, such as kinks, and, thereby, inhibits the spread of monomolecular steps on the crystal surface..." or "(2) magnesium may serve as a surface poison but is also incorporated into the growing crystal to such an extent that the solubility is markedly increased..." Discussion of his hypotheses seems to indicate that surface poisoning may be a minor factor, whereas bulk uptake of Mg^{2+} to form high-Mg calcite may be a greater factor (Berner, 1975).

Walter and Morse (1984) have found that under surface sea water conditions, 12 mol% magnesian calcite and aragonite are equivalent in thermodynamic stability (more correctly stated as equivalent in molar solubility). This value is substantiated by the work of Bischoff et al. (1987). The thermodynamic stability has

been found to be independent of initial solution pH, solid:solution ratio, and solution Mg:Ca molar ratio (Walter and Morse, 1984). From these results, it would be predicted that inorganic CaCO_3 precipitates in seawater would be in the form of aragonite or up to 12 mol% magnesian calcite at a temperature of 25°C .

Temperature also plays a role in Mg content of magnesian calcite. Mucci (1987) found a nearly linear relationship between the distribution coefficient of Mg and temperature between 5° and 40°C . The Mg distribution coefficient is defined as:

$$D_{\text{Mg}^{2+}}^{\text{C}} = \frac{X_{\text{MgCO}_3}^{\text{C}} / X_{\text{CaCO}_3}^{\text{C}}}{M_{\text{Mg}^{2+}}^{\text{L}} / M_{\text{Ca}^{2+}}^{\text{L}}}$$

where $X_{\text{MgCO}_3}^{\text{C}}$ and $X_{\text{CaCO}_3}^{\text{C}}$ refer to the mole fractions of MgCO_3 and CaCO_3 in the magnesian calcite overgrowth, and $M_{\text{Mg}^{2+}}^{\text{L}}$ and $M_{\text{Ca}^{2+}}^{\text{L}}$ are the molar concentrations of the parent solution in experimental precipitation studies (Mucci, 1987). An increase in Mg content was observed with an increase of temperature from 5° to 40°C (see Table 2). The experiments were performed in "artificial sea water" on pure calcite seeds. Unfortunately it was found that experimental values were generally lower than those found in nature. Mucci (1987) believes that this

may be due to differences in $[Mg^{2+}]/[Ca^{2+}]$ ratios found in microenvironments (i.e. algal bores, skeletal chambers, etc.) from those found in open surface sea water. Changes in Mg content in microenvironments may be a result of biochemical factors such as dissolved organic substances and/or mineralogy and nature of organic matrices in the host particles (Mackenzie et al., 1983).

Table 2. Average of experimental magnesium distribution coefficients, $D_{Mg^{2+}}^C$, in magnesian calcite overgrowths precipitated from seawater at various temperatures and their corresponding compositions in mole percent $MgCO_3$ (Mucci, 1987).

T (°C)	$D_{Mg^{2+}}^C$	Mole % $MgCO_3$
5	0.0121 ± .0013	5.8 ± 0.6
25	0.0172 ± .0022	8.1 ± 1.0
40	0.0271 ± .0013	12.3 ± 0.6

Cement types found to precipitate in warm shallow sea water are high-Mg calcite (usually 12-25 mol% $MgCO_3$ with decreasing % as water temperature decreases) and aragonite (Scoffin, 1987). High-Mg calcite cements occur as fine-grained fibrous or bladed crystals with pyramidal terminations, or as small rhombohedra (Scoffin, 1987). These crystals form fibrous crusts, spherulitic clusters, and pelloidal micrites (Scoffin, 1987). Scoffin (1987) describes pelloidal texture as "subspherical bodies 20-60 μ m in diameter composed of a

mosaic of roughly $1\mu\text{m}$ diameter equant calcite crystals, separated by coarser Mg calcite crystals $5\text{-}10\mu\text{m}$ in diameter." This texture has been observed as a cavity filling and is presently thought to be a precipitated cement (Marshall, 1986).

Aragonite cements form as loosely packed acicular fibers $50\text{-}300\mu\text{m}$ long, and as densely packed fibrous botryoidal masses (Aissaoui et al., 1986). The latter occurs in coral skeletons and grainstones; the former is found infilling primary reef cavities (Aissaoui et al., 1986).

Marshall (1986) found that acicular aragonite and bladed high-Mg calcite cements form at early and relatively late stages of lithification in the Great Barrier Reef. He noted that "early cements are found lining or filling coral pores and other skeletal chambers that may be followed by micrite or mesh cemented internal sediments. The later cements are more coarsely crystalline than their predecessors, and they line or fill either secondary borings or the remaining space within partly filled (usually geopetal) cavities."

On Rota, 50km north of Guam, 3 types of aragonite cement and 5 types of Mg calcite cement were found in emergent Holocene coralgall reefs analagous to the Merizo Limestone of this study (Bell and Siegrist, 1988). These were:

A₁ - Individual acicular crystals, frequently $200\mu\text{m}$ long,

with chisel-shaped terminations forming non-isopachous linings in aragonitic skeletal cavities.

A₂- Screen- or mesh-like cements formed by mutually interfering acicular or lath-shaped crystals growing from different locations in the pore wall.

A₃- isopachous closed fans of 200 μ m long fibrous aragonite crystals showing undulose extinction. These were noted to be similar to so-called botryoidal aragonite cements.

M₁- Micro- (1-4 μ m) and submicroscopic (<1 μ m) Mg calcite crystals frequently forming continuous pore linings or rims around bioclasts.

M₂- 4-20 μ m equant, blocky, rhomb, or loaf-shaped Mg calcite crystals frequently forming a mosaic above coarser M₁ cement.

M₃- 75-100 μ m long dentate bladed crystals forming semi-isopachous linings, individual crystals oriented perpendicular to pore walls.

M₄- 100-200 μ m long Roman sword shaped crystals perpendicular to nucleation surfaces, showing "picket fence" extinction.

M₅- Peloids of silt-size (60 μ m) made up of dense micrite (<1 μ m) with isopachous rims of M₃ or M₄ cement.

It is expected that many of these cements will be observed in the modern and Holocene rocks of this study. No studies of differences in cement morphology as a result of slight changes in surface sea water

temperature have been undertaken. Possible differences between cements in control and affected areas observed in this study will be discussed later.

Strontium:

Sr^{2+} concentrations can be used to track the progress of freshwater diagenesis (Kinsman, 1969). The overall affect of freshwater percolation through marine aragonite is to reduce the amount of Sr^{2+} . This appears to be related to the leaching of aragonite with simultaneous precipitation of calcite owing to freshwater phreatic and vadose diagenesis as discussed by Scoffin (1987). This effect has also been documented in the Red Sea region by Friedman and Brenner (1977) for corals of modern age, 110,000 years old, and 250,000+ years old. They found a decrease in strontium concentration paralleling the amount of aragonite which had been replaced by calcite in the ancient reef rocks studied. Initial Sr^{2+} concentrations range from 2500 to 9500 ppm due to differences in fractionation of strontium by various marine organisms (Scoffin, 1987). After diagenesis, observed Sr^{2+} concentrations average 200 ppm (Scoffin, 1987). The effects of diagenesis caused by a slight rise in temperature, as observed at Tanguisson, on Sr^{2+} concentrations has not been studied. Results of a study of strontium concentration at Tanguisson will be discussed later.

METHODS

Modern coral skeletal samples were collected along a transect normal to the shoreline located approximately 50 meters south of the power plant effluent channel (Transect B). This is the area where thermal impact of effluent is greatest in the affected area (Jones and Randall, 1973). *In situ* dead and living coral colonies, as well as heavily encrusted skeletons and loose cobbles, were removed. After collection in the affected area, the same coral genera and types of samples were taken from a control transect (Transect A) located approximately 450 meters north of Transect B (Figure 4). This was done to decrease bias which may be introduced as a result of selectivity of certain bioeroders for certain coral genera (Randall et al., 1990). Both transects extend from the shoreline, crossing the reef flat, reef margin, and upper reef slope (Figure 3).

Affected intertidal Holocene reef limestone samples were collected along a transect normal to the shoreline bordering the south edge of the effluent channel (Transect D). Coral skeletal and detrital facies were removed. Collection also included samples of Pleistocene Mariana Limestone. Unaffected Holocene samples similar in type to those in the affected area were collected from a control transect located approximately 1000 meters north of the power plant (Transect C). See Figure 4

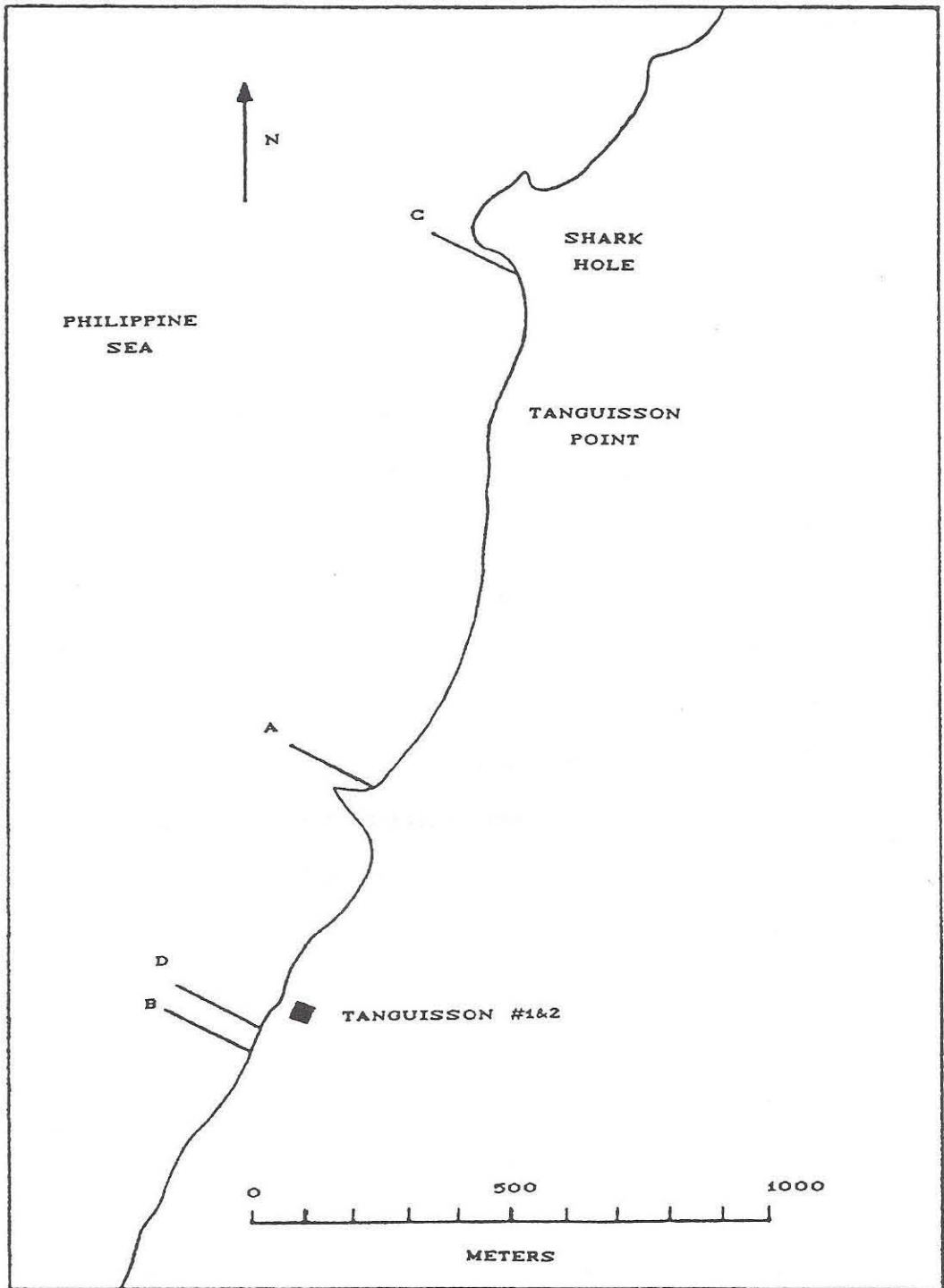


Figure 4. Location of sample transects. Transects A and B indicate modern reefs; Transects C and D indicate Holocene reefs.

A total of 41 recent reef samples, 19 from Transect A and 22 from Transect B, were slabbed vertically along the longest horizontal axis using diamond blade rock cutting saws. This was done to obtain a smooth areal surface for categorization and percentage estimation of skeletal framework, primary porosity, bioerosion, visible cement, and detrital infillings on a macroscopic scale.

Point counts of slabbed specimen surfaces were made using a clear plastic grid into which 500 points were punched with a nail punch. Points were generated from a random number table (Sokal and Rohlf, 1987) to assure randomness in the count.

One problem encountered was that of largely differing surface areas of samples. This was solved by projecting the sample onto a Sony video monitor using a CCD Color Camera M-852 equipped with a CCTV Precision Optics zoom lens installed on a light table which allows for vertical adjustment of the camera. The focal length of the camera was changed to allow sample surface areas to be brought within 95% of the area of a standard sample (RHR 1248-9A). Surface area of the standard sample and of the adjusted samples was measured using CUE 3 Image Analyzer Version 2.01 software (Olympus Corp., 1988). This program allows the surface area to be calculated by tracing the outside edge of the sample with a mouse. An areal readout of the traced area is given in the desired

units (for this study mm^2). The plastic grid was installed on the video screen, and counts were made directly from the screen. This technique allowed approximately 175-200 grid points to fall on each sample. Point counts and specimen descriptions are located in Appendix B.

Sample statistics for percent bioerosion for each of Transects A and B were calculated. Tests of significance consisted of two-way analyses of variance (ANOVA) for treatment (control vs. affected, or Transect A vs. Transect B) versus coral genera, and for treatment versus depth (Appendix A). Depth was studied because a stratification of hot water in the uppermost 1 meter was observed in the earlier study (Jones and Randall, 1973). Percent encrusting organisms also was studied in an identical statistical setup.

A thin section analysis of microboring algae and fungi also was done. Thin sections of 3 coral genera from Transect A and Transect B were systematically point counted and categorized as in the slab study. Sample statistics and analyses of variances (ANOVA) were generated using SYSTAT. Results will be discussed later. A short paper discussing this study in detail is located in Appendix C.

Bioerosion studies were not done for Holocene samples, as no appreciable modern bioerosion was observed on freshly cut surfaces.

Standard size polished thin sections of 30 μ m nominal thickness impregnated with blue-dyed epoxy were made of Holocene and modern reef samples by D.M. Organist Petrographic Laboratory, Newark, Delaware. Blue epoxy was used to allow easy identification of porosity under plane-polarized light. Sections were polished for SEM/WDS analysis.

Thin sections were studied using a Nikon transmitted light petrographic microscope equipped with 10x binocular and 4x, 10x, and 60x objective lenses. Samples were moved manually so that an entire scan of the section was completed at 40x magnification. Irregularities and visible cements also were observed at 100x and 600x magnifications. Scans normally were made with crossed polarizers, as it was found that the aragonite coral skeleton had a characteristic texture which was not always visible under plane-polarized light. Plane-polarized light was used to check porosity and contacts between cements and framework. Noted were framework type and condition, type of porosity (i.e. primary or secondary), presence and morphology of cements, as well as other diagenetic characteristics. Cements were also marked for SEM/WDS analysis during this procedure.

Samples of the 41 Recent corals, as well as 20 Holocene reef samples (10 from Transect C and 10 from Transect D) were crushed in a jaw crusher, then powdered

using a SPEX alumina shatterbox. Plastic sample cups (SPEX Industries, Inc., Catalog no. 3529) were filled with the sample powders and were covered with 2.5 μ m Spectro-Film Micro-Fine Mylar for x-ray fluorescence analysis.

Fourteen XRF samples were placed on a carousel in the Kevex 0700 XES Control, along with a working standard, for a total of 15 samples. Samples were analyzed automatically using a Quantex automatic command file titled 1DATACOL. See Appendix A. This allowed the carousel to be rotated to the next sample upon completion of collection of the previous sample. XRF sample spectra were saved on a file disk for later data reduction.

All samples were run for a preset time of 300 seconds. All were run on the Ag target. Kilovolt and milliamp settings different from published suggested values (Potts, 1987; Kevex Corporation, 1982) were used due to the relatively high concentrations of Ca and Sr present in these samples as opposed to those used to generate the published values. Kv and mA settings were changed to obtain an effective dead time of approximately 40% as suggested by the Kevex Corporation (1982). Exact settings can be found in Appendix D.

After run completion, stored spectra were analyzed using an automatic command file (Kevex Corporation, 1982) titled RBSRINT. This allowed for automatic removal

of escape peaks, smoothing, background removal, setting of peak gates, and integration of peak areas for the entire run. Program commands are listed in Appendix A.

A total of 3 runs per sample per target were done, providing raw intensities for Sr. Arithmetic means of the raw intensities from runs 1, 2, and 3 were calculated. A correction factor representing a peak intensity of strontium found on an analyzed blank (sample cup and mylar membrane with no powder) was subtracted from the mean intensities. Raw and calculated intensity data are located in Appendix D. Counting error for XRF work was calculated as the coefficient of variance (CV) expressed as a mean relative error (Appendix D). This was calculated to be 5.363%.

A total of 8 standards were chosen after XRF data was obtained. These were chosen from among the samples as those that were spread across the entire range of Sr intensities. These standards were sent out to XRAL Activation Services, Ann Arbor, Michigan for XRF analysis of Sr, Ca, Fe, S, P, Si, and Mg. The XRAL report and calibration curve are located in Appendix D.

A linear regression equation was generated using SYSTAT MGLH (Wilkinson, 1987). This formula takes the following general form:

$$I = mC + b_0$$

where C is the concentration of strontium in parts per million and I represents the XRF intensity of strontium.

Standard concentrations of Sr were used to generate the coefficients (m and b_0) by SYSTAT. The resulting formula was used to solve for the Sr concentrations of the unknown samples. See Appendix A. Error attributed to uncertainty in analysis of standards, sample analysis, and regression of standards and unknowns, was calculated using the formula (Appendix D) of Bennett and Franklin (1954) expressed as a mean relative error. This was calculated to be 2.211%

Various cements from 5 thin sections from each of the four transects (modern and Holocene) were analyzed for magnesium content using the JEOL JXA-840A Electron Probe Microanalyzer and Tracor Norther 5600 Computer Task System. The wavelength dispersive spectrometer was used at a setting of 15Kv with a sample current of 5nA. This sample current was used because volatilization of CO_2 occurred at beam currents of 10nA and higher. Total count times of 30 seconds were used. Calcium content was determined using a LiF (lithium fluoride) crystal, and magnesium was determined using a TAP (thallium hydrogen (acid) phthalate) crystal. Standards used were calcite containing 55.95 weight% CaO and 44.05 weight% CO_2 ; and dolomite containing 29.13 weight% CaO, 22.93 weight% MgO, and 47.94 weight% CO_2 . Both weight% CaO and MgO, and mol% $CaCO_3$ and $MgCO_3$ were calculated for the samples by the task system after count completion. Counting error for each analysis was calculated as a relative

error (Willard et al., 1974) for Mg and Ca by the Tracor Norther 5600 Computer Task System during automatic Bence-Albee correction procedures (Bence and Albee, 1968). Mean relative error for Mg is 19.92%; for Ca 1.178%.

After probe analyses, values of mol% MgCO_3 were grouped according to transect and cement type. Arithmetic means and standard deviations were calculated for each transect/cement type subgroup, which were then compared. Tests of significance were not attempted because of the low number of sample analyses (n) in each subgroup.

RESULTS

Bioerosion:

The mean percent bioerosion for Transect A, the control transect, based on 19 samples is 4.92 ± 4.77 (one standard deviation). That for Transect B, the affected transect, based on 22 samples is 9.81 ± 4.54 .

Two-way analyses of variance were performed for percentage bioerosion of Modern corals, treatment versus coral genera, and treatment versus depth. Treatments correspond to Transect A, the control area, and to Transect B, the effluent-affected area. Coral genera included in the analyses are *Goniastrea*, *Pocillopora*, *Acropora*, *Acropora* cobbles (studied as a separate generic group), *Favia*, *Favites*, and *Millepora*. All genera are scleractinian corals with the exception of *Millepora* which is a hydrozoan coral. Depths considered were 0 to 1 meters, 1.1 to 2 meters, and 2.1+ meters below mean sea level.

Table 3 shows the results for percent bioerosion as a function of treatment and coral genera. The table indicates that there is a significant difference ($p < 0.05$) in bioerosion between treatments. Although not significant ($p > 0.05$) in this experiment, there is a probable difference in susceptibility to bioerosion among coral genera. The interaction of treatment with coral genera is not significant ($p > 0.05$).

Table 3. Analysis of variance for percent bioerosion of Modern corals, treatment vs. coral genera. N=41.

<u>SOURCE</u>	<u>SS</u>	<u>DF</u>	<u>MS</u>	<u>F-RATIO</u>	<u>P</u>
Treatment	0.019	1	0.019	9.142	0.005
Genus	0.021	6	0.003	1.701	0.159
Interaction	0.006	6	0.001	0.462	0.830
Error	0.055	27	0.002		

Table 4. Analysis of variance for percent bioerosion of Modern corals, treatment vs. depth. N=41.

<u>SOURCE</u>	<u>SS</u>	<u>DF</u>	<u>MS</u>	<u>F-RATIO</u>	<u>P</u>
Treatment	0.022	1	0.022	12.348	0.001
Depth	0.011	2	0.005	3.071	0.059
Interaction	0.007	2	0.004	2.112	0.136
Error	0.062	35	0.002		

Table 4 shows the results for percent bioerosion as a function of treatment and depth. Again, a significant difference ($p < 0.05$) is shown between treatments. As with coral genera, the ANOVA indicates probable differences between depths, although not significant ($p > 0.05$) in this experiment. This is also evident in the interaction of treatment and depth.

The same experiments as shown in tables 3 and 4 were conducted for percentage bioerosion relative to available erodable substrate. This was done by excluding points counted for primary porosity, as these points represent surface area within the coral slab which is not available for bioerosion. Remaining point counts of

primary and secondary framework, cemented detritus, and bioerosion were recalculated to 100%. The results are shown in Tables 5 and 6.

Both tables show a significant difference ($p < 0.05$) between treatments. Of interest is the result for coral genera in table 5. This shows a higher probability of differences between coral genera than that shown in table 3. This result, however, was not significant ($p > 0.05$) for this experiment.

Table 5. Analysis of variance for percent bioerosion of Modern corals relative to erodable substrate, treatment vs. coral genera. N=41.

<u>SOURCE</u>	<u>SS</u>	<u>DF</u>	<u>MS</u>	<u>F-RATIO</u>	<u>P</u>
Treatment	0.022	1	0.022	8.850	0.006
Genus	0.036	6	0.006	2.371	0.057
Interaction	0.006	6	0.001	0.382	0.884
Error	0.068	27	0.003		

Table 6. Analysis of variance for percent bioerosion of Modern corals relative to erodable substrate, treatment vs. depth. N=41.

<u>SOURCE</u>	<u>SS</u>	<u>DF</u>	<u>MS</u>	<u>F-RATIO</u>	<u>P</u>
Treatment	0.028	1	0.028	11.037	0.002
Depth	0.011	2	0.006	2.298	0.115
Interaction	0.010	2	0.005	1.999	0.151
Error	0.088	35	0.003		

During the point counting procedure, it was observed that there may be a higher incidence of encrustation in

Transect B by various algae, vermetid molluscs, and other organisms. Mean percentage encrusters for Transect A is 6.75 ± 6.34 (one standard deviation), and that for Transect B is 13.6 ± 13.6 . Analyses of variance for percentage encrusting organisms as a function of treatment versus coral genera and treatment versus depth were performed. The results are shown in tables 7 and 8.

In both experiments, differences between treatments are not significant ($p > 0.05$), although a difference is probable. No significance was found between coral genera, or between depths, although again there is a high probability of differences in percent encrusters, which may be the basis for further study.

Table 7. Analysis of variance for percent encrusters on Modern corals, treatment vs. coral genera. N=41.

<u>SOURCE</u>	<u>SS</u>	<u>DF</u>	<u>MS</u>	<u>F-RATIO</u>	<u>P</u>
Treatment	0.037	1	0.037	3.078	0.091
Genus	0.135	6	0.022	1.883	0.121
Interaction	0.052	6	0.009	0.728	0.631
Error	0.322	27	0.012		

Table 8. Analysis of variance for percent encrusters on Modern corals, treatment vs. depth. N=41.

<u>SOURCE</u>	<u>SS</u>	<u>DF</u>	<u>MS</u>	<u>F-RATIO</u>	<u>P</u>
Treatment	0.034	1	0.034	3.216	0.082
Depth	0.044	2	0.022	2.071	0.141
Interaction	0.063	2	0.032	2.975	0.064
Error	0.373	35	0.011		

Strontium:

Concentration values in parts per million for Sr are shown in Tables 9 and 10. These values were obtained through linear regression as explained in Appendix A. The mean Sr concentration for Transect A is 6595 ± 576 (1 std. dev.) ppm. Mean concentration for Transect B is 6082 ± 759 ppm.

Transect C mean Sr concentration is 6472 ± 453 ppm. All samples are primarily original coral skeleton, although 89G006 and 89G016 had cemented detrital material present in moderate amounts. Transect D is made up of three sub-populations. Samples in table 9 with the lowest Sr concentration (89G022, 89G023, 89G029) are predominantly detrital, made up of calcite micrite and allochems. Samples of moderate values (89G021, 89G024, 89G025, 89G026) have been identified as Pleistocene Mariana Limestone. Thin section analysis shows total recrystallization of original aragonite coral skeleton to sparry calcite, with accompanying reduction of primary porosity to near zero by precipitation of more sparry calcite. Lower Sr concentration would be expected in both of these sample types. The remaining three samples are made up of primary aragonite coral skeleton along with various amounts of calcite micrite mud, with mean Sr concentration of 4371 ± 785 ppm.

Table 9. Strontium concentration in parts per million, Modern corals, Transects A and B.

TRANSECT A		TRANSECT B	
<u>SAMPLE</u>	<u>PPM Sr</u>	<u>SAMPLE</u>	<u>PPM Sr</u>
RHR1246-1A	6938	RHR1247-2A	6188
RHR1246-2A	6646	RHR1247-3A	5565
RHR1246-3A	6477	RHR1247-4A	4186
RHR1246-5A	6488	RHR1247-5A	5409
RHR1246-6A	6323	RHR1247-6A	5806
RHR1246-7A	5903	RHR1247-7A	4558
RHR1246-8A	7346	RHR1247-9A	5899
RHR1246-9A	6342	RHR1247-10A	5544
RHR1246-9AB	6971	RHR1247-11A	6408
RHR1246-10A	6854	RHR1247-13A	6049
RHR1246-11A	6806	RHR1247-14A	6918
RHR1246-12A	6235	RHR1247-15A	5504
RHR1249-1A	6383	RHR1247-16A	6039
RHR1249-3A	6632	RHR1248-1A	7145
RHR1249-5A	6923	RHR1248-2A&B	7096
RHR1249B-11A	7400	RHR1248-3A	6546
RHR1346-13A	4801	RHR1248-6A	6102
RHR1371-2A	6807	RHR1248-9A	6343
RHR1373-4A	7039	RHR1248-10A	6396
		RHR1258-1A	6351
		RHR1258-3A	7019
		RHR1258-4A	6731

Table 10. Strontium concentration in parts per million, Holocene corals, Transects C and D. Transect D samples in parentheses have been identified as Pleistocene Mariana Limestone.

TRANSECT C		TRANSECT D	
<u>SAMPLE</u>	<u>PPM Sr</u>	<u>SAMPLE</u>	<u>PPM Sr</u>
89G001	5972	89G019	4856
89G002	6610	89G020	4792
89G005	6225	(89G021)	1879
89G006	5805	89G022	439.4
89G013	6865	89G022A	3466
89G014	6600	89G023	381.7
89G015	7152	(89G024)	1746
89G016	5958	(89G025)	2271
89G017	6804	(89G026)	1943
89G018	6733	89G029	423.2

Table 11. Analysis of variance for strontium concentration in Modern corals, treatment vs. genus. Coral genera used were *Pocillopora* and *Goniastrea*.

<u>SOURCE</u>	<u>SS</u>	<u>DF</u>	<u>MS</u>	<u>F-RATIO</u>	<u>P</u>
Treatment	3546354.844	1	3546354.844	10.072	0.006
Genus	369935.268	1	369935.268	1.051	0.321
Interaction	560603.827	1	560603.827	1.592	0.225
Error	5633824.607	16	352114.038		

Table 12. Analysis of variance for strontium concentration in Modern corals, treatment vs. depth. Coral genera used were *Pocillopora* and *Goniastrea*.

<u>SOURCE</u>	<u>SS</u>	<u>DF</u>	<u>MS</u>	<u>F-RATIO</u>	<u>P</u>
Treatment	2556525.453	1	2556525.453	7.974	0.014
Depth	603269.522	2	301634.761	0.941	0.414
Interaction	1329699.037	2	664849.519	2.074	0.163
Error	4488462.333	14	320604.452		

Tables 11 and 12 show analyses of variance for Sr concentration in Modern corals as a function of treatment and coral genera, and of treatment and depth respectively. Samples of the coral genera *Pocillopora* and *Goniastrea* were chosen for these analyses, as they were the most abundant of the genera collected. A significant difference between treatments ($p < 0.05$) is evident in both analyses. No evidence of differences in strontium concentrations was found between the coral genera or depths studied.

Cements:

No observable difference in quantity of diagenetic CaCO_3 cements were found between control and affected transects for Modern or Holocene coral samples. Similar cement morphologies were observed in all transects. Characteristic aragonite cements observed in all transects were the A_1 and A_2 acicular type cements (Plate 1) of Bell and Siegrist (1988). These taken as a group contain from 0.00 to 0.29 mol% MgCO_3 . A_3 botryoidal or fan-shaped cement (Bell and Siegrist, 1988) was observed in Modern coral transects (Plate 1). These contained from 0.07 to 0.38 mol% MgCO_3 .

No calcite cements were observed in samples from the Modern coral transects. In the Holocene transects, M_1 cement (Bell and Siegrist, 1988) was observed as isopachous linings around bioclasts (Plate 2) and cementing detrital pelloidal material (fecal pellets). This cement contains from 9.64 to 18.1 mol% MgCO_3 . Acicular to bladed high Mg calcite cements (6.9 to 10.2 mol% MgCO_3) were observed in samples from Transect C, the Holocene control area (Plate 2). These most closely resembled the M_3 cement of Bell and Siegrist (1988).

Pleistocene coral samples showed total recrystallization of original aragonite skeletal material to calcite spar (Plate 2). Almost total reduction of primary porosity by infilling with calcite spar was evident. In some cases remnant first generation

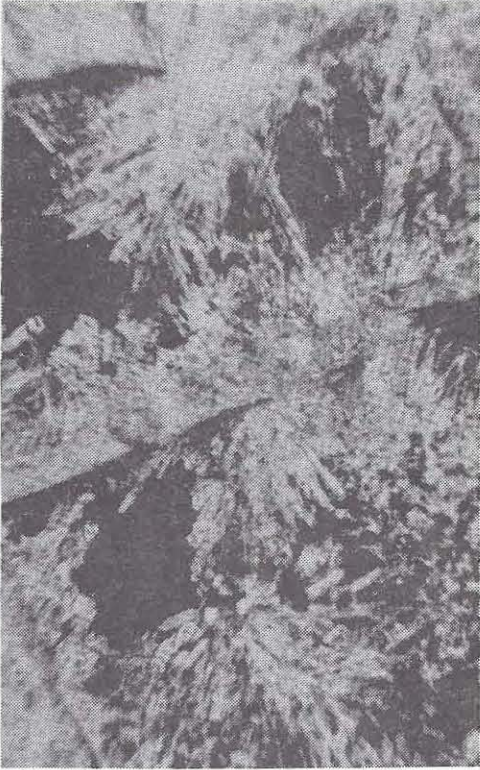
aragonite cements were still visible with growth perpendicular to pore surfaces. In most cases large calcite crystals were observed infilling the remaining pore as a second generation cement. This texture was used as a tool to correctly identify Holocene versus Pleistocene samples in Transect D.

Plates 1 and 2. All photographs taken under crossed polarizers at 125x magnification. Scale bars = 100 μ m. Dark areas are pore spaces.

Plate 1. Aragonite cements. A - Transect A, RHR1248-9A, A₁ cement (arrow). B - Transect B, RHR1247-7A, A₂ cement totally infilling pore at center of photo. C - Transect A, RHR1246-5A, A₃ cement (arrow).

Plate 2. Mg-calcite cements, etc. A - Transect C (Holocene), M₁ cement as isopachous linings within bioclast (arrow). B - Transect D (Holocene), M₃ cement (arrow). C - Transect D (Pleistocene), typical Pleistocene texture showing total recrystallization of aragonite coral to coarse calcite spar. Primary pores (arrow) are also infilled with calcite spar.

A



B



C

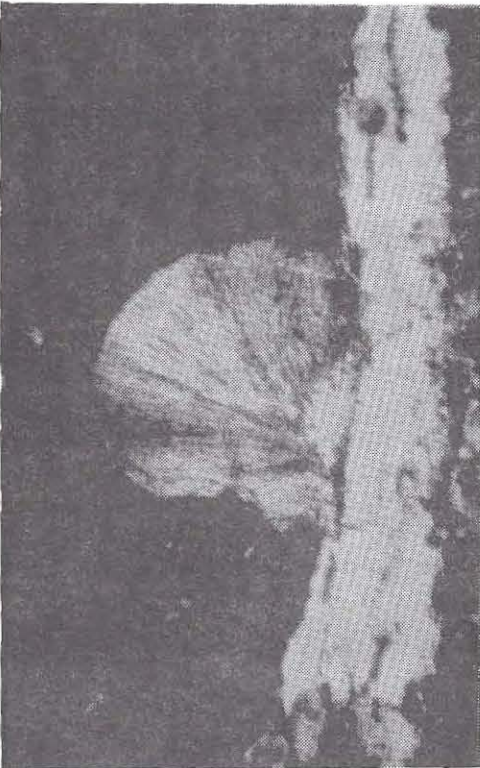
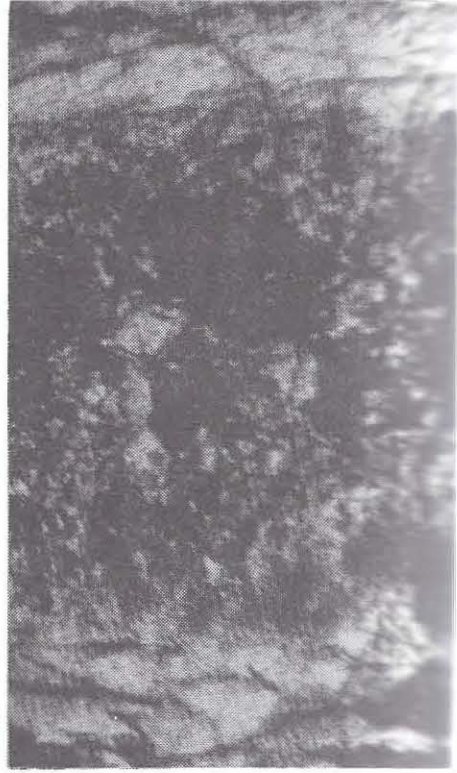


Plate 1.

A



B



C



Plate 2.

DISCUSSION

Bioerosion at Tanguisson:

The results of ANOVA indicate that there is a significant difference in percent bioerosion between samples in Transect A (control) and those in Transect B (affected). Mean percent bioerosion is greatest in Transect B. Visual survey of slabs indicated that polychaete borings are much more abundant in Transect B samples (Plates 3-5). Clionid sponge borings are observed in both transects, although in Transect A their occurrence was usually limited to the lower dead part or undersurface of the colony (Plates 3-5). Sponge borings were usually observed throughout the dead coral specimens in Transect B if present at all. Sipunculan borings are scarce in both transects.

Overall, bioeroder populations, with the exception of polychaetes, are similar in dead portions of corals in both transects. No distinct difference in major types of bioeroders between transects is evident.

Living parts of coral colonies in both transects are fairly bioeroder-free (Plates 3-5). One apparent exception is the presence of endolithic barnacles in *Goniastrea* sp. These are not true bioeroders however, as they grow along with the coral skeleton, in essence maintaining an open space in which to live (Bromley, 1978).

Plates 3-5. Cross-sections of slabbed reef samples. Divided scale bar is in centimeters.

Plate 3A and B, *Goniastrea* sp. A - Transect A, RHR1249-5A, large oval hole in upper left caused by growth of gastropod enclosed by coral growth. Smaller borings caused by clionid sponges. B - Transect B, RHR1247-11A, borings in interior caused by polychaetes. Note exterior coating of vermetid molluscs and red algae.

Plate 3C and D, *Pocillopora* sp. C - Transect A, RHR1246-1A, coral fairly clean except for a few clionid sponge borings (arrow). D - Transect B, RHR1247-10A, coral extensively bored by polychaetes and clionid sponges. Note exterior encrustation by red algae and vermetid molluscs.

Plate 4A and B, *Acropora* sp. A - Transect A, RHR1246-8A, coral free of bioeroders. Cavities at arrow are primary, infilled with detrital material. B - Transect B, RHR1247-14A, coral extensively bored by polychaetes and clionid sponges along a 2cm-thick exterior margin.

Plate 4C and D, *Millepora* sp. C - Transect A, RHR1246-12A, clionid sponge borings present along margin of earlier coral growth (arrow), now covered by new layer of coral skeleton. D - Transect B, RHR1247-13A, elongate borings are polychaetes. Clionid sponge borings are plentiful around margin. Note tufts of blue-green algae at upper right.

Plate 5A and B, *Favia* sp. A - Transect A, RHR 1246-11A, a few clionid sponge borings are located along margin (arrow). Dead basal area (lower right) encrusted by red algae and *Homotrema* sp. B - Transect B, RHR1248-10A, clionid sponge borings extensive along upper dead surface (left side of photo). Long openings in interior are possibly caused by endolithic barnacles.

Plate 5C and D, *Favites* sp. C - Transect A, RHR1371-2A, small lineations of clionid sponge chambers are located between corallites (arrow). D - Transect B, RHR1248-3A, clionid sponge borings extensive with polychaete borings present in interior of coral. Note upper surface (left side of photo) encrusted by blue-green algae.

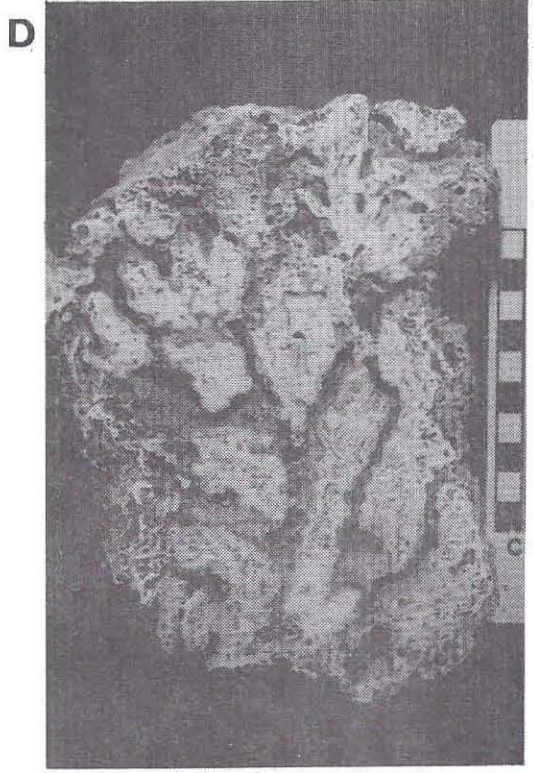
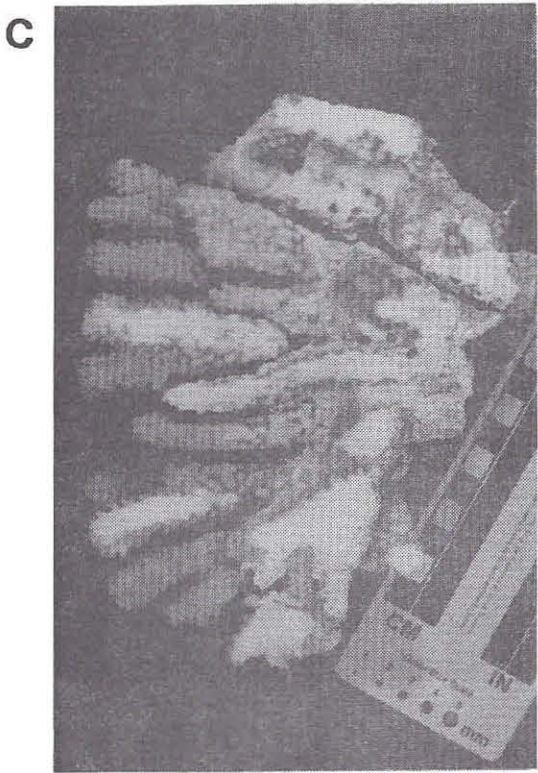
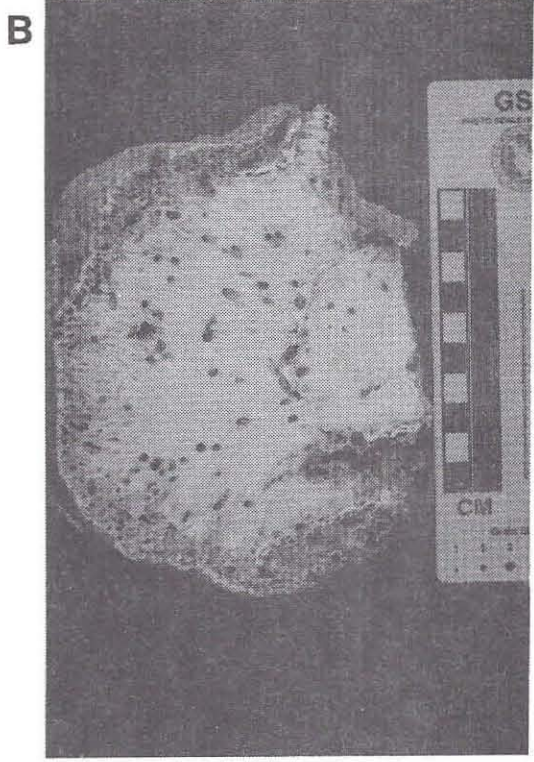
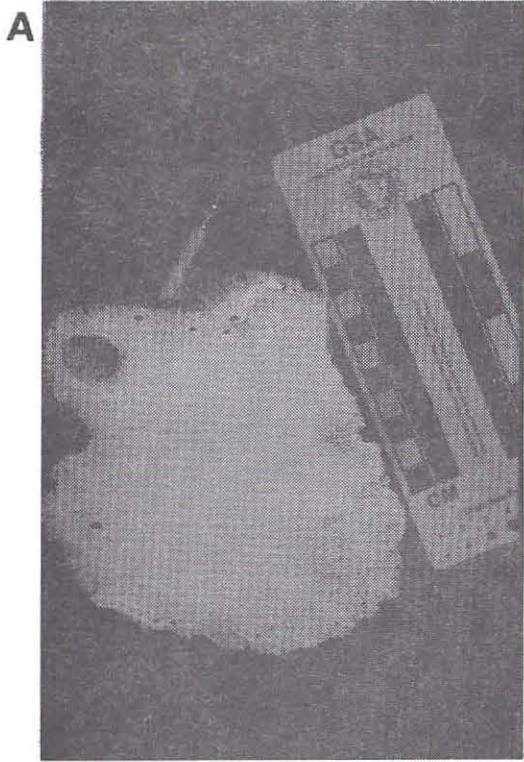
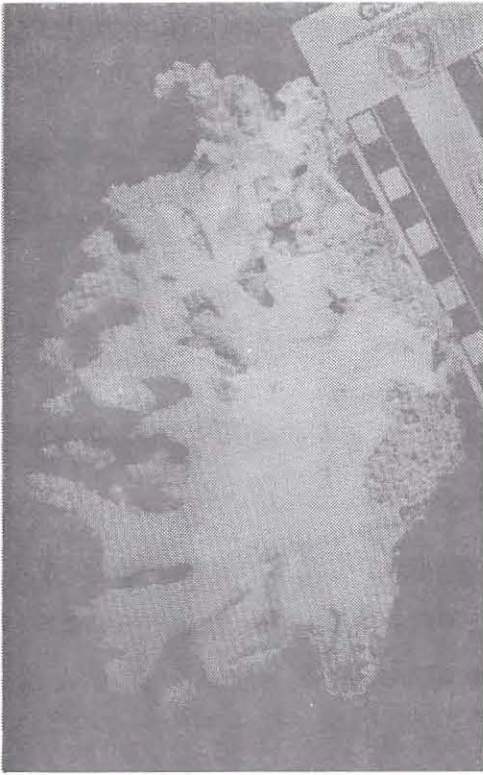
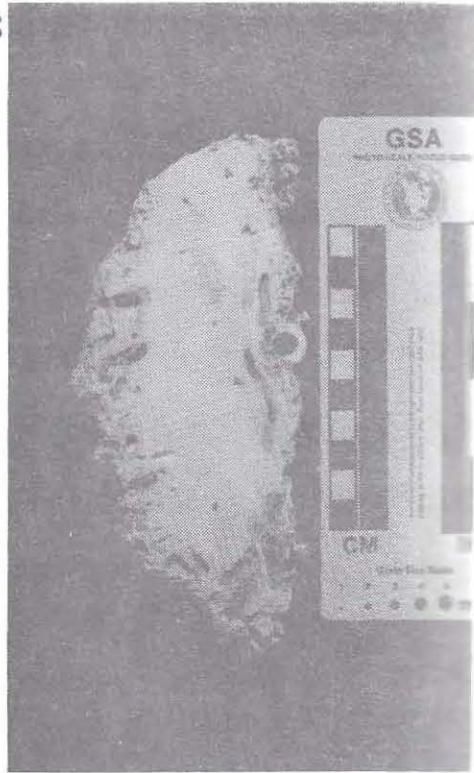


Plate 3.

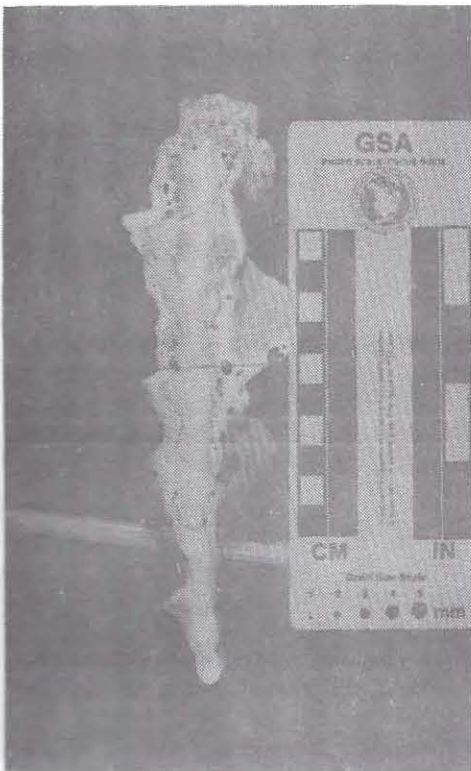
A



B



C



D

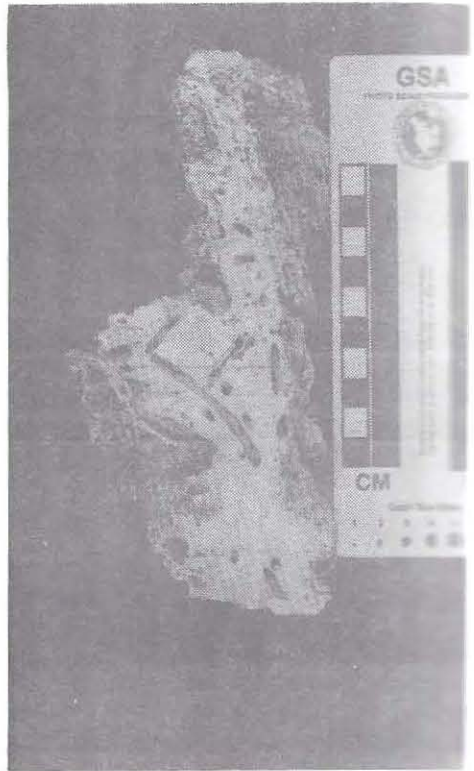


Plate 4.

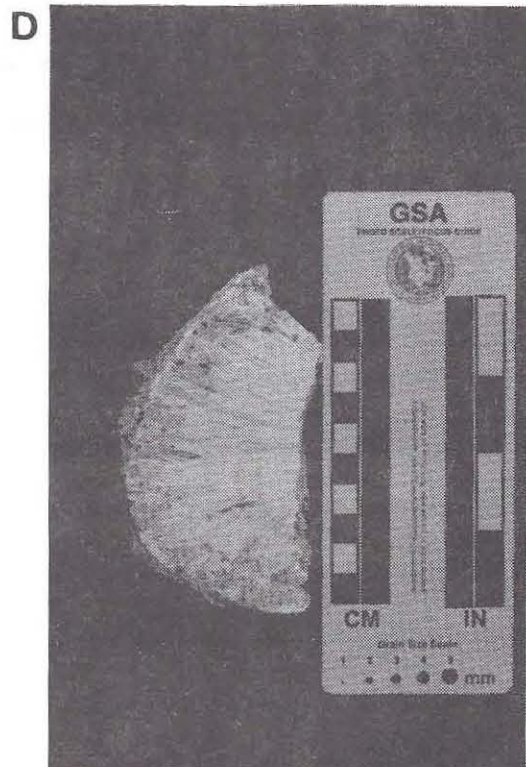
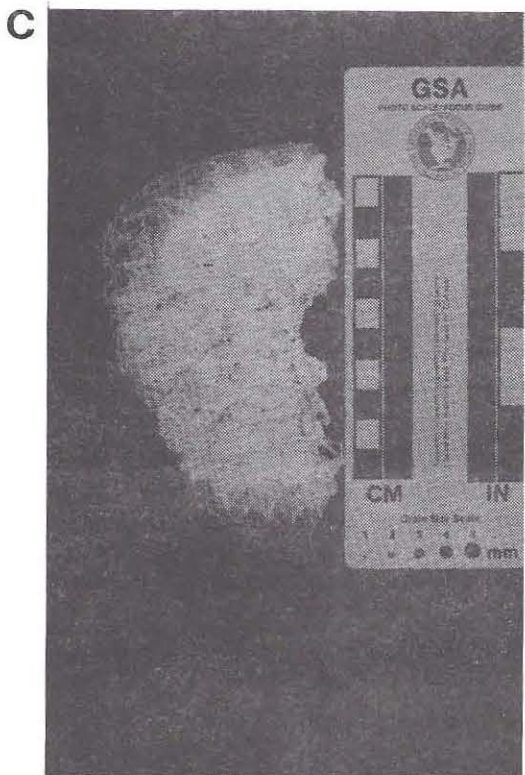
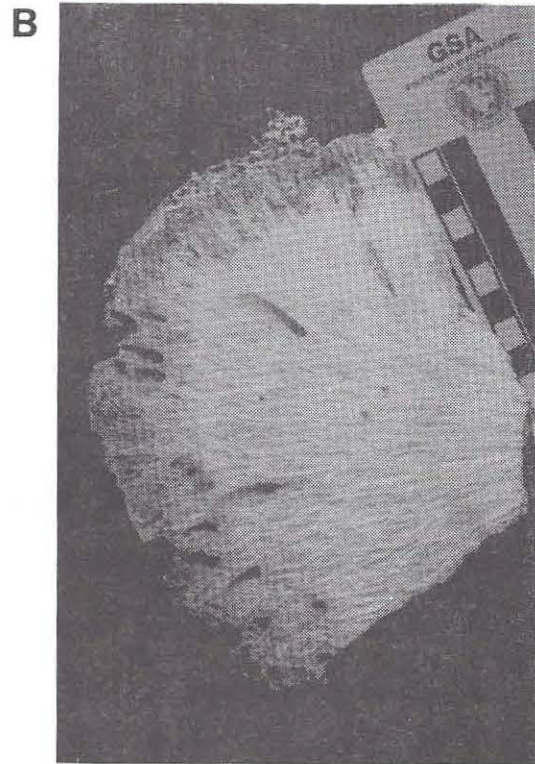
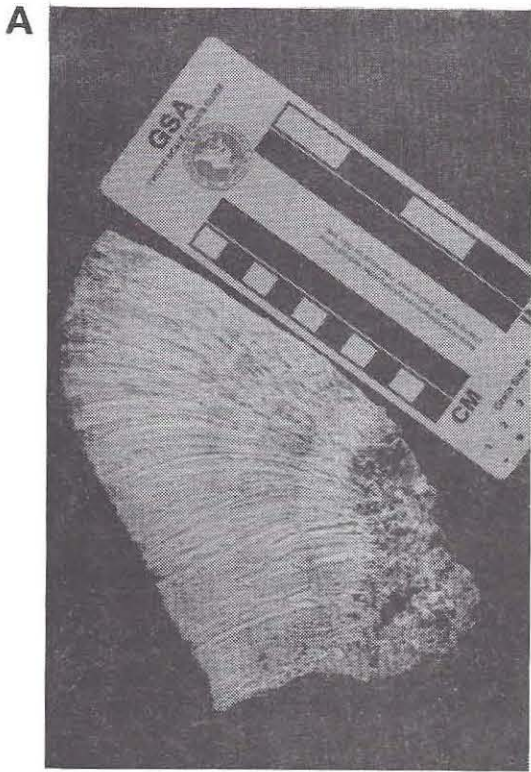


Plate 5.

From the above results and observations, it appears that the main reason for increased bioerosion in the affected area is the lack of living coral cover. The absence of a veneer of coral polyps allows for open areas on the reef skeletal framework surface suitable for the settlement of the larvae of bioeroding organisms. Subsequent growth and activity of borers can then riddle the skeleton with tubes and holes (Plates 3, 4, 5). Because living corals in both transects are primarily bioeroder-free, the presence of living coral polyps must have an inhibiting effect on bioeroder larval settlement.

Unfortunately a true analysis of differences in types of bioeroders owing to the effects of hot water effluent was not possible because a comparison of living control corals to dead affected corals was made. A study of dead corals in both areas would be necessary to yield such information. An adequate number of dead Transect A samples was not available.

Although not statistically significant ($p > .05$) in this experiment, an apparent difference in degree of bioerosion in different coral genera is evident. Visual study of slabs seemed to indicate that some coral genera had higher percentages of borings along with differing dominant bioeroder types. For instance, *Pocillopora sp.* appears to be favored by clionid sponges. Point count data indicate that the corals with the highest

susceptibility to bioerosion are *Pocillopora sp.* and *Goniastrea sp.*

Another apparent trend ($p < .06$) is that of bioerosion versus depth. Jones and Randall (1973) indicated some stratification of the hot water in the uppermost one meter of the water column in the affected area. Grouping of percent bioerosion according to depth appears to indicate more bioerosion occurring in the uppermost one meter. This seems to indicate that there may be an enhancement of bioeroder activity in this warmer upper stratified layer.

The thin section study of microbioeroders (Appendix C) showed no significant difference in percent microbioerosion between samples in Transect A and Transect B. Since it has been shown that the presence of endolithic blue-green algae is primarily a surficial feature (Bathurst, 1976), it is conjectured that the presence of microborings within the coral skeleton interior is a remnant of bioerosion occurring during coral skeletal growth. In Transect B, this would have occurred before the area was affected by hot water effluent.

Encrustation at Tanguisson:

Percent encrustation (Tables 7, 8) may vary on natural versus heat stressed samples. Although not significant at the 95% probability level, The ANOVA

($p < .09$, $p < .10$), along with visual evidence give credence to a probable increased rate of settlement of encrusting organisms in Transect B. Visual evidence includes the fact that most dead coral surfaces in Transect B were totally covered by a combination of predominantly crustose coralline red algae, vermetid molluscs, and blue-green algae (Plates 3-5). Encrusting foraminiferids, especially the bright red *Homotrema* sp., are also observed. Dead coral surfaces in Transect A were usually covered with the same encrusting forms as those found in Transect B.

It appears that the presence of encrusting forms, like bioeroders, is a function of the presence of uninhabited dead coral skeletal surfaces available for settlement and growth. When the corals in the affected area died, the bare rock surfaces that were created were readily inhabited by encrusters and bioeroders alike. The point count method used in this study may not be adequate to accurately measure encrustation. When a slice through the interior of a sample is studied, encrusters are usually represented as a relatively thin (<1cm) veneer around the edge. The encruster veneer thickness is usually not constant, and relatively thick deposits of encrusters can be discerned when a sample is studied in three dimensions. A method which probably would yield more accurate results would be to compare volume of coral skeleton per volume of encrusters

present in a sample of given dimensions. It is apparent that more study is needed to verify the incidence of increased encrustation as a result of hot water effluent.

Strontium Anomalies at Tanguisson:

Mean concentrations of strontium are significantly lower (Tables 11 and 12) in Transect B samples (6082 ppm versus 6595 ppm in Transect A). However, concentration values in samples from Transect B range from 4186 to 7145 ppm (Table 9), with 14 out of 21 values falling within one standard deviation of the mean concentration of Transect A samples. From this it is apparent that the occurrence of lower strontium values is not a consistent feature of the affected transect.

Lower strontium values in Transect B were observed to occur regularly in samples with a higher point-counted percentage of encrusting organisms. Because most of these encrusters grow skeletons of calcite containing low strontium concentrations relative to aragonite coral skeletons (Scoffin, 1987), lower whole rock Sr concentrations would be expected with increasing percentages of encrusters. It appears that low strontium values in Transect B are a result of dilution of coral skeletal material with calcite skeletal material from encrusting organisms. This finding also gives support to the suggestion that the affected area has experienced a

higher rate of growth of encrusting organisms since the coral mass mortality event of 1971.

Carbonate Cements:

As indicated in the RESULTS section, no difference in rate of cement deposition or types of cements present was observed between Transects A and B. It appears that carbonate cements cannot be used as indicators of hot water effluent diagenesis, at least when temperature differences similar to those found at Tanguisson (approx. 6°C) are involved.

Holocene:

As indicated, recent bioerosion was insubstantial in the Holocene transects. Studies of strontium concentrations and carbonate cements in the Holocene samples revealed no discernible differences. It is apparent that no observable diagenetic overprint has been left on the Holocene intertidal reef framework as a result of hot water effluent at Tanguisson.

Diagenetic Model:

The results of this study have made it possible to construct a tentative model for diagenesis of a modern tropical coral reef after massive mortality of living corals resulting from power plant hot water effluent. When reef limestone remains in a marine diagenetic

environment, observable features include the increased presence of bioeroders, possibly dominated by clionid sponges and polychaetes. Mean slabbed surface area percentages for bioerosion (borings) may approach 9.8 ± 4.5 , as opposed to a control value of $4.9 \pm 4.8\%$. This may be accompanied by an increased percentage of encrusting organisms present as veneers and/or infilled pockets, possibly dominated by vermetid molluscs and crustose coralline red algae. These features will be accompanied by a whole rock decrease in strontium concentration caused by the dilution of relatively high Sr-bearing aragonite coral skeletons with encrusting organisms having calcite skeletons of relatively low Sr content. As percentage of encrusters increases, whole rock strontium concentration will generally decrease. No discernible differences in carbonate cement types, morphologies, precipitation rates, or magnesium content within these cements, are expected.

If the reef limestone has been introduced into a freshwater diagenetic environment, it is probable that the above model features will be obscured as seen in the Pleistocene Mariana Limestone (Plate 2). Original skeletal textures and bioerosion may be discernible only when cathodoluminescence or ultraviolet/blue light fluorescence microscopy (Dravis and Yurewicz, 1985) are used. The original strontium signature would be obliterated during freshwater diagenesis (Kinsman, 1969).

Implications at Tanguisson:

The structural integrity of the affected reef at Tanguisson is undoubtedly being reduced as a result of increased bioerosion. Many of the observed slabs were fragile and riddled with borings. Some addition of material by encrusting red algae and vermetid gastropods is occurring, but does not appear to outweigh the loss of reef rock from bioerosion. No strong cementation is occurring to help strengthen the interior of this reef.

It is probable that over the next few years wave activity from large storms and typhoons will physically break up this area of already weakened reef, increasing the potential for damage to the Tanguisson shoreline and the power plant. This also may be indicative of what may happen as a result of coral mortality caused by other man-induced problems such as pollution and reef siltation (Dahl and Salvat, 1988) on Guam and elsewhere in the tropics.

Global Implications:

The effect of El Niño-Southern Oscillation (ENSO) which appears to be most important to reef-building coral survival is that of temperature. The 1982-83 major ENSO event caused a rise in surface sea temperature in the Eastern Pacific of from 1° to 5°C (Glynn et al., 1988). This was accompanied by coral bleaching (loss of zooxanthellae) and eventual death of coral polyps over

several weeks. From these observations it has been postulated that abnormally high (30-31°C in the Eastern Pacific) surface seawater temperatures present for prolonged periods (4-5 months) are responsible for reef-building coral mortality (Glynn, 1988).

As for recovery of corals after the 1982-83 ENSO event, Glynn (1988) observed little recruitment of new corals in the Eastern Pacific, and also noted that intense bioerosion of dead coral substrate has occurred.

It appears that the temperature effects noted at Tanguisson are similar to those of natural sudden abnormal surface seawater temperature rises such as those during the 1982-83 ENSO. Intense bioerosion following major ENSO events may lead to physical destruction of affected reefs. This in turn may allow for increased damage to shorelines which were once protected by these reefs.

The model of reef diagenesis at Tanguisson may also be applied to the identification of past large-scale ENSO events. Such events possibly can be noted in the stratigraphic record by identifying skeletal limestones with increased bioerosion, along with encrusters occurring as veneers over a large areal extent. This paleoecological data may be accompanied by a whole rock depletion in strontium owing to the increased presence of encrusters.

CONCLUSION

The results of this study have made it possible to generate a tentative model for modern reef diagenesis occurring as a result of sudden abnormal increases in surface seawater temperature beyond coral tolerances.

Model diagenetic effects occur after mass mortality of reef-building corals in the elevated temperature area.

For the marine diagenetic environment, we can expect:

A. an increased percentage of bioerosion, probably caused by the availability of inhabitable substrate after death of the corals. Mean slabbed areal percentages may be approximately $9.8 \pm 4.5\%$ in the tropical Western Pacific;

B. an increased percentage of encrusting forms present as extensive veneers and filling irregular pockets on the reef rock surface. Presence of encrusters also is probably due to increased available substrate after coral death;

C. a decrease in whole rock strontium concentration from that of 100% coral skeletal material due to an increase in low Sr-bearing encrusting forms.

If the reef limestone is moved into a freshwater diagenetic environment, the above features may become obscured or obliterated upon dissolution of aragonite with subsequent precipitation of calcite.

At Tanguisson, an area of sustained elevated surface

seawater temperature, the eventual physical breakup of the affected reef, already weakened by bioerosion, is likely. The Tanguisson shoreline and the power plant will be more susceptible to storm damage due to the absence of this protective reef.

Large scale El Niño-Southern Oscillation events may be followed by a similar sequence of events as those at Tanguisson. Slow recovery after the 1982-83 ENSO is probably at least partly responsible for an increase in bioerosion in these areas. The Tanguisson model also may be of use as a tool in pinpointing past major ENSO events in the stratigraphic record.

APPENDIX A. Statistical Methods and Computer Programs

Analysis of Variance:

Tests of significance for bioerosion, encrustation, and strontium concentration were performed using two-way analysis of variance (ANOVA) with replication (Sokal and Rohlf, 1987). A two-way ANOVA table with explanation is given in Table A-1.

Table A-1. Schematic two-way ANOVA table for results in text table 3.

Source of Variation	df	SS	MS	F _s
A (columns; treatments)	1	0.019	0.019	*
B (rows; genera)	6	0.021	0.003	*
A x B (interaction)	6	0.006	0.001	*
Within subgroups (error)	27	0.055	0.002	
Total	40	0.101		

The first column indicates source of variation as between treatments; between coral genera; interaction of A and B, the two main effects (dependence of the effect of one factor on the other factor); within subgroups; and a total (all groups taken as a single sample).

The second column gives degrees of freedom (df). Calculations can be found in Sokal and Rohlf (1987, page 190). The third column gives calculated sums of squares (SS). Calculations can be found in Sokal and Rohlf (1987, pages 187-189). The fourth column indicates mean

squares (MS), simply calculated as SS/df . The last column of the standard ANOVA table gives an F value to be used in an F-test of significance as described by Sokal and Rohlf (1987). Values are not presented in Table A-1, as SYSTAT software was used to calculate the ANOVA values (Wilkinson, 1987). Output from SYSTAT gives a probability value (p) of acceptance of the null hypothesis, as an F-test is done along with the ANOVA calculations. P-values are shown in the last column of the textual ANOVA tables.

Simple Regression:

A simple regression of strontium values for eight standardized samples (APPENDIX D) was done using the regression formula $I = mC + b_0$ where $I =$ XRF intensity, and $C =$ Sr concentration in parts per million. SYSTAT software (Wilkinson, 1987) was used to calculate values for m (0.080) and b_0 (0.528). The SYSTAT generated r^2 for the standard calibration curve is 0.999. Unknown sample concentrations were determined by solving the regression formula for C .

X-Ray Fluorescence Automatic Command Files:

Automatic command files (ATO's) are a sequence of recorded commands which will perform desired data collection and reduction tasks on an automatic basis (Kevex Corporation, 1982). This gives one the ability to

collect spectra for an entire platter of samples on computer disk, and then analyze each spectrum in identical fashion with limited input from the operator.

To save spectra, the following manual commands were made:

1. Set detector to desired Kv and mA settings, and move to desired target manually.

2. Computer commands:

PRE - sets desired preset count time.

SETEV - sets spectrometer to desired EV/CH (electron volts per channel).

SETLA - sets the last sample position.

SETID - allows input of sample identification to correspond to its platter position.

For this study, a data collection ATO entitled 1DATACOL was used to collect and save spectra. This program was activated by typing ATO,1DATACOL. The series of commands included in the ATO are as follows:

RON,1DATACOL - record on, activates storage of chained commands and names ATO.

CLR1 - clears spectrometer for spectrum acquisition.

ACQ1 - acquires spectrum.

WAI - display of WAIT-ACQUIRING banner.

REA - reads spectrum into data file.

SAV - saves spectrum to disk.

1 - directs spectrum to be saved on disk drive #1.

SETPO - directs platter to move to next sample position.

+ - directs platter to move to next higher position.

LOOP - repeat execution of ATO on next sample.

ROF - command recording off.

Sample spectra were analyzed using an ATO entitled RBSRINT. This was activated by typing ATO,RBSRINT. The series of commands included in the ATO are:

RON,RBSRINT - same as 1DATACOL.

RCL - recalls spectrum from disk and displays it on screen.

1 - directs the recall command to recall from disk drive #1.

ESC - removal of escape peaks.

SMO - smoothing of spectrum.

BKZ - removes previous background models.

BKM - allows for construction of new background model (during ATO input, desired background must be marked for removal. For this study, background was marked at 13.32, 13.64, 14.50, and 14.76 Kev.)

BKS - subtracts background.

SETGA - sets area of intensity peak to be integrated.

(during ATO input, desired peak gates must be marked. For this study, gates were set at 13.84-14.44 Kev.)

INT - integrates area of intensity peak indicated.

SETPO - same as 1DATACOL.

+ - same as 1DATACOL.

LOOP - same as 1DATACOL.

ROF - same as 1DATACOL.

Appendix B: Macrobioerosion Point Count Data and Slab Descriptions

TRANSECT A

Sample # RHR1246-1A

CUE 3 Area 21935.3

<u>GRAIN TYPE</u>	<u>POINT COUNT</u>	<u>PERCENTAGE</u>
Primary Framework	124	71.26
Secondary Framework		
Encrusters	2	1.15
Other	0	0.00
Bioerosion (Borings)	4	2.30
Cemented Detritus	0	0.00
Primary Porosity (Cavities)	44	25.29
TOTAL	174	100.00

Notes: Live *Pocillopora setchelli*.

Reef Front Slope, Upper Part, 1.0m depth.

Eroders-clionid sponges exclusively, small <1mm borings along coral fingers. Encrusters-*Homotrema sp.* and red algae near base, vermetid molluscs.

Sample # RHR1246-2A

CUE 3 Area 22407.6

<u>GRAIN TYPE</u>	<u>POINT COUNT</u>	<u>PERCENTAGE</u>
Primary Framework	121	67.60
Secondary Framework		
Encrusters	19	10.61
Other	0	0.00
Bioerosion (Borings)	26	14.53
Cemented Detritus	0	0.00
Primary Porosity (Cavities)	13	7.26
TOTAL	179	100.00

Notes: Partly dead *Goniastrea retiformis*.

Reef Front Slope, 1.0m depth.

Eroders-Clionid sponge predominates. Infestation with barnacles evident at earlier growth stage.

Encrusters-red algae, vermetid molluscs, *Homotrema sp.*

Sample # RHR1246-3A

CUE 3 Area 23152.5

<u>GRAIN TYPE</u>	<u>POINT COUNT</u>	<u>PERCENTAGE</u>
Primary Framework	169	88.48
Secondary Framework		
Encrusters	3	1.57
Other	0	0.00
Bioerosion (Borings)	4	2.09
Cemented Detritus	0	0.00
Primary Porosity (Cavities)	15	7.85
TOTAL	191	99.99

Notes: Dead *Goniastrea retiformis*.

Reef Front Slope, Channel Wall, 1.5m depth.

Eroders-Polychaetes and clionid sponge.

Encrusters-*Homotrema sp.*, red algae, blue-green algae, vermetid molluscs.

Sample # RHR1246-5A

CUE 3 Area 21232.1

<u>GRAIN TYPE</u>	<u>POINT COUNT</u>	<u>PERCENTAGE</u>
Primary Framework	141	78.77
Secondary Framework		
Encrusters	16	8.94
Other	0	0.00
Bioerosion (Borings)	8	4.47
Cemented Detritus	0	0.00
Primary Porosity (Cavities)	14	7.82
TOTAL	179	100.00

Notes: Live *Goniastrea retiformis*.

Reef Front Slope, Channel Wall Margin, 1.25m depth.

Endolithic barnacles present at surface, alive at time of collection. Eroders-clionid sponge.

Encrusters-vermetid molluscs, *Homotrema sp.*

Sample # RHR1246-6A

CUE 3 Area 23332.1

<u>GRAIN TYPE</u>	<u>POINT COUNT</u>	<u>PERCENTAGE</u>
Primary Framework	96	53.33
Secondary Framework		
Encrusters	27	15.00
Other	0	0.00
Bioerosion (Borings)	18	10.00
Cemented Detritus	1	0.56
Primary Porosity (Cavities)	38	21.11
TOTAL	180	100.00

Notes: Partly live *Pocillopora setchelli*.

Reef Front Slope, 1.5m depth.

Eroders-extensive clionid sponge borings.

Encrusters-red algae, vermetid molluscs, *Homotrema sp.*

Sample # RHR1246-7A

CUE 3 Area 26442.2

<u>GRAIN TYPE</u>	<u>POINT COUNT</u>	<u>PERCENTAGE</u>
Primary Framework	166	75.80
Secondary Framework		
Encrusters	11	5.02
Other	0	0.00
Bioerosion (Borings)	26	11.87
Cemented Detritus	0	0.00
Primary Porosity (Cavities)	16	7.31
TOTAL	219	100.00

Notes: Live *Millepora platyphylla*.

Outer Reef Margin, 0.25m depth.

Eroders-clionid sponge, polychaetes.

Encrusters-red algae overlain by new coral growth. Also blue-green algae, vermetid molluscs, *Homotrema sp.*

Sample # RHR1246-8A

CUE 3 Area 23503.2

<u>GRAIN TYPE</u>	<u>POINT COUNT</u>	<u>PERCENTAGE</u>
Primary Framework	144	78.26
Secondary Framework		
Encrusters	13	7.07
Other	0	0.00
Bioerosion (Borings)	0	0.00
Cemented Detritus	2	1.09
Primary Porosity (Cavities)	25	13.59
TOTAL	184	100.01

Notes: Live *Acropora digitifera*.

Reef Front Slope, 1.5m depth.

Eroders-scattered small clionid sponge borings.

Encrusters-vermetid molluscs, red algae, *Homotrema sp.*

Sample # RHR1246-9A

CUE 3 Area 22011.0

<u>GRAIN TYPE</u>	<u>POINT COUNT</u>	<u>PERCENTAGE</u>
Primary Framework	95	53.37
Secondary Framework		
Encrusters	19	10.67
Other	0	0.00
Bioerosion (Borings)	18	10.11
Cemented Detritus	0	0.00
Primary Porosity (Cavities)	46	25.84
TOTAL	178	99.99

Notes: Live *Pocillopora setchelli*.

Reef Margin, 0.5m depth.

Eroders-large clionid sponge borings at base.

Encrusters-vermetid molluscs, red algae, *Homotrema sp.*

Sample # RHR1246-9AB

CUE 3 Area 23484.3

<u>GRAIN TYPE</u>	<u>POINT COUNT</u>	<u>PERCENTAGE</u>
Primary Framework	142	72.08
Secondary Framework		
Encrusters	41	20.81
Other	0	0.00
Bioerosion (Borings)	4	2.03
Cemented Detritus	0	0.00
Primary Porosity (Cavities)	10	5.08
TOTAL	197	100.00

Notes: Dead *Acropora* sp.

Reef Front Slope, Channel Floor, 2.5m depth.

Eroders-polychaetes, clionid sponge.

Encrusters-red algae, vermetid molluscs, *Homotrema* sp.

Sample # RHR1246-10A

CUE 3 Area 21647.6

<u>GRAIN TYPE</u>	<u>POINT COUNT</u>	<u>PERCENTAGE</u>
Primary Framework	128	68.09
Secondary Framework		
Encrusters	0	0.00
Other	0	0.00
Bioerosion (Borings)	10	5.32
Cemented Detritus	0	0.00
Primary Porosity (Cavities)	50	26.60
TOTAL	188	100.01

Notes: Live *Pocillopora setchelli*.

Reef Front Slope, 1.5m depth.

Eroders-clionid sponge borings along margins of digits.

Encrusters-red algae, vermetid molluscs, *Homotrema* sp.

Sample # RHR1246-11A

CUE 3 Area 22410.1

<u>GRAIN TYPE</u>	<u>POINT COUNT</u>	<u>PERCENTAGE</u>
Primary Framework	167	94.35
Secondary Framework		
Encrusters	6	3.39
Other	0	0.00
Bioerosion (Borings)	2	1.13
Cemented Detritus	0	0.00
Primary Porosity (Cavities)	2	1.13
TOTAL	177	100.00

Notes: Live *Favia matthaii*.

Reef Front Slope, Channel Wall Shelf, 1.5m depth.

Eroders-clionid sponge.

Encrusters-dead basal area contains red algae, *Homotrema* sp.

Sample # RHR1246-12A

CUE 3 Area 22049.9

<u>GRAIN TYPE</u>	<u>POINT COUNT</u>	<u>PERCENTAGE</u>
Primary Framework	155	87.08
Secondary Framework		
Encrusters	18	10.11
Other	0	0.00
Bioerosion (Borings)	3	1.69
Cemented Detritus	0	0.00
Primary Porosity (Cavities)	2	1.12
TOTAL	178	100.00

Notes: Live *Millepora platyphylla*.

Reef Front Slope, 1.0m depth.

Eroders-very few borings, clionid sponge, sipunculans, polychaetes. Encrusters-red algae and vermetid molluscs overlain by new coral growth.

Sample # RHR1249-1A

CUE 3 Area 21759.1

<u>GRAIN TYPE</u>	<u>POINT COUNT</u>	<u>PERCENTAGE</u>
Primary Framework	120	69.77
Secondary Framework		
Encrusters	33	19.19
Other	0	0.00
Bioerosion (Borings)	9	5.23
Cemented Detritus	0	0.00
Primary Porosity (Cavities)	10	5.81
TOTAL	172	100.00

Notes: Live *Millepora platyphylla* encrusting dead *Lobophyllia hemprichii*. Reef Front Slope, Channel Wall, 2.5m depth. Eroders-clionid sponge, polychaetes in *Millepora*; large polychaetes in *Lobophyllia*. Encrusters-vermetid molluscs, red algae.

Sample # RHR1249-3A

CUE 3 Area 21624.2

<u>GRAIN TYPE</u>	<u>POINT COUNT</u>	<u>PERCENTAGE</u>
Primary Framework	178	97.27
Secondary Framework		
Encrusters	2	1.09
Other	0	0.00
Bioerosion (Borings)	2	1.09
Cemented Detritus	0	0.00
Primary Porosity (Cavities)	1	0.55
TOTAL	183	100.00

Notes: Live *Favia rotumana*.

Reef Front Slope, Channel Floor on a Block, 2.0m depth.

Endolithic barnacle near surface. Eroders-irregular boring near upper surface may be clionid sponge.

Encrusters-red algae, *Homotrema sp.* on underside.

Sample # RHR1249-5A

CUE 3 Area 21780.6

<u>GRAIN TYPE</u>	<u>POINT COUNT</u>	<u>PERCENTAGE</u>
Primary Framework	171	92.43
Secondary Framework		
Encrusters	11	5.95
Other	0	0.00
Bioerosion (Borings)	3	1.62
Cemented Detritus	0	0.00
Primary Porosity (Cavities)	0	0.00
TOTAL	185	100.00

Notes: Live *Goniatrea retiformis*.

Reef Front Slope, 2.5m depth.

Eroders-clionid sponge. Large cavity may represent older excavation by unknown eroder.

Encrusters-red algae on exposed dead surfaces.

Sample # RHR1249B-11A

CUE 3 Area 22030.0

<u>GRAIN TYPE</u>	<u>POINT COUNT</u>	<u>PERCENTAGE</u>
Primary Framework	186	98.41
Secondary Framework		
Encrusters	1	0.53
Other	0	0.00
Bioerosion (Borings)	2	1.06
Cemented Detritus	0	0.00
Primary Porosity (Cavities)	0	0.00
TOTAL	189	100.00

Notes: Loose cobble of *Acropora sp.*

Reef Front Slope, Channel Floor, 3.0m depth.

Eroders-1 polychaete boring.

Encrusters-sparse blue-green algae.

Sample # RHR1346-13A

CUE 3 Area 22243.4

<u>GRAIN TYPE</u>	<u>POINT COUNT</u>	<u>PERCENTAGE</u>
Primary Framework	135	80.84
Secondary Framework		
Encrusters	8	4.79
Other	0	0.00
Bioerosion (Borings)	24	14.37
Cemented Detritus	0	0.00
Primary Porosity (Cavities)	0	0.00
TOTAL	167	100.00

Notes: Dead *Acropora sp.* (corymbose form).

Reef Margin, 1.2m depth.

Eroders-clionid sponge, polychaetes.

Encrusters-red algae, blue-green algae, *Homotrema sp.*

Sample # RHR1371-2A

CUE 3 Area 21663.6

<u>GRAIN TYPE</u>	<u>POINT COUNT</u>	<u>PERCENTAGE</u>
Primary Framework	167	94.89
Secondary Framework		
Encrusters	2	1.14
Other	0	0.00
Bioerosion (Borings)	5	2.84
Cemented Detritus	0	0.00
Primary Porosity (Cavities)	2	1.14
TOTAL	176	100.01

Notes: Live *Favites abdita*.

Outer Reef Flat Platform, 0.3m depth.

Eroders-small clionid sponge borings between corallites.

Encrusters-vermetid molluscs.

Sample # RHR1373-4A

CUE 3 Area 21240.4

<u>GRAIN TYPE</u>	<u>POINT COUNT</u>	<u>PERCENTAGE</u>
Primary Framework	124	71.26
Secondary Framework		
Encrusters	2	1.15
Other	0	0.00
Bioerosion (Borings)	3	1.72
Cemented Detritus	0	0.00
Primary Porosity (Cavities)	45	25.86
TOTAL	174	99.99

Notes: Live *Pocillopora setchelli*.

Reef Margin, 0.4m depth.

Eroders-few sponge borings at bases of digits.

Encrusters-vermetid molluscs, *Homotrema sp.* at base.

TRANSECT B

Sample # RHR1247-2A

CUE 3 Area 22685.8

<u>GRAIN TYPE</u>	<u>POINT COUNT</u>	<u>PERCENTAGE</u>
Primary Framework	150	78.53
Secondary Framework		
Encrusters	12	6.28
Other	0	0.00
Bioerosion (Borings)	29	15.18
Cemented Detritus	0	0.00
Primary Porosity (Cavities)	0	0.00
TOTAL	191	99.99

Notes: Dead *Goniastrea retiformis*.

Outer Reef Margin, Surge Channel Margin, 1.0m depth.

Eroders-polychaetes, clionid sponge near surface,

sipunculid. Encrusters-vermetid molluscs, red algae, blue-green algae.

Sample # RHR1247-3A

CUE 3 Area 21982.4

<u>GRAIN TYPE</u>	<u>POINT COUNT</u>	<u>PERCENTAGE</u>
Primary Framework	79	45.93
Secondary Framework		
Encrusters	34	19.77
Other	0	0.00
Bioerosion (Borings)	24	13.95
Cemented Detritus	0	0.00
Primary Porosity (Cavities)	35	20.35
TOTAL	172	100.00

Notes: Dead *Pocillopora setchelli*.
Reef Front Slope, Upper Part, 0.5m depth.
Eroders-clionid sponge, polychaetes.
Encrusters-blue-green algae, red algae, vermetid molluscs, *Homotrema sp.*

Sample # RHR1247-4A

CUE 3 Area 22846.4

<u>GRAIN TYPE</u>	<u>POINT COUNT</u>	<u>PERCENTAGE</u>
Primary Framework	49	25.79
Secondary Framework		
Encrusters	81	42.63
Other	1	0.53
Bioerosion (Borings)	18	9.47
Cemented Detritus	0	0.00
Primary Porosity (Cavities)	41	21.58
TOTAL	190	100.00

Notes: Dead *Pocillopora setchelli*.
Reef Margin, 0.7m depth.
Eroders-extensive clionid sponge borings, polychaetes.
Encrusters-highly covered with red algae, vermetid molluscs, *Homotrema sp.*, small byssally attached mussels.

Sample # RHR1247-5A

CUE 3 Area 22907.8

<u>GRAIN TYPE</u>	<u>POINT COUNT</u>	<u>PERCENTAGE</u>
Primary Framework	62	33.51
Secondary Framework		
Encrusters	105	56.76
Other	0	0.00
Bioerosion (Borings)	13	7.03
Cemented Detritus	0	0.00
Primary Porosity (Cavities)	5	2.70
TOTAL	185	100.00

Notes: Dead *Millepora platyphylla*.
Reef Front Slope, 1.0m depth.
Eroders-clionid sponge, polychaetes. Encrusters-vermetid molluscs, blue-green algae, *Homotrema sp.*

Sample # RHR1247-6A

CUE 3 Area 23430.3

<u>GRAIN TYPE</u>	<u>POINT COUNT</u>	<u>PERCENTAGE</u>
Primary Framework	111	58.42
Secondary Framework		
Encrusters	42	22.11
Other	0	0.00
Bioerosion (Borings)	24	12.63
Cemented Detritus	0	0.00
Primary Porosity (Cavities)	13	6.84
TOTAL	190	100.00

Notes: Dead *Pocillopora setchelli*.
Reef Front Slope, Upper Part, 1.2m depth.
Eroders-clionid sponge, polychaetes.
Encrusters-vermetid molluscs, blue-green algae.

Sample # RHR1247-7A

CUE 3 Area 21962.5

<u>GRAIN TYPE</u>	<u>POINT COUNT</u>	<u>PERCENTAGE</u>
Primary Framework	90	56.60
Secondary Framework		
Encrusters	18	11.32
Other	0	0.00
Bioerosion (Borings)	25	15.72
Cemented Detritus	0	0.00
Primary Porosity (Cavities)	26	16.35
TOTAL	159	99.99

Notes: Dead *Pocillopora setchelli*.
Reef Margin, Outer Part, 0.5m depth.
Eroders-polychaetes, extensive clionid sponge borings.
Encrusters-vermetid molluscs, blue-green algae, small
byssally attached mussels.

Sample # RHR1247-9A

CUE 3 Area 21402.8

<u>GRAIN TYPE</u>	<u>POINT COUNT</u>	<u>PERCENTAGE</u>
Primary Framework	126	71.19
Secondary Framework		
Encrusters	30	16.95
Other	0	0.00
Bioerosion (Borings)	13	7.34
Cemented Detritus	0	0.00
Primary Porosity (Cavities)	8	4.52
TOTAL	177	100.00

Notes: Dead *Acropora sp.*
Reef Front Slope, Mid Part, 1.5m depth.
Eroders-polychaetes, clionid sponge.
Encrusters-vermetid molluscs, red algae, blue green
algae, *Homotrema sp.*, *Halimeda sp.*

Sample # RHR1247-10A

CUE 3 Area 23542.6

<u>GRAIN TYPE</u>	<u>POINT COUNT</u>	<u>PERCENTAGE</u>
Primary Framework	102	51.26
Secondary Framework		
Encrusters	41	20.60
Other	0	0.00
Bioerosion (Borings)	17	8.54
Cemented Detritus	0	0.00
Primary Porosity (Cavities)	39	19.60
TOTAL	199	100.00

Notes: Dead *Pocillopora setchelli*.
Reef Front Slope, Upper Part, 1.0m depth.
Eroders-clionid sponge, polychaetes.
Encrusters-heavily covered with vermetid molluscs and red algae. Surface coated with blue-green algae.

Sample # RHR1247-11A

CUE 3 Area 21751.8

<u>GRAIN TYPE</u>	<u>POINT COUNT</u>	<u>PERCENTAGE</u>
Primary Framework	128	68.82
Secondary Framework		
Encrusters	18	9.68
Other	0	0.00
Bioerosion (Borings)	31	16.67
Cemented Detritus	0	0.00
Primary Porosity (Cavities)	9	4.84
TOTAL	186	100.01

Notes: Dead *Goniastrea retiformis*.
Outer Reef Margin, Upper Surge Channel, 1.0m depth.
Eroders-polychaetes, clionid sponge near surface.
Endolithic barnacle cavities in basal part.
Encrusters-blue-green algae, vermetid molluscs, red algae.

Sample # RHR1247-13A

CUE 3 Area 23171.2

<u>GRAIN TYPE</u>	<u>POINT COUNT</u>	<u>PERCENTAGE</u>
Primary Framework	105	58.01
Secondary Framework		
Encrusters	17	9.39
Other	0	0.00
Bioerosion (Borings)	25	13.81
Cemented Detritus	0	0.00
Primary Porosity (Cavities)	34	18.78
TOTAL	181	99.99

Notes: Dead *Millepora platyphylla*.
Reef Front Slope, 1.0m depth.
Eroders-polychaetes, clionid sponge.
Encrusters-blue-green algae, vermetid molluscs.

Sample # RHR1247-14A

CUE 3 Area 21738.3

<u>GRAIN TYPE</u>	<u>POINT COUNT</u>	<u>PERCENTAGE</u>
Primary Framework	114	65.14
Secondary Framework		
Encrusters	27	15.43
Other	0	0.00
Bioerosion (Borings)	22	12.57
Cemented Detritus	0	0.00
Primary Porosity (Cavities)	12	6.86
TOTAL	175	100.00

Notes: Dead *Acropora sp.*

Reef Front Slope Near Reef Margin, 0.5m depth.

Eroders-clionid sponge near surface, polychaetes.

Encrusters-vermetid molluscs, blue-green algae, red algae.

Sample # RHR1247-15A

CUE 3 Area 22496.7

<u>GRAIN TYPE</u>	<u>POINT COUNT</u>	<u>PERCENTAGE</u>
Primary Framework	116	63.74
Secondary Framework		
Encrusters	30	16.48
Other	0	0.00
Bioerosion (Borings)	26	14.29
Cemented Detritus	0	0.00
Primary Porosity (Cavities)	10	5.49
TOTAL	182	100.00

Notes: Dead *Goniastrea retiformis*.

Reef Front Slope, Inner Part

Eroders-polychaetes, sipunculids, clionid sponge near surface.

Encrusters-red algae, blue-green algae, vermetid molluscs.

Sample # RHR1247-16A

CUE 3 Area 22631.1

<u>GRAIN TYPE</u>	<u>POINT COUNT</u>	<u>PERCENTAGE</u>
Primary Framework	101	55.80
Secondary Framework		
Encrusters	15	8.29
Other	0	0.00
Bioerosion (Borings)	23	12.71
Cemented Detritus	0	0.00
Primary Porosity (Cavities)	42	23.20
TOTAL	181	100.00

Notes: Dead *Pocillopora setchelli*.

Reef Front Slope, Upper Part.

Eroders-polychaetes, clionid sponge. Encrusters-vermetid molluscs, red algae, blue-green algae, *Homotrema sp.*

Sample # RHR1248-1A

CUE 3 Area 21637.7

<u>GRAIN TYPE</u>	<u>POINT COUNT</u>	<u>PERCENTAGE</u>
Primary Framework	174	97.75
Secondary Framework		
Encrusters	0	0.00
Other	0	0.00
Bioerosion (Borings)	4	2.25
Cemented Detritus	0	0.00
Primary Porosity (Cavities)	0	0.00
TOTAL	178	100.00

Notes: *Acropora sp.* cobble.

Reef Front Slope, Channel Floor, 2.5m depth.

Eroders-polychaetes.

Encrusters-none.

Sample # RHR1248-2A&B

CUE 3 Area 21654.5

<u>GRAIN TYPE</u>	<u>POINT COUNT</u>	<u>PERCENTAGE</u>
Primary Framework	180	97.83
Secondary Framework		
Encrusters	0	0.00
Other	0	0.00
Bioerosion (Borings)	4	2.17
Cemented Detritus	0	0.00
Primary Porosity (Cavities)	0	0.00
TOTAL	184	100.00

Notes: *Acropora sp.* cobble.

Reef Front Slope, Channel Floor, 2.5m depth.

Eroders-polychaetes.

Encrusters-blue-green algae, *Homotrema sp.*

Sample # RHR1248-3A

CUE 3 Area 23542.4

<u>GRAIN TYPE</u>	<u>POINT COUNT</u>	<u>PERCENTAGE</u>
Primary Framework	154	85.56
Secondary Framework		
Encrusters	6	3.33
Other	0	0.00
Bioerosion (Borings)	20	11.11
Cemented Detritus	0	0.00
Primary Porosity (Cavities)	0	0.00
TOTAL	180	100.00

Notes: Dead *Favites abdita*.

Reef Front Slope, 2.0m depth.

Eroders-clionid sponge, polychaetes.

Encrusters-blue-green algae, *Homotrema sp.*

Sample # RHR1248-6A CUE 3 Area 22362.3

<u>GRAIN TYPE</u>	<u>POINT COUNT</u>	<u>PERCENTAGE</u>
Primary Framework	134	72.83
Secondary Framework		
Encrusters	27	14.67
Other	0	0.00
Bioerosion (Borings)	16	8.70
Cemented Detritus	0	0.00
Primary Porosity (Cavities)	7	3.80
TOTAL	184	100.00

Notes: Dead *Favia matthaii*.
Reef Front Slope, Channel Wall, 1.7m depth.
Eroders-clionid sponge near surface, polychaetes.
Encrusters-heavy coating of red algae, vermetid molluscs, *Homotrema sp.*

Sample # RHR1248-9A CUE 3 Area 22735.8

<u>GRAIN TYPE</u>	<u>POINT COUNT</u>	<u>PERCENTAGE</u>
Primary Framework	154	84.62
Secondary Framework		
Encrusters	14	7.69
Other	0	0.00
Bioerosion (Borings)	10	5.49
Cemented Detritus	0	0.00
Primary Porosity (Cavities)	4	2.20
TOTAL	182	100.00

Notes: Dead *Favia matthaii* overgrown by *Goniastrea retiformis*.
Reef Front Slope, 3.0m depth. Eroders-clionid sponge near surface, polychaetes. Encrusters-red algae, blue-green algae, vermetid molluscs.

Sample # RHR1248-10A CUE 3 Area 21703.5

<u>GRAIN TYPE</u>	<u>POINT COUNT</u>	<u>PERCENTAGE</u>
Primary Framework	151	84.36
Secondary Framework		
Encrusters	10	5.59
Other	0	0.00
Bioerosion (Borings)	16	8.94
Cemented Detritus	0	0.00
Primary Porosity (Cavities)	2	1.12
TOTAL	179	100.01

Notes: Dead *Favia matthaii*.
Reef Front Slope, Channel Wall, 2.5m depth.
Possible endolithic barnacles near base and radiating upward. Eroders-clionid sponge. Encrusters-vermetid molluscs, red algae, *Halimeda sp.*, *Homotrema sp.*

Sample # RHR1258-1A

CUE 3 Area 22032.7

<u>GRAIN TYPE</u>	<u>POINT COUNT</u>	<u>PERCENTAGE</u>
Primary Framework	150	81.97
Secondary Framework		
Encrusters	19	10.38
Other	0	0.00
Bioerosion (Borings)	14	7.65
Cemented Detritus	0	0.00
Primary Porosity (Cavities)	0	0.00
TOTAL	183	100.00

Notes: Partly dead *Goniastrea retiformis*.

Reef Front Slope, 2.5m depth.

Eroders-clionid sponge, polychaetes.

Encrusters-red algae, vermetid molluscs.

Sample # RHR1258-3A

CUE 3 Area 22223.3

<u>GRAIN TYPE</u>	<u>POINT COUNT</u>	<u>PERCENTAGE</u>
Primary Framework	160	87.43
Secondary Framework		
Encrusters	5	2.73
Other	0	0.00
Bioerosion (Borings)	1	0.55
Cemented Detritus	0	0.00
Primary Porosity (Cavities)	17	9.29
TOTAL	183	100.00

Notes: Live *Acropora surculosa*.

Reef Front Slope, 2.75m depth.

Eroders-clionid sponge along dead lower surface.

Encrusters-red algae, vermetid molluscs, *Homotrema sp.*
on dead lower surface.

Sample # RHR1258-4A

CUE 3 Area 23785.0

<u>GRAIN TYPE</u>	<u>POINT COUNT</u>	<u>PERCENTAGE</u>
Primary Framework	84	47.46
Secondary Framework		
Encrusters	0	0.00
Other	0	0.00
Bioerosion (Borings)	16	9.04
Cemented Detritus	0	0.00
Primary Porosity (Cavities)	77	43.50
TOTAL	177	100.00

Notes: Live *Pocillopora elegans*.

Reef Front Slope, 2.7m depth.

Eroders-polychaete borings in center of coral digits.

Encrusters-none.

APPENDIX C: Changes in Density of Endolithic Algal
Borings in Modern Reefal Carbonates Due to Temperature

INTRODUCTION

Studies of reef bioerosion have been undertaken for many reasons. Among these are identification of borings and borers (Golubic, 1969; Golubic et al, 1975; Warne, 1975), and the implications of degradation of reefal material (Tudhope and Risk, 1985). This study is primarily concerned with the latter, and will be limited to microborers, although macroborers such as polychaetes are also important removers of reef material.

The study area is located on Guam, Mariana Islands. Tanguisson Point, located on the west coast, is the site of a well-developed sand beach surrounded by steep limestone cliffs. A pronounced gap in the cliffs, once a coconut plantation, was chosen for the construction of the Tanguisson No. 1 and No. 2 thermoelectric plant in 1971 (Jones and Randall, 1973). Turbines are cooled by intake of seawater. Hot effluent seawater is pumped out of the plant directly onto the reef flat. When the plant began operation in 1971, corals in the effluent area were killed due to a rise in seawater temperature of approximately 6°C (Jones and Randall, 1973). See thesis text Figure 1.

This paper is part of a larger project to study the diagenetic effects observed at this site today. An

analysis of macrobioerosion in coral slabs from a control area compared to those from the hot water effluent area (see thesis text Figure 4) has been done. Results show that there is a greater amount of bioerosion in the effluent area due to either absence of living coral cover, hot water effects, or a combination of these. A similar analysis of microbioeroders is presented here to ascertain whether this trend holds true at the microscopic level.

Endolithic blue-green algae (Cyanophyta) are the most abundant microborer group in the intertidal zone (Golubic, 1969). Other microborers present here include red and green algae (Golubic, 1969) and fungi (Golubic et al, 1975).

Golubic (1969) describes actively boring endolithic algae as those having specialized filaments for penetration into the substrate. Penetration is attained presumably by dissolution of the rock. Cells are generally embedded in a gelatinous sheath, with those in the endolithic filaments spaced by gelatinous material. Photosynthetic pigments are present in the filaments (Fay, 1983). Borings are generally 4 to 15 μm in diameter (Golubic 1969). Boring algae are found in marine and freshwater environments, and are found in the supratidal zone down to the base of the photic zone (approximately 70 m) (Golubic et al, 1975).

Warne (1975) describes endolithic fungi as having

branching hyphae creating borings from 1 to 3 μm in diameter, with bulbous sporangia from 20 to 50 μm in diameter. Kohlmeyer (1969) indicates that fungi begin by roughening the surface until the substrate becomes spongy. Branching hyphae then penetrate further, reducing the integrity of the substrate. Golubic et al (1975) indicate that boring fungi are found in the intertidal zone but increase in abundance at depth in the oceans. This is due to the absence of the ability to photosynthesize, eliminating the need for sunlight penetration.

Bathhurst (1976) identifies major features which distinguish algal borings from those made by fungi. These features were taken from Bromley (1965).

"1. Fungal borings are on the whole finer than those of algae.

"2. The diameter of fungal borings is generally more or less constant while that of algae varies considerably.

"3. The mode of branching is characteristically 'false ramification' in algae, the thicker main borings giving the appearance of having been occupied by a bundle of threads which, separating individually, simulate branching. As a result of true ramification in fungi there is normally no sensible reduction in diameter from stem to branch. True ramification is also found in algae, however.

"4. The angle at which branches leave the major axis is very much more constant in fungi, and is often between 60° and 90° . Dichotomy is also common. Algae frequently branch very irregularly.

"5. Likewise the articles [cells] in fungi tend to be more or less straight or gently curved, while those of algae are sometimes very irregular. Overcrowding probably induces irregularity in some species of both types, but some fungi appear to remain invariably straight."

METHODS

Thin sections of four genera of corals from a control area and an area affected by hot water effluent (Transect B) were systematically point counted using a petrographic microscope equipped with a manual point counting stage. A total of 200 points were counted on each slide. Sections were counted at a magnification of 390x. Counts were grouped into the categories indicated in Figure 3.

The number of microborings counted (algae and fungi combined) was normalized by transforming it to a percentage of available substrate (available substrate equals total points counted minus primary porosity).

Sample statistics were calculated and a two-way analysis of variance (control vs. Transect B and genus vs. genus) was conducted (Sokal and Rohlf, 1987) to test

the null hypothesis that there is no significant difference in bioerosion between the control group and Transect B group.

RESULTS

Thin sections were predominantly made up of coral skeleton and primary porosity present within corallites. Lesser amounts of detritus and diagenetic cement were seen. See Table 1. Some specimens also were encrusted with polychaete tubes. Tubes were counted along with coral skeleton in the "skeletal" point count category of Table 1.

TABLE 1. Point Count Data. Numbers=Actual Number of Counted Points. L=Longitudinal Section, T=Transverse Section for *Goniastrea*.

1247-9A+B	Tran B	Acropora	1246-8A	Control	Acropora
Skeletal		97			113
Algal		15			20
Detritus		4			3
Cement		1			0
Macropores		83			64
Total		200			200

1247-2A	Tran B	<i>Goniastrea</i> (T)	1246-2A	Control	Gon(T)
Skeletal		94			96
Algal		16			29
Detritus		1			4
Cement		0			0
Macropores		89			71
Total		200			200

1247-11A	Tran B	<i>Goniastrea</i> (L)	1246-3A	Control	Gon(L)
Skeletal		78			85
Algal		17			14
Detritus		0			5
Cement		0			0
Macropores		105			96
Total		200			200

TABLE 1 Cont'd. Point Count Data. Numbers=Actual Number of Counted Points. L=Longitudinal Section, T=Transverse Section for Goniastrea.

1247-10A	Tran B	Pocillopora	1246-1A	Control	Poc
Skeletal		88		98	
Algal		12		21	
Detritus		6		0	
Cement		8		1	
Macropores		86		80	
Total		200		200	

Adjusted percentages of algal bioerosion were averaged for the control and the affected (Transect B) groups. These were calculated to be 17.04 ± 4.00 and 13.91 ± 3.09 respectively. Surprisingly, the mean of the control was greater than that of the affected area. A T-test of these means shows that they are not significantly different from each other ($p < .05$), so it is appropriate to assume that the amount of microbioerosion is not a function of increase in water temperature or absence of living coral cover at this scale.

A two-way analysis of variance was also performed to indicate significant differences in microbioerosion between coral genera, as well as between control and affected groups. The ANOVA showed no significant difference between coral genera ($p < .01$), and again no significant difference between treatment groups ($0.05 < p < .10$). See Table 2.

TABLE 2. Analysis of Variance.

ANALYSIS OF VARIANCE

SOURCE	Sum-Of-Squares	DF	Mean-Square	F-Ratio
Treatment	0.002	1	0.002	0.010
Genus	0.003	3	0.001	0.005
Treatment* Genus	0.005	3	0.002	0.009
Error	0.192	1	0.192	

DISCUSSION

At the microscopic level studied here, it appears that neither an increase in ambient water temperature or loss of coral cover and increase in available substrate are mechanisms that will increase or decrease bioerosion by endolithic algae and fungi. Borings did not show a preferred orientation (longitudinal to corallites vs. transverse to corallites) as tested in the *Goniastrea* slides. Some areas within a slide showed a greater abundance of borings, but this averaged out when the point count was complete.

Golubic (1969) noted that borings in fresh unbored calcite blocks penetrated only to a depth of approximately 50μ . This indicates that algal borings most likely occur close to the coral skeletal surface, and that as the coral skeleton grows up over the borings, algae tend to bore to a finite depth. Deeper

calcite (greater than a few millimeters maximum) is no longer available, probably due to decreased light penetration.

Most of the borings counted here are probably no longer active, as they are centimeters deep within the coral skeleton. Possibly overall boring and micritization at the surface of the affected coral skeletons would be greater than normal, but this was not observed. Affected corals were completely covered with epilithic algae, possibly discouraging colonization by boring forms.

In conclusion, the activity of endolithic algae and fungi as a group are not effected by increase in water temperature or loss of living coral cover. Algae and fungi borings appear to occur as the coral skeleton continues to grow, leaving inactive borings throughout the coral skeleton.

Appendix D: X-Ray Fluorescence Data

Table D-1. Strontium

Detector set at 35 Kv, 1.7 mA. Preset time 300 seconds, Spectrometer set on Ag secondary target, 20 ev/ch. Integration of Sr K_{α} lines from 13.84-14.44 keV, bkg removed.

SAMPLE NO.	INTENSITY DATA				
	RUN 1	RUN 2	RUN 3	MEAN	CORRECTED
(Tran A)					
RHR1246-1A	561.12	552.19	553.80	555.70	555.58
RHR1246-2A	534.80	533.38	528.91	532.36	532.24
RHR1246-3A	523.17	516.81	516.32	518.77	518.65
RHR1246-5A	523.69	518.33	517.14	519.72	519.60
RHR1246-6A	502.20	507.46	509.73	506.46	506.34
RHR1246-7A	470.00	473.34	475.43	472.92	472.80
RHR1246-8A	585.84	589.72	589.31	588.29	588.17
RHR1246-9A	504.96	508.31	510.29	507.85	507.73
RHR1246-9AB	555.81	558.15	560.94	558.30	558.18
RHR1246-10A	548.22	549.43	549.17	548.94	548.82
RHR1246-11A	543.62	546.85	544.92	545.13	545.01
RHR1246-12A	497.21	499.79	501.31	499.44	499.32
RHR1249-1A	510.42	512.61	510.80	511.28	511.16
RHR1249-3A	528.90	531.47	533.15	531.17	531.05
RHR1249-5A	553.92	554.46	555.09	554.49	554.37
RHR1249B-11A	592.59	592.55	592.89	592.68	592.56
RHR1346-13A	384.84	382.74	386.67	384.75	384.63
RHR1371-2A	545.24	546.64	543.79	545.22	545.10
RHR1373-4A	564.71	562.85	563.82	563.79	563.67
(Tran B)					
RHR1247-2A	494.28	495.31	497.53	495.71	495.59
RHR1247-3A	446.59	443.74	447.18	445.84	445.72
RHR1247-4A	334.15	336.33	336.11	335.53	335.41
RHR1247-5A	432.28	432.35	435.54	433.39	433.27
RHR1247-6A	463.00	466.64	465.64	465.09	464.97
RHR1247-7A	361.64	367.64	366.56	365.28	365.16
RHR1247-9A	461.74	477.84	478.19	472.59	472.47
RHR1247-10A	441.00	442.71	448.67	444.13	444.01
RHR1247-11A	509.43	515.11	515.30	513.28	513.16
RHR1247-13A	481.19	485.76	486.84	484.60	484.48
RHR1247-14A	550.54	555.51	556.09	554.05	553.93
RHR1247-15A	437.59	442.60	442.71	440.97	440.85
RHR1247-16A	481.38	484.16	485.64	483.73	483.61
RHR1248-1A	570.90	572.60	573.35	572.28	572.16
RHR1248-2A&B	558.06	571.58	575.45	568.36	568.24
RHR1248-3A	509.60	530.24	533.20	524.35	524.23
RHR1248-6A	475.55	493.98	496.79	488.77	488.65
RHR1248-9A	491.38	516.29	516.50	508.06	507.94
RHR1248-10A	498.58	518.38	519.99	512.32	512.20
RHR1258-1A	496.15	513.80	516.17	508.71	508.59
RHR1258-3A	561.64	564.30	560.63	562.19	562.07
RHR1258-4A	531.33	535.94	550.03	539.10	538.98

Table D-1 Cont'd

<u>SAMPLE NO.</u>	<u>INTENSITY DATA</u>				
	<u>RUN 1</u>	<u>RUN 2</u>	<u>RUN 3</u>	<u>MEAN</u>	<u>*CORRECTED</u>
(Tran C)					
89G001	479.43	480.81	474.97	478.40	478.28
89G002	531.62	531.83	524.95	529.46	529.34
89G005	498.75	501.97	495.25	498.66	498.54
89G006	467.55	466.73	460.83	465.04	464.92
89G013	551.63	551.78	546.10	549.84	549.72
89G014	528.88	529.63	527.44	528.65	528.53
89G015	575.45	574.05	568.90	572.80	572.68
89G016	479.04	477.21	475.54	477.26	477.14
89G017	545.18	547.69	542.10	544.99	544.87
89G018	538.71	542.00	537.10	539.27	539.15
(Tran D)					
89G019	391.00	387.88	388.57	389.15	389.03
89G020	386.66	384.32	381.13	384.04	383.92
89G021	152.25	150.39	150.29	150.98	150.86
89G022	36.05	36.18	35.17	35.80	35.68
89G022A	280.49	276.47	276.74	277.90	277.78
89G023	31.39	30.55	31.59	31.18	31.06
89G024	140.91	140.52	139.47	140.30	140.18
89G025	184.43	181.98	180.63	182.35	182.23
89G026	157.97	154.63	155.60	156.07	155.95
89G029	35.23	33.95	34.31	34.50	34.38
MYLARONLY	0.14	0.08	0.13	0.12	-----

* Note: Corrected values are obtained by subtracting MYLARONLY mean intensity from sample mean intensities.

Next two pages: Certified report of chemical analysis of standards.

XRAL ACTIVATION SERVICES INCORPORATED



3915 RESEARCH PARK, SUITE A-12, ANN ARBOR, MICHIGAN, 48108

PHONE: (800) 232-4130 FAX: (313) 662-3260

CERTIFICATE OF ANALYSIS

TO: UNIVERSITY OF MARYLAND
ATTN: RAYMOND G. BOWMAN
GEOLOGY DEPARTMENT
COLLEGE PARK, MD
20742

CUSTOMER NO. 99/01/06

DATE SUBMITTED
12-JUN-90

REPORT: 1674

FILE NUMBER: 1669

8 SAMPLES

WERE ANALYZED AS FOLLOWS:

ELEMENTS	DETECTION LIMIT	UNITS	METHOD	ELEMENTS	DETECTION LIMIT	UNITS	METHOD
SiO2	0.0100	%	XRF	FE	3.0000	PPM	XRF
CAO	0.0100	%	XRF	S	50.0000	PPM	XRF
MGO	0.0100	%	XRF	SR	2.0000	PPM	XRF

COMMENTS:

THIS IS A FINAL REPORT.

DATE 06-JUL-90

XRAL ACTIVATION SERVICES INC.

CERTIFIED BY

REPORTING ACTIVATION

DATE: 06-JUL-90

REPORT: 1674

FILE NUMBER: 1669

XRAL ACTIVATION SERVICES INCORPORATED

DATE: 06-JUL-90

REPORT: 1674

FILE NUMBER: 1669

PAGE: 1

S A M P L E	SI02 %	CAD %	MGD %	FE	PPM S	PPM SR	PPM
89G019	0.14	51.2	2.42	116	<50	4800	
89G023	0.16	53.9	1.43	122	<50	385	
89G024	0.11	54.6	0.96	119	<50	1740	
89G025	0.09	54.5	0.78	113	<50	2350	
RHR 1246-6A	0.20	51.8	0.82	122	<50	6460	
RHR 1246-8A	0.07	52.0	0.32	124	<50	7300	
RHR 1247-4A	0.09	50.0	2.56	337	<50	4110	
RHR 1247-10A	0.13	51.1	1.35	289	<50	5680	

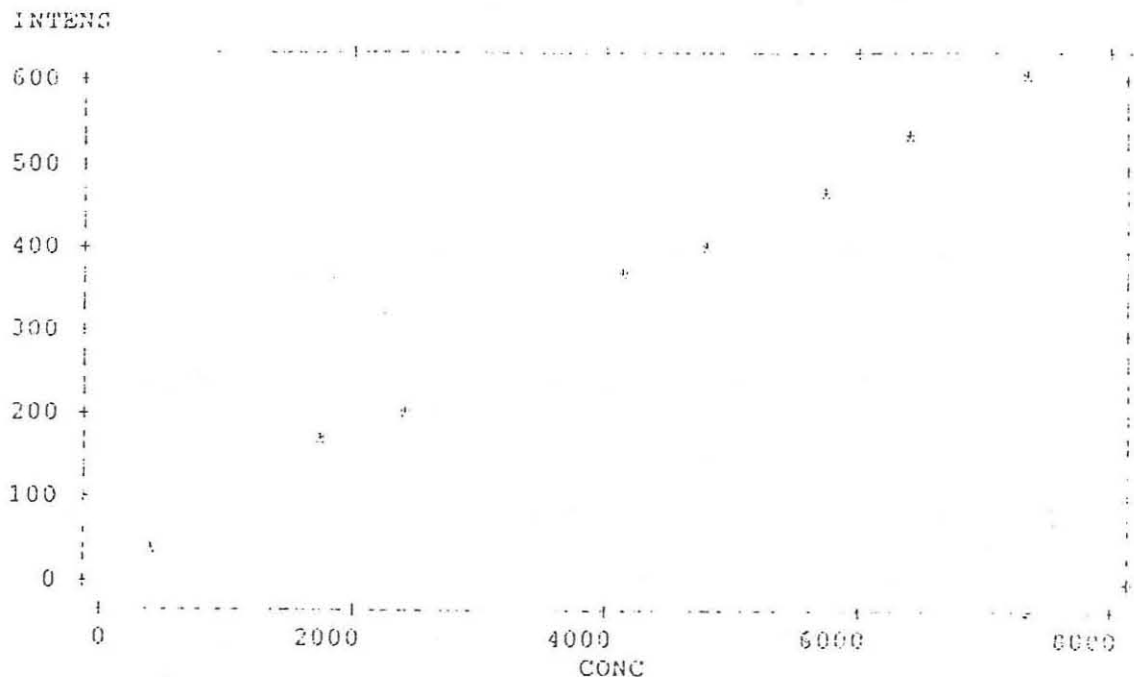
Table D-2. Linear regression of standards (by SYSTAT)

Dependent Variable: Intensity N: 8
 Multiple R: 0.999 Squared Multiple R: 0.999
 Adjusted Squared Multiple R: 0.999
 Standard Error of Estimate: 7.295

<u>Variable</u>	<u>Coefficient</u>	<u>STD Error</u>	<u>STD Coefficient</u>
Constant	0.528 (b ₀)	5.328	0.000
Concentration	0.080 (m)	0.001	0.999

<u>Variable</u>	<u>T</u>	<u>P(2 Tail)</u>
Constant	0.099	0.924
Concentration	70.041	0.000

Figure D-1. Strontium standard calibration curve based on regression data in Table D-2.



Errors:

Counting error for XRF analysis was taken as the coefficient of variance (CV) related to calculated intensity data. This was found by solving the following equation (Sokal and Rohlf, 1987):

$$CV = 1/\sqrt{I} \cdot 100$$

where CV is expressed as a percentage and I = XRF intensity. Mean relative counting error was calculated as $\sum CV/n$ where n = number of samples (n = 61). Calculated mean relative counting error for this experiment is 5.363%.

A calculation of the error associated with an estimation of sample concentrations from the standard linear regression was done utilizing the following formula (Bennett and Franklin, 1954):

$$\text{var}(x_o) \approx \sigma^2/b^2 [(1/m + 1/n) + (y_o - \bar{y})^2/b^2 \sum (x_i - \bar{x})^2]$$

where m = number of observations, n = number of analysis runs, and b = slope. This equation provides an approximate 95% confidence interval for concentrations estimated from the regression. Confidence intervals were expressed as a percentage of the estimated concentration (= relative error). Mean relative error (RE) was calculated as $\sum RE/n$ where n = number of samples (n = 61). Calculated mean relative error for this experiment is 2.211%. The Bennett and Franklin equation was calculated using a computer data reduction program

created by Mr. Richard Miller, University of Maryland
Department of Geology.

Total error for this experiment was taken as $\Sigma CV/n +$
 $\Sigma RE/n$ (= 7.574%).

APPENDIX E. SEM/WDS calcite cement analyses for
magnesium.

TRANSECT A

Sample No.	RHR1246-2A	Cement Type:	Acicular
OXIDE	NORMALIZED WT%	CALCULATED WT%	
CaO	55.99	55.77	
MgO	0.03	0.03	
CO ₂	43.98	43.80	STOICH
TOTAL		99.60	
MOL% CaCO ₃ :	99.91	MgCO ₃ :	0.09

Sample No.	RHR1246-11A	Cement Type:	Acicular
OXIDE	NORMALIZED WT%	CALCULATED WT%	
CaO	56.00	55.02	
MgO	0.03	0.03	
CO ₂	43.98	43.21	STOICH
TOTAL		98.25	
MOL% CaCO ₃ :	99.93	MgCO ₃ :	0.07

Sample No.	RHR1246-9A (Analysis A)	Cement Type:	Acicular
OXIDE	NORMALIZED WT%	CALCULATED WT%	
CaO	55.92	52.76	
MgO	0.09	0.09	
CO ₂	43.99	41.50	STOICH
TOTAL		94.35	
MOL% CaCO ₃ :	99.76	MgCO ₃ :	0.23

Sample No.	RHR1246-9A (Analysis B)	Cement Type:	Acicular
OXIDE	NORMALIZED WT%	CALCULATED WT%	
CaO	56.01	53.29	
MgO	0.01	0.01	
CO ₂	43.97	41.84	STOICH
TOTAL		95.15	
MOL% CaCO ₃ :	99.96	MgCO ₃ :	0.04

Sample No.	RHR1371-2A (Analysis A)	Cement Type:	Botryoidal
OXIDE	NORMALIZED WT%	CALCULATED WT%	
CaO	55.97	52.42	
MgO	0.05	0.05	
CO ₂	43.98	41.19	STOICH
TOTAL		93.66	
MOL% CaCO ₃ :	99.86	MgCO ₃ :	0.13

Sample No.	RHR1371-2A (Analysis B)	Cement Type:	Botry
OXIDE	NORMALIZED WT%	CALCULATED WT%	
CaO	55.97	56.84	
MgO	0.05	0.05	
CO ₂	43.98	44.67	STOICH
TOTAL		101.57	
MOL% CaCO ₃ :	99.86	MgCO ₃ :	0.13

Sample No.	RHR1371-2A	Cement Type:	Acicular
OXIDE	NORMALIZED WT%	CALCULATED WT%	
CaO	56.03	54.34	
MgO	0.00	0.00	
CO ₂	43.97	42.64	STOICH
TOTAL		96.98	
MOL% CaCO ₃ :	100.00	MgCO ₃ :	0.00

Sample No.	RHR1246-5A	Cement Type:	Botry
OXIDE	NORMALIZED WT%	CALCULATED WT%	
CaO	55.96	53.97	
MgO	0.06	0.05	
CO ₂	43.98	42.41	STOICH
TOTAL		96.43	
MOL% CaCO ₃ :	99.86	MgCO ₃ :	0.14

Sample No.	RHR1246-5A	Cement Type:	Botry 2
OXIDE	NORMALIZED WT%	CALCULATED WT%	
CaO	56.00	56.95	
MgO	0.03	0.03	
CO ₂	43.98	44.72	STOICH
TOTAL		101.69	
MOL% CaCO ₃ :	99.93	MgCO ₃ :	0.07

Sample No.	RHR1246-5A	Cement Type:	Acicular
OXIDE	NORMALIZED WT%	CALCULATED WT%	
CaO	55.96	55.64	
MgO	0.06	0.05	
CO ₂	43.98	43.72	STOICH
TOTAL		99.42	
MOL% CaCO ₃ :	99.86	MgCO ₃ :	0.14

TRANSECT B

Sample No.	RHR1248-9A	Cement Type:	Acicular
OXIDE	NORMALIZED WT%	CALCULATED WT%	
CaO	55.96	53.21	
MgO	0.06	0.06	
CO ₂	43.98	41.82	STOICH
TOTAL		95.09	
MOL% CaCO ₃ :	99.85	MgCO ₃ :	0.15

Sample No.	RHR1248-9A	Cement Type:	Botry
OXIDE	NORMALIZED WT%	CALCULATED WT%	
CaO	55.91	57.03	
MgO	0.10	0.10	
CO ₂	43.99	44.87	STOICH
TOTAL		102.00	
MOL% CaCO ₃ :	99.75	MgCO ₃ :	0.25

Sample No.	RHR1248-1A	Cement Type:	Acicular 1
OXIDE	NORMALIZED WT%	CALCULATED WT%	
CaO	56.03	52.64	
MgO	0.00	0.00	
CO ₂	43.97	41.31	STOICH
TOTAL		93.95	
MOL% CaCO ₃ :	100.00	MgCO ₃ :	0.00

Sample No.	RHR1248-1A	Cement Type:	Acicular 2
OXIDE	NORMALIZED WT%	CALCULATED WT%	
CaO	55.91	55.61	
MgO	0.10	0.10	
CO ₂	43.99	43.75	STOICH
TOTAL		99.45	
MOL% CaCO ₃ :	99.75	MgCO ₃ :	0.25

Sample No.	RHR1258-1A	Cement Type:	Botry
OXIDE	NORMALIZED WT%	CALCULATED WT%	
CaO	55.85	51.71	
MgO	0.15	0.14	
CO ₂	44.00	40.73	STOICH
TOTAL		92.58	
MOL% CaCO ₃ :	99.62	MgCO ₃ :	0.38

Sample No.	RHR1258-1A	Cement Type:	Acicular 1
OXIDE	NORMALIZED WT%	CALCULATED WT%	
CaO	55.95	52.89	
MgO	0.07	0.06	
CO ₂	43.98	41.57	STOICH
TOTAL		94.53	
MOL% CaCO ₃ :	99.83	MgCO ₃ :	0.16

Sample No.	RHR1258-1A	Cement Type:	Acicular 2
OXIDE	NORMALIZED WT%	CALCULATED WT%	
CaO	55.90	51.34	
MgO	0.12	0.11	
CO ₂	43.99	40.41	STOICH
TOTAL		91.85	
MOL% CaCO ₃ :	99.71	MgCO ₃ :	0.29

Sample No.	RHR1247-7A	Cement Type:	Acicular 1
OXIDE	NORMALIZED WT%	CALCULATED WT%	
CaO	55.98	53.68	
MgO	0.05	0.04	
CO ₂	43.98	42.17	STOICH
TOTAL		95.89	
MOL% CaCO ₃ :	99.88	MgCO ₃ :	0.11

Sample No.	RHR1247-7A	Cement Type:	Acicular 2
OXIDE	NORMALIZED WT%	CALCULATED WT%	
CaO	56.03	52.20	
MgO	0.00	0.00	
CO ₂	43.97	40.96	STOICH
TOTAL		93.16	
MOL% CaCO ₃ :	100.00	MgCO ₃ :	0.00

Sample No.	RHR1247-7A	Cement Type:	Acicular 3
OXIDE	NORMALIZED WT%	CALCULATED WT%	
CaO	56.01	54.98	
MgO	0.02	0.02	
CO ₂	43.97	43.16	STOICH
TOTAL		98.16	
MOL% CaCO ₃ :	99.95	MgCO ₃ :	0.04

TRANSECT C

Sample No. 89G002		Cement Type: Acicular 1
OXIDE	NORMALIZED WT%	CALCULATED WT%
CaO	55.99	56.18
MgO	0.03	0.03
CO ₂	43.98	44.12 STOICH
TOTAL		100.34
MOL% CaCO ₃ : 99.91	MgCO ₃ : 0.08	

Sample No. 89G002		Cement Type: Acicular 2
OXIDE	NORMALIZED WT%	CALCULATED WT%
CaO	56.01	56.65
MgO	0.02	0.02
CO ₂	43.97	44.47 STOICH
TOTAL		101.14
MOL% CaCO ₃ : 99.96	MgCO ₃ : 0.04	

Sample No. 89G002		Cement Type: Acic-Blade
OXIDE	NORMALIZED WT%	CALCULATED WT%
CaO	52.71	53.41
MgO	2.83	2.87
CO ₂	44.46	45.04 STOICH
TOTAL		101.31
MOL% CaCO ₃ : 93.05	MgCO ₃ : 6.95	

Sample No. 89G005 (Analysis A)		Cement Type: Acicular 1
OXIDE	NORMALIZED WT%	CALCULATED WT%
CaO	56.03	53.10
MgO	0.00	0.00
CO ₂	43.97	41.67 STOICH
TOTAL		94.77
MOL% CaCO ₃ : 100.00	MgCO ₃ : 0.00	

Sample No. 89G005 (Analysis B)		Cement Type: Acicular 1
OXIDE	NORMALIZED WT%	CALCULATED WT%
CaO	55.97	56.48
MgO	0.05	0.06
CO ₂	43.98	44.39 STOICH
TOTAL		100.93
MOL% CaCO ₃ : 99.86	MgCO ₃ : 0.14	

Sample No.	89G005 (Analysis A)	Cement Type: Acic-Blade
OXIDE	NORMALIZED WT%	CALCULATED WT%
CaO	50.32	55.31
MgO	4.87	5.36
CO ₂	44.81	49.26 STOICH
TOTAL		109.93
MOL% CaCO ₃ :	88.12	MgCO ₃ : 11.87

Sample No.	89G005 (Analysis B)	Cement Type: Acic-Blade
OXIDE	NORMALIZED WT%	CALCULATED WT%
CaO	51.90	53.95
MgO	3.52	3.66
CO ₂	44.58	46.33 STOICH
TOTAL		103.94
MOL% CaCO ₃ :	91.37	MgCO ₃ : 8.62

Sample No.	89G006 (Analysis A)	Cement Type: Detrital
OXIDE	NORMALIZED WT%	CALCULATED WT%
CaO	47.49	47.85
MgO	7.29	7.34
CO ₂	45.23	45.57 STOICH
TOTAL		100.76
MOL% CaCO ₃ :	82.40	MgCO ₃ : 17.60

Sample No.	89G006 (Analysis B)	Cement Type: Detrital
OXIDE	NORMALIZED WT%	CALCULATED WT%
CaO	47.01	49.13
MgO	7.69	8.04
CO ₂	45.30	47.34 STOICH
TOTAL		104.51
MOL% CaCO ₃ :	81.45	MgCO ₃ : 18.55

Sample No.	89G006	Cement Type: Drusy
OXIDE	NORMALIZED WT%	CALCULATED WT%
CaO	50.67	51.53
MgO	4.57	4.65
CO ₂	44.76	45.51 STOICH
TOTAL		101.69
MOL% CaCO ₃ :	88.85	MgCO ₃ : 11.15

Sample No. 89G016		Cement Type: Acicular 1
OXIDE	NORMALIZED WT%	CALCULATED WT%
CaO	55.94	55.66
MgO	0.07	0.07
CO ₂	43.98	43.76 STOICH
TOTAL		99.50
MOL% CaCO ₃ : 99.82	MgCO ₃ : 0.18	

Sample No. 89G016		Cement Type: Acicular 2
OXIDE	NORMALIZED WT%	CALCULATED WT%
CaO	55.96	47.13
MgO	0.06	0.05
CO ₂	43.98	37.04 STOICH
TOTAL		84.21
MOL% CaCO ₃ : 99.85	MgCO ₃ : 0.15	

Sample No. 89G017		Cement Type: Acicular 1
OXIDE	NORMALIZED WT%	CALCULATED WT%
CaO	56.01	55.40
MgO	0.02	0.02
CO ₂	43.97	43.49 STOICH
TOTAL		98.91
MOL% CaCO ₃ : 99.96	MgCO ₃ : 0.04	

Sample No. 89G017		Cement Type: Acicular 2
OXIDE	NORMALIZED WT%	CALCULATED WT%
CaO	56.00	57.04
MgO	0.03	0.03
CO ₂	43.97	44.79 STOICH
TOTAL		101.86
MOL% CaCO ₃ : 99.93	MgCO ₃ : 0.07	

Sample No. 89G017		Cement Type: Acicular 3
OXIDE	NORMALIZED WT%	CALCULATED WT%
CaO	55.97	55.58
MgO	0.05	0.05
CO ₂	43.98	43.68 STOICH
TOTAL		99.31
MOL% CaCO ₃ : 99.87	MgCO ₃ : 0.13	

TRANSECT D

Sample No. 89G019		Cement Type: Isopachous
OXIDE	NORMALIZED WT%	CALCULATED WT%
CaO	51.41	52.70
MgO	3.94	4.04
CO ₂	44.65	45.77 STOICH
TOTAL		102.51
MOL% CaCO ₃ : 90.35	MgCO ₃ : 9.64	

Sample No. 89G019		Cement Type: Acicular 1
OXIDE	NORMALIZED WT%	CALCULATED WT%
CaO	55.95	52.31
MgO	0.06	0.06
CO ₂	43.98	41.12 STOICH
TOTAL		93.49
MOL% CaCO ₃ : 99.84	MgCO ₃ : 0.16	

Sample No. 89G019		Cement Type: Acicular 2
OXIDE	NORMALIZED WT%	CALCULATED WT%
CaO	55.92	52.07
MgO	0.09	0.08
CO ₂	43.99	40.95 STOICH
TOTAL		93.10
MOL% CaCO ₃ : 99.77	MgCO ₃ : 0.22	

Sample No. 89G019		Cement Type: Acicular 3
OXIDE	NORMALIZED WT%	CALCULATED WT%
CaO	55.99	57.57
MgO	0.03	0.03
CO ₂	43.98	45.21 STOICH
TOTAL		102.81
MOL% CaCO ₃ : 99.92	MgCO ₃ : 0.07	

Sample No. 89G019		Cement Type: Acicular 4
OXIDE	NORMALIZED WT%	CALCULATED WT%
CaO	55.99	54.65
MgO	0.03	0.03
CO ₂	43.98	42.92 STOICH
TOTAL		97.61
MOL% CaCO ₃ : 99.92	MgCO ₃ : 0.07	

Sample No. 89G020 (Analysis A)	Cement Type: Isopachous	
OXIDE	NORMALIZED WT%	CALCULATED WT%
CaO	45.73	43.40
MgO	8.78	8.33
CO ₂	45.48	43.16 STOICH
TOTAL		94.89
MOL% CaCO ₃ : 78.92	MgCO ₃ : 21.08	

Sample No. 89G020 (Analysis B)	Cement Type: Isopachous	
OXIDE	NORMALIZED WT%	CALCULATED WT%
CaO	50.07	45.88
MgO	5.09	4.66
CO ₂	44.85	41.10 STOICH
TOTAL		91.65
MOL% CaCO ₃ : 87.61	MgCO ₃ : 12.39	

Sample No. 89G020	Cement Type: Acicular	
OXIDE	NORMALIZED WT%	CALCULATED WT%
CaO	56.01	53.75
MgO	0.02	0.02
CO ₂	43.97	42.20 STOICH
TOTAL		95.97
MOL% CaCO ₃ : 99.95	MgCO ₃ : 0.05	

Sample No. 89G022	Cement Type: Bladed	
OXIDE	NORMALIZED WT%	CALCULATED WT%
CaO	55.88	54.63
MgO	0.13	0.13
CO ₂	43.99	43.01 STOICH
TOTAL		97.77
MOL% CaCO ₃ : 99.68	MgCO ₃ : 0.32	

Sample No. 89G022	Cement Type: Spar	
OXIDE	NORMALIZED WT%	CALCULATED WT%
CaO	54.55	51.17
MgO	1.26	1.18
CO ₂	44.19	41.45 STOICH
TOTAL		93.80
MOL% CaCO ₃ : 96.88	MgCO ₃ : 3.12	

Sample No. 89G024 (Pleistocene)	Cement Type: Acicular 1	
OXIDE	NORMALIZED WT%	CALCULATED WT%
CaO	55.94	51.61
MgO	0.08	0.07
CO ₂	43.98	40.58 STOICH
TOTAL		92.27
MOL% CaCO ₃ :	99.80	MgCO ₃ : 0.20

Sample No. 89G024 (Pleistocene)	Cement Type: Acicular 2	
OXIDE	NORMALIZED WT%	CALCULATED WT%
CaO	55.88	53.54
MgO	0.13	0.13
CO ₂	43.99	42.15 STOICH
TOTAL		95.82
MOL% CaCO ₃ :	99.67	MgCO ₃ : 0.33

Sample No. 89G024 (Pleistocene)	Cement Type: Acicular 3	
OXIDE	NORMALIZED WT%	CALCULATED WT%
CaO	55.60	47.87
MgO	0.36	0.31
CO ₂	44.03	37.91 STOICH
TOTAL		86.10
MOL% CaCO ₃ :	99.09	MgCO ₃ : 0.90

Sample No. 89G025 (Pleistocene)	Cement Type: Acicular	
OXIDE	NORMALIZED WT%	CALCULATED WT%
CaO	55.97	54.92
MgO	0.05	0.05
CO ₂	43.98	43.15 STOICH
TOTAL		98.12
MOL% CaCO ₃ :	99.87	MgCO ₃ : 0.12

Counting errors for the above analyses were calculated by the Tracor Norther 5600 Computer Task System as a relative error. The formula used for the calculation is:

$$\% = \frac{\sqrt{\text{counts} - \text{background}}}{\text{counts} - \text{background}} \cdot 100$$

This method is presented in Willard et al. (1974).

Relative errors for Ca and Mg were averaged to provide a

mean relative error for the analyses as a whole (mean

$\% \sigma_{Ca} = 1.178$, mean $\% \sigma_{Mg} = 19.92$).

REFERENCES CITED

- Aissaoui, D.M, Buigues, D., and Purser, B.H., 1986, Model of reef diagenesis: Mururoa Atoll, French Polynesia: in Schroeder, J.H., and Purser, B.H., eds., Reef Diagenesis, Springer-Verlag, New York, pub., p. 27-52.
- Bathurst, R.G.C., 1976, Carbonate sediments and their diagenesis: Elsevier Scientific Publishing Company, New York, pub., pp. 231-457, 381-392.
- Bell, S.C., and Siegrist, H.G. Jr., 1988, Patterns in reef diagenesis: Rota, Mariana Islands: Proceedings of the 6th International Coral Reef Symposium, Australia, v. 3, p. 547-552.
- Bence, A.E., and Albee, A.L., 1968, Empirical correction factors for the electron microanalysis of silicates and oxides: Journal of Geology, v. 76, p. 382-403.
- Bennett, C.A., and Franklin, N.L., 1954, Statistical analysis in chemistry and the chemical industry: John Wiley & Sons, Inc., New York, pub., p. 222-234.
- Berner, R.A., 1975, The role of magnesium in the crystal growth of calcite and aragonite from sea water: Geochimica et Cosmochimica Acta, v. 39, p. 489-504.
- Bischoff, W.D., Mackenzie, F.T., and Bishop, F.C., 1987, Stabilities of synthetic magnesian calcites in aqueous solution: comparison with biogenic materials: Geochimica et Cosmochimica Acta, v. 51, p. 1413-1423.

- Bromley, R.G., 1965, Studies in the lithology and conditions of sedimentation of the Chalk Rock and comparable horizons: Thesis, University of London, unpublished, 355pp.
- Bromley, R.G., 1978, Bioerosion of Bermuda reefs: Palaeogeography, Palaeoclimatology, Palaeoecology, v. 23, p. 169-197.
- Cobb, W.R., 1969, Penetration of calcium carbonate substrates by the boring sponge, *Cliona*: American Zoologist, v. 9, p. 783-790.
- Dahl, A.L., and Salvat, B., Are human impacts, either through traditional or contemporary uses, stabilizing or destabilizing to reef community structure?: Proceedings of the 6th International Coral Reef Symposium, Australia, v. 1, p. 63-69.
- Dravis, J.J., and Yurewicz, D.A., 1985, Enhanced carbonate petrography using fluorescence microscopy: Journal of Sedimentary Petrology, v. 55, no. 6, p. 795-804.
- Fay, P., 1983, The blue-greens: Institute of Biology Studies in Biology no. 160, Edward Arnold Ltd., Melbourne, pub., 88 pp.
- Friedman, G.M., and Brenner, I.B., 1977, Progressive diagenetic elimination of strontium in Quaternary to Late Tertiary coral reefs of Red Sea: sequence and time scale: in Frost, S.H., Weiss, M.P., and Saunders, J.B., eds., Reef and Related Carbonates - Ecology and

Sedimentology, AAPG Studies in Geology No. 4,
p. 353-355.

Fütterer, D.K., 1974, Significance of the boring sponge
Cliona for the origin of fine grained material of
carbonate sediments: Journal of Sedimentary
Petrography, v. 44, p. 79-84.

Glynn, P.W., 1988, El Niño-Southern Oscillation
1982-1983: nearshore population, community, and
ecosystem responses: Ann. Rev. Ecol. Syst., v. 19,
p. 309-345.

Glynn, P.W., Cortes, J., Guzman, H.M., and Richmond,
R.H., 1988, El Niño (1982-83) associated coral
mortality and relationship to sea surface temperature
deviations in the tropical Eastern Pacific:
Proceedings of the 6th International Coral Reef
Symposium, Australia, v. 3, p. 237-243.

Golubic, S., 1969, Distribution, taxonomy and boring
patterns of marine endolithic algae: American
Zoologist, no. 9, p. 747-751.

Golubic, S., Perkins, R.D., and Lukas, K.J., 1975,
Boring microorganisms and microborings in carbonate
substrates: in Frey, R.W. ed., The Study of Trace
Fossils, Springer-Verlag, New York, pub., p. 229-259.

Haigler, S.A., 1969, Boring mechanism of *Polydora*
websteri inhabiting *Crassostrea virginica*: American
Zoologist, v. 9, p. 821-828.

- Hutchings, P.A., 1986, Biological destruction of coral reefs: *Coral Reefs*, v. 4, p. 239-252.
- Jones, R.S., and Randall, R.H., 1973, A study of biological impact caused by natural and man-induced changes on a tropical reef: University of Guam, Marine Laboratory Technical Report no. 7, 182 pp.
- Kevex Corporation, 1982, Kevex xrf Quantex-Ray software user's manual: Kevex Corporation, Foster City, California, p. 4-1 to 4-41, 11-1 to 11-20.
- Kiene, W.E., 1988, A model of bioerosion on the Great Barrier Reef: Proceedings of the 6th International Coral Reef Symposium, Australia, v. 3, p. 449-454.
- Kinsman, D.J.J., 1969, Interpretation of Sr⁺² concentrations in carbonate minerals and rocks: *Journal of Sedimentary Petrology*, v. 39, no. 2, p. 486-508.
- Kohlmeyer, J., 1969, The role of marine fungi in the penetration of calcareous substances: *American Zoologist*, no. 9, p. 741-746.
- Mackenzie, F.T., Bischoff, W.D., Bishop, F.C., Loijens, M., Schoonmaker, J.E., and Wollast, R., 1983, Magnesian calcites: Low temperature occurrence, solubility and solid-solution behavior: in Ribbe, P.H., ed., *Carbonates: Mineralogy and Chemistry, Reviews in Mineralogy*, no. 11, p. 97-144.
- Marshall, J.F., 1986, Regional distribution of submarine cements within an epicontinental reef system: *Central*

- Great Barrier Reef, Australia: in Schroeder, J.H., and Purser, B.H., eds., Reef Diagenesis, Springer-Verlag, New York, pub., p. 8-26.
- Milliman, J.D., 1974, Marine carbonates: Springer-Verlag, New York, pub., p. 3-15.
- Mucci, A., 1987, Influence of temperature on the composition of magnesian calcite overgrowths precipitated from seawater: *Geochimica et Cosmochimica Acta*, v. 51, p. 1977-1984.
- Olympus Corporation, 1988, Cue 3 image analyzer version 2.01: Galai.
- Potts, P.J., 1987, A handbook of silicate rock analysis: Chapman and Hall, New York, pub., pp. 226-285, 326-382.
- Randall, R.H., 1983, Guide to the coastal resources of Guam, volume ii-the corals: University of Guam Press, p. 12.
- Randall, R.H., and Siegrist, H.G. Jr., 1988, Geomorphology of the fringing reefs of northern Guam in response to Holocene sea level changes: Proceedings of the 6th International Coral Reef Symposium, Australia, v. 3, p. 473-477.
- Randall, R.H., Tsuda, R.T., and Bowman, R.G., 1990, A reassessment of reef-building corals, an assessment of framework bioerosion, and a reassessment of marine benthic algae in the reef area affected by thermal effluent at Tanguisson Point, Guam (DRAFT REPORT): University of Guam Marine Laboratory, 44 pp.

- Rice, M.E., 1969, Possible boring structures of sipunculids: *American Zoologist*, v. 9, p. 803-812.
- Scoffin, T.P., 1987, An introduction to carbonate sediments and rocks: Chapman and Hall, New York, pub., pp. 40-52, 64-70, 89-145.
- Sokal, R.R., and Rohlf, F.J., Introduction to biostatistics, second edition: W.H. Freeman and Company, New York, pub., 363 pp.
- Tracey, J.R. Jr., Schlanger, S.O., Stark, J.T., Doan, D.B., and May, H.G., 1964, General geology of Guam: U.S. Geological Survey Professional Paper 403-A, 104 pp.
- Tudhope, A.W., and Risk, M.J., 1985, Rate of dissolution of carbonate sediments by microboring organisms, Davies Reef, Australia: *Journal of Sedimentary Petrology*, no. 55, p. 440-447.
- Walter, L.M., and Morse, J.W., 1984, Magnesian calcite stabilities: a reevaluation: *Geochimica et Cosmochimica Acta*, v. 48, p. 1059-1069.
- Warme, J.E., 1975, Borings as trace fossils, and the processes of marine bioerosion: in Frey, R.W., ed., *The Study of Trace Fossils*, Springer-Verlag, New York, pub., p. 181-227.
- Warme, J.E., 1977, Carbonate borers-their role in reef ecology and preservation: in Frost, S.H., Weiss, M.P., and Saunders, J.B., eds., *Reef and Related Carbonates - Ecology and Sedimentology*, AAPG Studies in Geology No. 4, p. 261-279.

- Wilkinson, L., 1987, SYSTAT: the system for statistics:
Systat, Inc., Evanston, IL.
- Willard, H.H., Merritt, L.L. Jr., and Dean, J.A., 1974,
Instrumental methods of analysis, fifth edition:
D. Van Nostrand Company, New York, pub., pp. 320-322.

ACKNOWLEDGEMENTS

I would like to thank Richard H. Randall, Henry G. Siegrist, and other workers at the University of Guam Marine Laboratory for the creation of and assistance with this project. Their technical support and sample collection are much appreciated.

Thanks also go out to my committee: Peter B. Stifel, Philip A. Candela, Ann G. Wylie, and Marjorie L. Reaka. They provided much needed assistance at the University of Maryland. More importantly, they convinced me that this whole thing was worth doing when it seemed hopeless.

I also thank the grads and undergrads at the University of Maryland for their advice and support, especially Richard Miller and Phillip Piccoli. The help of Curtis Lure and Barbara Linder is much appreciated. I could not have gotten it done without them.

Most of all I would like to thank my wife, Colleen Bowman. She paid the bills for two years, and kept me going even when things got almost out of control. Without her love and support this all would never have happened. I also thank the rest of my family for being there to listen to my complaining about this thing.

Thanks to all.

TABLE OF CONTENTS

<u>Section</u>	<u>Page</u>
Acknowledgements	ii
List of Tables	iv
List of Figures	v
List of Plates	vi
Introduction	1
General Geology	4
Bioerosion	9
Cementation	11
Strontium	18
Methods	20
Results	29
Bioerosion	29
Strontium	33
Cements	36
Discussion	41
Bioerosion at Tanguisson	41
Encrustation at Tanguisson	47
Strontium Anomalies at Tanguisson	49
Carbonate Cements	50
Holocene	50
Diagenetic Model	50
Implications at Tanguisson	52
Global Implications	52
Conclusion	54
Appendix A Statistical Methods and Computer Programs	56
Appendix B Macrobioerosion Point Count Data and Slab Descriptions	61
Appendix C Changes in Density of Endolithic Algal Borings	75
Appendix D X-Ray Fluorescence Data	83
Appendix E SEM/WDS Calcite Cement Analyses for Magnesium	90
References Cited	101

ABSTRACT

Title of Thesis: DIAGENETIC EFFECTS RELATED TO HOT WATER
EFFLUENT IN MODERN AND HOLOCENE REEF
LIMESTONES ON GUAM

Name of degree candidate: Raymond G. Bowman

Degree and Year: Master of Science, 1990

Thesis directed by: Peter B. Stifel, Associate
Professor, Department of Geology

In 1971, scleractinian corals were affected by hot water effluent from an oil-fired thermoelectric plant near Tanguisson Point, Guam. Corals were damaged or killed in an approximately 10,000 square meter area of the reef flat. This work is a reassessment of the affected area and an area of intertidal Holocene reef rock, including a study of bioerosion, cementation, and trace element geochemistry of coral skeletons and cements in the modern reef.

Percentages of bioerosion and encrusting organisms were determined using a random number grid point count method of coral cross-sections. A significant ($p < .05$) increase in percent bioerosion was noted in the affected area versus a control area. A trend toward a higher rate

of encrustation was also noted in the affected area.

Strontium concentrations were determined by x-ray fluorescence. Significantly less strontium, probably due to a higher percentage of encrusters, was noted in the affected area.

Thin section analyses of carbonate cements yielded no differences in cement types or morphologies. No differences in magnesium concentrations, determined by SEM/WDS, within cement types were noted.

A model for diagenesis related to hot water effluent in the modern reef includes increased bioerosion and encrustation, and a decrease in whole rock strontium concentration. No diagenetic alteration was observed within the Holocene reef material.

The observed increase in bioerosion in the vicinity of the hot water effluent at Tanguisson may lead to loss of the fringing reef. Larger scale effects may be related to El Niño-Southern Oscillation (ENSO). Loss of living coral cover similar to that at Tanguisson occurred over a large area of the Eastern Pacific during the 1982-83 ENSO event. Slow recovery of living corals, along with an increase in bioerosion, may lead to physical damage to reefs affected by ENSO events.

LIST OF TABLES

<u>Number</u>	<u>Page</u>
1. Factors favoring aragonite and calcite precipitation	12
2. Average of experimental Mg distribution coefficients and compositions	15
3. ANOVA for % bioerosion, treatment vs. genera	30
4. ANOVA for % bioerosion, treatment vs. depth	30
5. ANOVA for % relative bioerosion, treatment vs. genera	31
6. ANOVA for % relative bioerosion, treatment vs. depth	31
7. ANOVA for % encrusters, treatment vs. genera	32
8. ANOVA for % encrusters, treatment vs. depth	32
9. Strontium concentration in ppm, Modern corals	34
10. Strontium concentration in ppm, Holocene corals	34
11. ANOVA for strontium concentration, treatment vs. genus	35
12. ANOVA for strontium concentration, treatment vs. depth.	35

LIST OF FIGURES

<u>Number</u>	<u>Page</u>
1. Area or reef flat affected by hot water effluent as of January, 1973	2
2. Map of Guam showing the Tanguisson Point study area	6
3. Vertical profile of the fringing reef system at Tanguisson Point	7
4. Location of sample transects	21

LIST OF PLATES

<u>Number</u>	<u>Page</u>
1. Aragonite cements	39
2. Mg-calcite cements and Pleistocene texture	40
3. Cross-sections of slabbed reef samples, <i>Goniastrea</i> and <i>Pocillopora</i>	43
4. Cross-sections of slabbed reef samples, <i>Acropora</i> and <i>Millepora</i>	44
5. Cross-sections of slabbed reef samples, <i>Favia</i> and <i>Favites</i>	45